

STABLE AROMATIC ORGANOBORANE MATERIALS

by
Heidi Lee van de Wouw

A dissertation submitted to the Johns Hopkins University in conformity
with the requirements for the degree of Doctor of Philosophy.

Baltimore, Maryland
January 2019

© Heidi Lee van de Wouw 2019
All rights reserved.

Abstract

The work included herein describes the synthesis and study of stable aromatic organoborane materials. The materials synthesized are based upon the architecture of 1,2-azaborines, aromatic hydrocarbons with a single CC for BN bond substitution. The aromaticity and electronics of both molecular and macromolecular materials are investigated. A large portion of this work is focused on the development of the monomer BN 2-vinylnaphthalene (BN2VN) and homo- and copolymers of BN2VN resulting from radical polymerization. BN2VN functionalized polymers can be converted to novel materials owing to the implicit reactivity of organoboranes.

Advisor: Professor Rebekka S. Klausen

Reader: Professor J.D. Tovar

Reader: Professor Thomas J. Kempa

Dedicated to all those whom

just keep pushing on.

Acknowledgements

Many people have helped to make my graduate school career a success and I could not have succeeded without the support from many different people, in many different capacities.

Firstly, I thank my advisor, Professor Rebekka S. Klausen, for her warm mentorship. From the first weeks of working side-by-side unpacking boxes of glassware, to seeing me off as an accomplished chemical researcher, Rebekka has always challenged me to perform to the best of my abilities. To the first members of the Klausen Lab, Dr. Eric Moshe Press and Dr. Sravan Surampudi, I thank you for inviting me into your families and for continually being available to discuss all facets of my research.

I thank my mother and father, Monica and John van de Wouw, for raising me to be an independent go-getter and granting me the freedom to choose my own path. I thank my sister, Jody van de Wouw, for always being there for me. To my aunts, Kim Hayashi and Leslie Rosen, thank you for challenging me to succeed academically and helping me navigate my course through higher education. Thanks to my grandparents, Ba-chan, Ji-chan, Grams, Tutu, and Opa, for always providing me with unconditional love, and especially my grandmothers for teaching me to be open and gregarious.

My day-to-day as a graduate student has been continually brightened by the many undergraduate students with whom I have mentored over the years, Mr. Jae Young (Jake) Lee, Mr. Elorm C. Awuyah, and Ms. Jodie I. Baris. I am privileged to have lead such a lot of astute and dedicated mentees, each allowing me to learn from them as they arose to meet the challenge of becoming thoughtful researchers. Our shared comradery and commiseration allowed us to grow not just as researchers, but as young adults, together.

Eduardo Silva and Zachary Inscho, I thank you both for standing by my side and offering support for both my technical and artistic aspirations. You both have helped me to create balance within my life and to enjoy my time in a completely different world, the East Coast. Rachel Harris,

your hospitality and understanding throughout my last month in Baltimore has been invaluable and I will forever admire your generosity.

I would like to thank the members of the Klausen Research Group. With you we are able to support one another, build upon each other's accomplishments, and grow as professionals. Yuyang Ji and Qifeng Zhang, thank you especially for your friendship and introducing me to new cultures and allowing me to share mine with you.

I would like to thank the Johns Hopkins University, Department of Chemistry, especially: Prof. J. D. Tovar, Prof. Sara Thoi, Prof. Howard Fairbrother, Prof. Howard Katz, Boris Steinberg, Lauren McGhee, Dr. Joel Tang, Dr. Maxime Siegler, and Dr. Phil Mortimer. I was further supported by the department through both the Ernest M. Marks Award and the Harry and Cleio Greer Fellowship. Thank you Prof. Carmen F. Works for urging me to apply to Johns Hopkins University and continuing to be my mentor.

Lastly, the work included in this dissertation and future directions of the BN sub-group is funded by the American Chemical Society, Petroleum Research Fund (Grant# 56380-DNI7: Controlling Polarization in Polystyrene) and the National Science Foundation (Grant# CHE-1752791: Hydrophobic and Hydrophilic Polymers from Boron-Containing Polyolefins).

Publications Drawing Upon this Dissertation

1. van de Wouw, H. L.; Lee, J. Y.; Siegler, M. A.; Klausen, R. S. "Innocent BN Bond Substitution in Anthracene Derivatives." *Org. Biomol. Chem.* **2016**, *14*, 3256–3263.
2. van de Wouw, H. L.; Lee, J. Y.; Klausen, R. S. "Gram-Scale Free Radical Polymerization of an Azaborine Vinyl Monomer." *Chem. Commun.* **2017**, *53*, 7262–7265.
3. van de Wouw, H. L.; Lee, J. Y.; Awuyah, E. C.; Klausen, R. S. "A BN Aromatic Ring Strategy for Tunable Hydroxy Content in Polystyrene." *Angew. Chem., Int. Ed.* **2018**, *57*, 1673–1677.
4. van de Wouw, H. L.; Awuyah, E. C.; Baris, J. I.; Klausen, R. S. "An Organoborane Vinyl Monomer with Styrene-like Radical Reactivity: Reactivity Ratios and Role of Aromaticity." *Macromol.* **2018**, *51*, 6359–6368.
5. van de Wouw, H. L.; Klausen, R. S. "BN Polystyrenes: Emerging Optical Materials & Versatile Intermediates." *J. Org. Chem.* **2019**, *84*, 1117–1125.

Publication not Included in this Dissertation

1. van de Wouw, H. L.; Chamorro, J.; Quintero, M.; Klausen, R. S. "Opposites Attract: Organic Charge Transfer Salts." *J. Chem. Educ.* **2015**, *92*, 2134–2139.

Table of Contents

Title Page	i
Abstract	ii
Dedication	iii
Acknowledgements	iv
Publication Drawing Upon this Dissertation	vi
Publications not included in this Dissertation	vi
Table of Contents	vii
List of Tables	x
List of Figures	xi
List of Schemes	xii
List of Abbreviations	xiii

Chapter 1: Introduction

1.1	Introduction	1
1.2	Synthesis of BN Aromatic Vinyl Monomers Vinyl Borazine BN Styrene (BNSt) and Substituted Styrenes BN 2-Vinylnaphthalene (BN2VN)	4
1.3	Radical Polymerization Free Radical Homopolymerization Controlled Radical Polymerization	6
1.4	Copolymerization N-Methyl BN Styrene and 2-Methylstyrene BN2VN and 2-Vinylnaphthalene BN2VN and Styrene	10
1.5	Postpolymerization Modification	14
1.6	Stereoregular Polymers and Coordination-Insertion Polymerization	21
1.7	Outlook	23

Chapter 2: BN Anthracenes

2.1	Introduction	24
2.2	<i>B</i> -Aryl Anthracene Synthesis	26
2.3	Single Crystal X-ray Crystallography	27
2.4	2-Arylanthracene Syntheses and X-Ray Structures	30
2.5	Calculated Structure	32
2.6	Absorbance Spectroscopy	32
2.7	Electrochemistry	34
2.8	Electronic Structure Calculations	36
2.9	Conclusion	38

Chapter 3: Development of BN₂VN and Homopolymerization

3.1	Introduction	39
3.2	Azaborine Monomer Development	40
3.3	Free Radical Polymerization	42
3.4	Conclusion	44

Chapter 4: Copolymers of BN₂VN and 2-Vinylnaphthalene

4.1	Introduction	45
4.2	Determination of Copolymer Composition	46
4.3	Structural Characteristics of Copolymers	48
4.4	Conclusion	50

Chapter 5: Copolymers of BN2VN and Styrene

5.1	Introduction	51
5.2	Theoretical Considerations for Monomer Coreactivity Molecular Geometries NCIS Calculations Bond Dissociation Energies	52
5.3	BN2VN and Styrene Copolymerization	57
5.4	Determination of Copolymer Composition	59
5.5	Conclusion	60

Chapter 6: A BN Aromatic Ring Strategy for Tunable Hydroxy Content in Polystyrene

6.1	Introduction	61
6.2	Oxidative Strategy	61
6.3	Model Oxidation	63
6.4	BN2VN-Styrene Copolymer Oxidation	64
6.5	Conclusion	67

Chapter 7: Reactivity Ratios

7.1	Introduction	68
7.2	Determination by Linearization Methods	71
7.3	Determination by NLLS Method	75
7.4	Insights into Polymer Microstructure	77
7.5	Conclusion	79

Appendix I: Experimental Details	80
---	----

Appendix II: Bibliography	129
----------------------------------	-----

Appendix III: Curriculum Vitae	145
---------------------------------------	-----

List of Tables

Table 1.1	Free radical polymerization of BN aromatic vinyl monomers.
Table 1.2	Selected BN polystyrene photophysical data compared to hydrocarbon polymers.
Table 1.3	Reactivity Ratios for the Copolymerization of BN Aromatic Vinyl Monomers and Styrene.
Table 2.1	Exocyclic torsion angles and bond distances.
Table 2.2	Experimental optical properties for compounds synthesized.
Table 2.3	Electrochemical properties for compounds synthesized.
Table 3.1	PBN2VN molecular weight characteristics.
Table 3.2	Absence of thermal BN2VN auto-polymerization.
Table 4.1	P(BN2VN- <i>co</i> -2VN) molecular weight and optical properties.
Table 5.1	Cyclic bond angles in monomers.
Table 5.2	Bond lengths in monomers.
Table 5.3	Electrostatic and NICS comparison of monomers.
Table 5.4	P(BN2VN- <i>co</i> -S) molecular weight and optical properties.
Table 7.1	Low conversion P(BN2VN- <i>co</i> -S) molecular weight characteristics.
Table 7.2	Reactivity ratios of BN2VN and styrene via linearization.
Table 7.3	Reactivity ratios of vinyl alcohol precursors and styrene.
Table 7.4	Prediction of P(BN2VN- <i>co</i> -S) thermal properties.

List of Figures

- Figure 1.1** Diversity in polystyrene.
- Figure 1.2** Styrene-BN2VN reactivity ratios.
- Figure 2.2** BN Acenes.
- Figure 2.4** BN Anthracene crystal packing.
- Figure 2.7** Absorbance spectroscopy in THF.
- Figure 2.8** Potential dependence on Hammett electronic properties.
- Figure 2.9** Frontier M.O. energy dependence on Hammett electronic properties.
- Figure 3.1** ^1H NMR spectra of 2VN and BN2VN
- Figure 4.1** Absorbance spectroscopy in THF of BN2VN and 2VN.
- Figure 4.2** ^1H NMR spectra of P(BN2VN-*co*-2VN).
- Figure 4.3** ^{11}B NMR spectra of P(BN2VN-*co*-2VN).
- Figure 5.1** Aromatic vinyl borane monomers.
- Figure 5.2** Reactive radical computations.
- Figure 5.3** P(BN2VN-*co*-S) GPC chromatograms.
- Figure 5.4** P(BN2VN-*co*-S) composition calibration.
- Figure 6.1** ^1H NMR analysis of NaOOH-mediated oxidation of a model compound.
- Figure 6.2** Oxy. P(BN2VN-*co*-S) GPC curves
- Figure 6.3** Spectral signatures of P(BN2VN-*co*-S) oxidation.
- Figure 6.4** Oxy. P(BN2VN-*co*-S) differential scanning calorimetry.
- Figure 7.5** BN2VN and styrene copolymerization.
- Figure 7.6** Low conversion P(BN2VN-*co*-S) thermal properties.

List of Schemes

- Scheme 1.1** Synthesis of BN styrenes.
- Scheme 1.2** Gram-scale homopolymerization of BN2VN initiated by AIBN.
- Scheme 1.3** Controlled radical polymerization.
- Scheme 1.4** Borane strategy for polyalcohol synthesis.
- Scheme 1.5** Postfunctionalization of BN2VN copolymers.
- Scheme 1.6** Stereoregular polymers.
- Scheme 2.1** Synthesis for BN anthracene starting material.
- Scheme 2.2** BN Anthracene synthesis.
- Scheme 2.3** Synthesis of 2-arylanthracenes.
- Scheme 3.1** Vinyl borane monomer strategy.
- Scheme 3.2** Poly(BN 2-vinylnaphthalene).
- Scheme 4.1** Free radical copolymerization of BN2VN and 2VN.
- Scheme 5.1** Free radical copolymerization of BN2VN and styrene.
- Scheme 6.1** Borapolyolefin oxidation.
- Scheme 7.1** Reactivity ratios in vinyl comonomers.

List of Abbreviations

∠	angle
°C	degrees Celsius
μL	microliter
μm	micrometer
2MeS	2-methylstyrene
2VN	2-vinylnaphthalene
4-ABSt	4-azaborinylstyrene
Å	angstrom
ABS	acrylonitrile-butadiene-styrene
abu	absorbance (arbitrary) units
ACHN	1,1'-azobis(cyanocyclohexane)
AIBN	azoisobutyronitrile; 2,2'-azobis(2-methylpropionitrile)
aPS	atactic polystyrene
aPVA	atactic poly(vinyl alcohol)
ATRP	atom transfer radical polymerization
BDE	bond dissociation enthalpy
BN2EtN	BN 2-ethylnaphthalene
BN2VN	BN 2-vinylnaphthalene
BNEtB	BN 2-ethylbenzene
BNSt	BN styrene
Bq	ghost atom
br	broad
ca.	circa
CAM	Coulomb-attenuated method
CIP	coordination-insertion polymerization
cm	centimeter
Cp*	pentamethylcyclopentadiene
CPME	cyclopentyl methyl ether
CRP	controlled radical polymerization
CTA	chain transfer agent
d	doublet
\mathcal{D}	dispersity (M_w/M_n)
DDMAT	2-(dodecylthiocarbonothioylthio)-2-methylpropionic acid
DFT	density functional theory

DMF	dimethylformamide
DMSO	dimethyl sulfoxide
DSC	differential scanning calorimetry
EA	elemental analysis
E_g	optical band gap
EI	electron ionization
$E_{p,a}$	peak anodic potential
$E_{p,c}$	peak cathodic potential
ESP	electrostatic potential
EtB	ethylbenzene
eV	electronvolt
EVA	ethylene-vinyl acetate
f_{BN2VN}	fractional composition of BN2VN in the monomer feed
F_{BN2VN}	fractional composition of BN2VN in the copolymer
Fc	ferrocene
FR	Fineman-Ross
g	gram
GIAO	gauge-independent atomic orbital
GPC	gel permeation chromatography
h	hour
Hz	hertz
I	nuclear spin
iPS	isotactic polystyrene
iPVA	isotactic poly(vinyl alcohol)
IR	infrared
J	coupling constant
JCI	joint confidence interval
JHU	Johns Hopkins University
kcal	kilocalorie
kDa	kilodalton
KT	Kelen-Tüdös
LDA	lithium diisopropylamide
M	Molar concentration
m	<i>meso</i>
m	multiplet

mg	milligram
min	minute
mL	milliliter
mm	millimeter
M_n	number average molecular weight
mol	mole
mol%	mole percent
M_w	weight average molecular weight
NaOOH	sodium hydroperoxide
NICS	nucleus independent chemical shift
NLLS	non-linear least squares
nm	nanometer
NMe2VAB	N-methyl 2-vinylazaborine
NMP	nitroxide mediated polymerization
NMR	nuclear magnetic resonance
P(4-ABS)	poly(4-azaborinylstyrene)
P2MeS	poly(2-methylstyrene)
P2VN	poly(2-vinylnaphthalene)
PBN2VN	poly(BN 2-vinylnaphthalene)
PBNMeS	poly(N-methyl 2-vinylazaborine)
PBNS	poly(BN styrene)
PEE	polyethylene
PMMA	poly(methyl methacrylate)
ppm	parts per million
PS	polystyrene
PSS	polystyrene sulfonate
PVA	poly(vinyl alcohol)
PVB	poly(vinyl borazine)
PVBP	poly(vinyl biphenyl)
q	quartet
<i>r</i>	<i>racemo</i>
RAFT	radical addition-fragmentation
RCM	ring closing metathesis
RI	refractive index
s	singlet

sPBN2VN	syndiotactic poly(BN 2-vinylnaphthalene)
sPS	syndiotactic polystyrene
sPVA	syndiotactic poly(vinyl alcohol)
St	styrene
SVA	styrene-vinyl alcohol
t	triplet
TBAF	tetrabutylammonium fluoride
TBS	<i>t</i> -butyldimethylsilyl
T_g	glass transition temperature
THF	tetrahydrofuran
T_m	melting temperature
TMS	trimethylsilyl
UV-vis	ultraviolet-visible
VAc	vinyl acetate
VB	vinyl borazine
VSi	vinyl silanes
wt%	weight percent
ϵ	extinction coefficient
λ_{em}	wavelength of emission
λ_{max}	longest wavelength of absorption
λ_{onset}	wavelength of absorption onset

1.1 Introduction

Polyolefin commodity chemicals have revolutionized the landscape of consumer goods by providing light weight and durable materials for both packaging and manufacturing. In 2015 more than 178 million tons of polyolefin materials were produced.^{1,2} Truly tunable, plastics can be made to possess a plethora of properties by varying monomer identity, degree of polymerization, and polymer architecture. Commercially, there are over 300 grades of polyolefins, each offering unique mechanical properties.³ Beyond this, comonomer composition, polymer stereoregularity, and post polymerization modification have profound ability to further expand the functionality of polymeric materials.

Vinylaromatic monomers, of most fame styrene, offer a dynamic insight into polyolefin polymerization. Conjugated aromatic groups provide the ability to stabilize propagating reactive ethylenic species through inclusion of resonance and aromatic stabilization energies. Styrene is a versatile monomer that is polymerized under free and controlled radical, thermal, anionic, cationic, and transition metal-catalyzed conditions.⁴ Polystyrene's macromolecular properties are exquisitely controlled by synthesis (Figure 1a). Free radical polymerization yields amorphous polystyrene (PS) for packaging applications.⁵ Coordination-insertion polymerization provides crystalline high-melting

stereoregular PS.⁶ Controlled radical polymerization (CRP) yields well-defined block copolymers which self-assemble into nanoscale patterned domains.⁷

PS derivatives with functionalized aryl side chains are important materials in their own right. Cross-linking and Friedel–Crafts sulfonylation provides polystyrene sulfonate (PSS), the major component of the ion exchange resin Dowex.⁸ Functionalization with polar groups is particularly desirable to improve adhesion to polar surfaces.⁹ Boron-functionalized organic polymers are an active research area.^{10,11} Tricoordinate boron-functionalized materials have found wide application in sensing,¹² non-linear optics,¹³ and *n*-type charge transport.¹⁴ Isosteric and isoelectronic BN for CC bond substitution in aromatic compounds is an attractive approach to developing stable organoboranes.^{15,16} BN for CC substitution in polymer backbones, either as poly(aminoborane)s^{17–22} or as conjugated polymers (Figure 1.1b),^{23–25} is well-precedented.

Vinyl monomers with BN aromatic side chains are less explored. Interest in these structures stem from several distinct motivations:

i. Reactivity. Styrene's synthetic versatility arises from the utility of the benzylic reactive intermediates implicated in styrene polymerization. How does a BN aromatic ring influence the reactivity of a benzylic radical, anion, or other reactive intermediate relevant to polymerization?

ii. Photophysics. BN aromatics have unusual photophysical properties compared to benzene, including bathochromically shifted absorption and emission.

iii. Postfunctionalization. Organoboranes are workhorse intermediates in chemical synthesis.^{26,27} The C–B bond of *B*-vinyl polymers introduces opportunities for postpolymerization chemical modification, addressing long-standing challenges in the synthesis of functional polymers containing both polar and nonpolar functional groups.

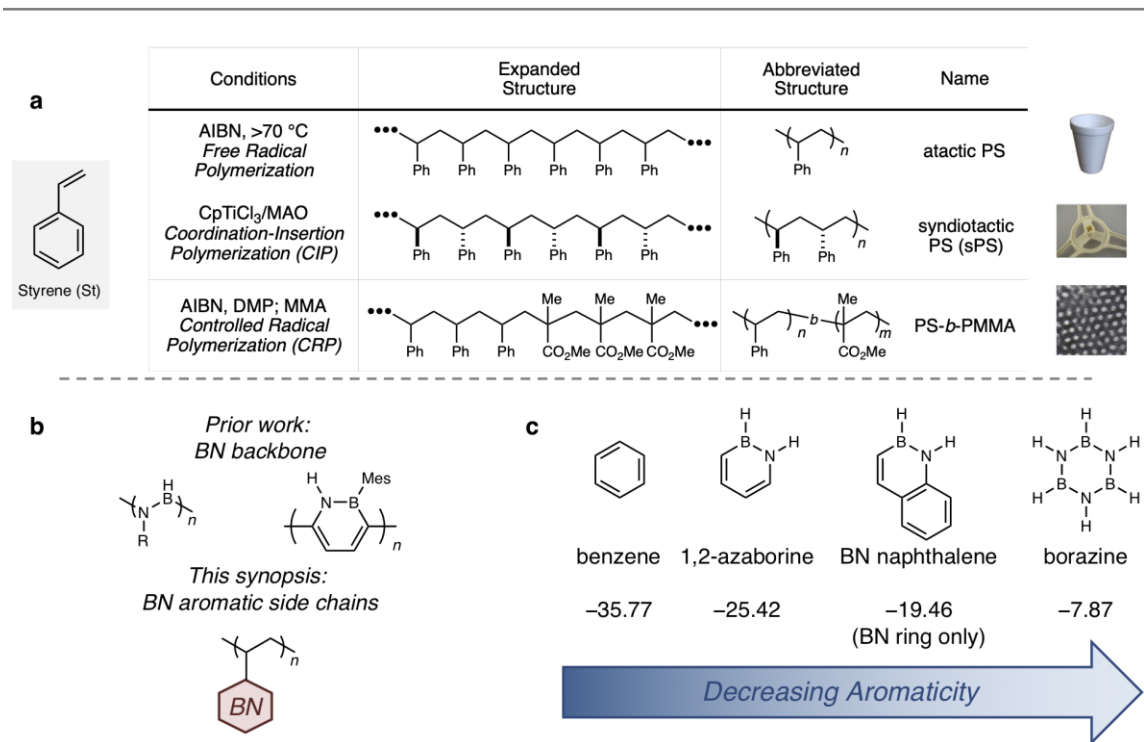
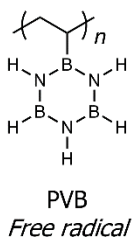


Figure 1.1. Diversity in polystyrene. a) Styrene polymerization & applications of polystyrene architectures. b) Prior work in BN for CC isosterism in polymeric materials. c) BN for CC isosterism and aromaticity. NICS(0)_{nzz} (ppm) values excerpted from Baranac–Stojanović et al.^{28,29}

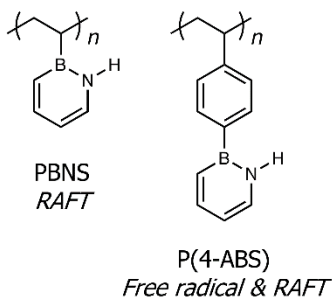
This chapter focuses on “BN polystyrenes”, defined as polymers arising from vinyl monomers with BN aromatic side chains (Chart 1.1). As a systematic nomenclature for BN aromatic rings and polymeric derivatives is still evolving,^{15,16} materials in Chart 1 are named to emphasize similarity to a hydrocarbon polymer (e.g. PS, polystyrene vs. PBNS, poly(BN styrene)). BN aromatic heterocycles incorporated as polyolefin side chains include borazine (Sneddon, 1991),³⁰ 1,2-azaborine and BN biphenyl (Liu and Jäkle, 2016),³¹ *N*-methyl-1,2-azaborine (Sönnichsen and Staubitz, 2017),³² and BN naphthalene (Klausen, 2017).^{33–36} BN aromatic rings, as determined by nucleus independent chemical shift (NICS) calculations, are less aromatic than benzene and aromaticity decreases with increasing BN substitution (Figure 1.1c).^{28,29} Localization of electrons over boron and nitrogen perturb the aromaticity of cyclic and polycyclic aromatic ring systems over

their hydrocarbon counterparts. This electronic consequence has inspired researchers to develop innovative chemistries for the synthesis of a variety of azaborine compounds.

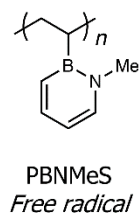
Sneddon 1991



Liu & Jäkle 2016



Staubitz 2017



Klausen 2017 & 2018

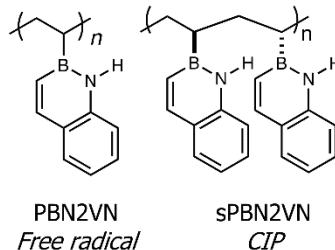


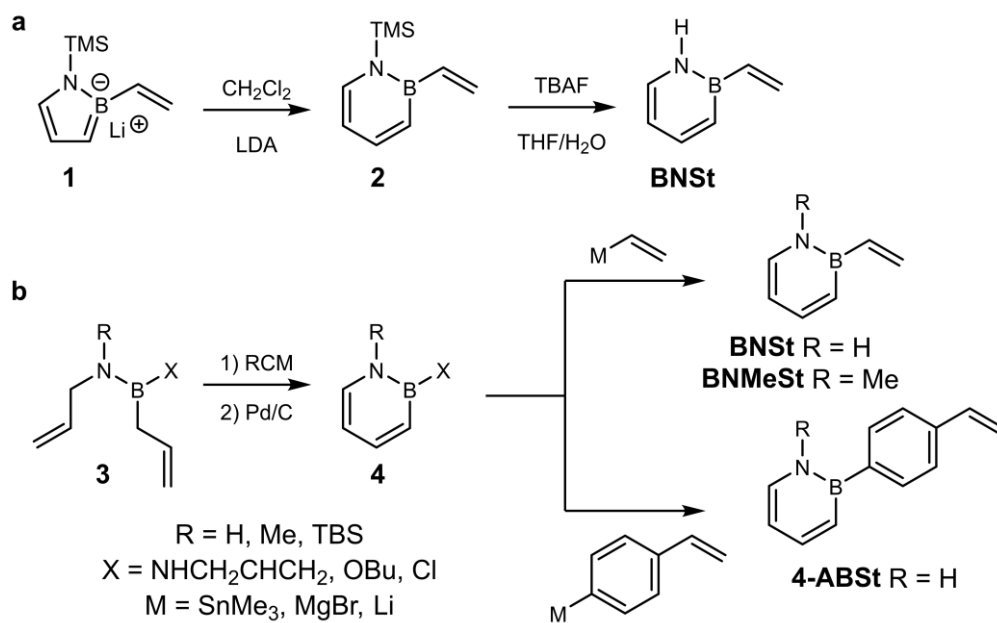
Chart 1.1. Polyolefins with BN aromatic side chains. PVB = poly(vinyl borazine),³⁰ PBNS = BN polystyrene;³¹ P(4-ABS) = poly(4-azaborinylstyrene);³¹ PBNMeS = poly(1-methyl-2-vinyl-1,2-azaborine);³² PBN2VN = poly(BN 2-vinylnaphthalene);^{33,35,36} sPBN2VN = syndiotactic PBN2VN.³⁴ RAFT = radical addition-fragmentation; CIP = coordination-insertion polymerization.

1.2 Synthesis of BN Aromatic Vinyl Monomers.

M. J. Dewar reported the first syntheses of BN aromatic structures such as BN phenanthrene³⁷ and BN naphthalene³⁸ in the 1950's and 1960's. Azaborine, the benzene analog with the general formula C₄H₆BN, has three isomers, which remained elusive for decades after Dewar's initial work.^{15,16} In recent years, modern methods enabled fresh synthetic approaches that simplified access to monocyclic azaborines.³⁹ Despite significant advances, there remains a need for synthetic methods suitable for gram-scale and larger synthetic approaches.⁴⁰

1.2.1. Vinyl Borazine (VB). Sneddon reported the synthesis and polymerization of *B*-vinylborazine (VB) in 1991.³⁰ VB was synthesized by transition metal-catalyzed coupling of borazine ($B_3N_3H_6$) and acetylene.⁴¹ Alkylated variants of VB (e.g. *B*-vinylpentamethylborazine) were synthesized by substitution reactions of *B*-haloborazines with Grignard reagents.⁴²

1.2.2. BN Styrene (BNSt) and Substituted Styrenes. Ashe reported the first synthesis of BNSt in 2009 via ring expansion of 1,2-azaborolide **1**.⁴³ The six-step synthesis proceeded in 6% overall yield (Scheme 1a). The authors reported that the BNSt anion acted as a π -ligand in transition metal complexes, but did not explore vinyl polymerization.



Scheme 1.1. Synthesis of BN styrenes (BNSt). a) Ashe: Ring expansion and deprotection of 1,2-azaborolide **1** provides BNSt.⁴³ b) Liu: Ring-closing metathesis (RCM) and aromatization provides **4**, a versatile intermediate in the synthesis of BN aromatic vinyl monomers.^{32,44} LDA = lithium diisopropylamide; TMS = trimethylsilyl; TBAF = tetrabutylammonium fluoride; TBS = *t*-butyldimethylsilyl.

Building on Ashe's 2000 report on ring-closing metathesis routes to 1,2-azaborines,³⁹ in 2013 Liu described a ring closing metathesis (RCM)/aromatization sequence (Scheme 1b) to 1,2-

azaborines.⁴⁴ Structures of the general type **4** serve as a common intermediate in the preparation of functionalized monocyclic BN aromatics. In 2016, Liu and Jäkle described derivatization of **4** with vinyl and *p*-styryl organometallic reagents to provide BNSt and 4-azaborinylstyrene respectively.³¹ Sönnichsen and Staubitz reported the synthesis of BNMeSt by modification of the RCM/aromatization strategy (four steps, 15% overall yield).³²

1.2.3 BN 2-Vinylnaphthalene (BN2VN). The key step in Dewar's 1959 synthesis of BN naphthalene is the condensation of 2-vinylaniline with trichloroborane, followed by reduction.³⁸ More recently, Molander reported the synthesis of dozens of substituted BN naphthalenes via the one pot condensation of vinylanilines with dichloroorganoboranes generated *in situ* from potassium organotrifluoroborate salts.⁴⁵ Based on this precedent, we targeted bicyclic BN 2-vinylnaphthalene (BN2VN) as a more synthetically accessible monomer compared to monocyclic structures. We developed a two step, multigram scale synthesis of BN2VN (55% overall yield).^{35,36} Synthetic details are described in Chapter 3.

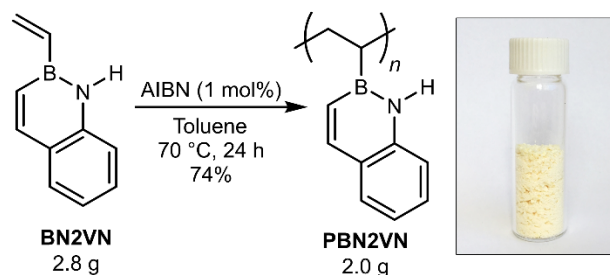
1.3 Radical Polymerization

Free radical polymerization is the most widely explored approach to BN polystyrene synthesis and free radical polymerization of all of the monomers in Section 1.3 has been reported. Table 1.1 summarizes representative results. In addition to free radical polymerization, there is one report each of controlled radical and coordination-insertion polymerization, from Liu & Jäkle and us respectively. The potential for future investigation is significant, including both further development of existing methods, as well as unexplored avenues like anionic polymerization.

1.3.1 Free Radical Homopolymerization. Sneddon reported VB polymerization initiated by azoisobutyronitrile (AIBN), which provided two fractions: a major fraction consisting of soluble, moderate molecular weight ($M_n = 10.7$ kDa) material assigned to a polyolefin with borazine side chains and a smaller fraction (<15-20%) of high molecular weight material arising from crosslinking of the borazine side chains.^{30,46} Alkylated vinylborazines did not polymerize under free radical conditions.^{42,47}

Free radical polymerization of vinyl monomers with 1,2-azaborine-derived substituents proceeds under similar conditions as reported for VB (AIBN, 70-90 °C). No side chain cross-linking was observed. BN2VN, BNMeSt, and 4-ABSt polymerization provided high molecular weight polymers (Table 1), but PBNS was only isolated in low molecular weight ($M_n = 1.6$ kDa). The origin of this divergent reactivity is not yet clear. Free radical polymerization of vinyl boronic esters is known,^{48,49} suggesting that α -boryl radicals are generally suitable for polymerization, an observation further supported by the high reactivity of BN2VN and BNMeSt. A potential explanation is chain transfer to monomer, the phenomenon in which the polymer radical abstracts a weakly bonded atom from the monomer. The formation of a molecular radical at the expense of a polymeric radical results in short chain lengths. However, calculations suggest that azaborine's C-H and N-H bonds are strong, with bond dissociation enthalpies ranging between 105–112 kcal mol⁻¹ (CAM-B3LY/6-311G(d,p)).⁵⁰ Other pathways for early chain termination have neither been explored nor ruled out.

To date, only BN2VN polymerization has been carried out on multigram scale (Scheme 1.2). BNSt polymerization was reported on 10 mg scale and BNMeSt polymerization on ca. 150 mg scale.



Scheme 1.2. Klausen: Gram-scale homopolymerization of BN2VN initiated by AIBN.

All BN polystyrenes showed optical properties distinct from hydrocarbon analogs (Table 2); for example, PBN2VN is pale yellow (Scheme 3, inset), whereas P2VN is white. In general, the

longest wavelength absorption (λ_{\max}) bathochromically shifted and intensified upon BN substitution. The magnitude of the bathochromic shift varied from 16 nm (PS vs. PBNS) to 43 nm (P2VN vs. PBN2VN). The emission spectra of BN polystyrenes also differed from hydrocarbon polymers, with larger Stokes shifts seen in BN polystyrenes than in hydrocarbon polymers. Similar trends are observed in molecular systems, including the monomers themselves.⁵¹

Table 1.1. Free radical polymerization of BN aromatic vinyl monomers. AIBN = 2,2'-azobis(2-methylpropionitrile); ACHN = 1,1'-azobis(cyanocyclohexane).

Entry	Monomer (solvent)	Radical Initiator	Temperature	Time	Yield	M_n (kDa)	\bar{D}	Ref.
1	VB (C ₆ H ₆)	AIBN (1 mol%)	80 °C	20 h	25%	10.7	1.68	30
2	BNSt (C ₆ D ₆)	ACHN (1 mol%)	90 °C	72 h	50% ^a	1.6	1.33	31
3	BNMeSt (neat)	AIBN (1 mol%)	85 °C	72 h	51%	16.5	1.51	32
4	BN2VN (neat)	AIBN (1 mol%)	70 °C	24 h	75%	20.5	3.87	36
5	4-ABSt (THF)	AIBN (2.5 mol%)	70 °C	20 h	>99% ^a	38.5	3.91	31

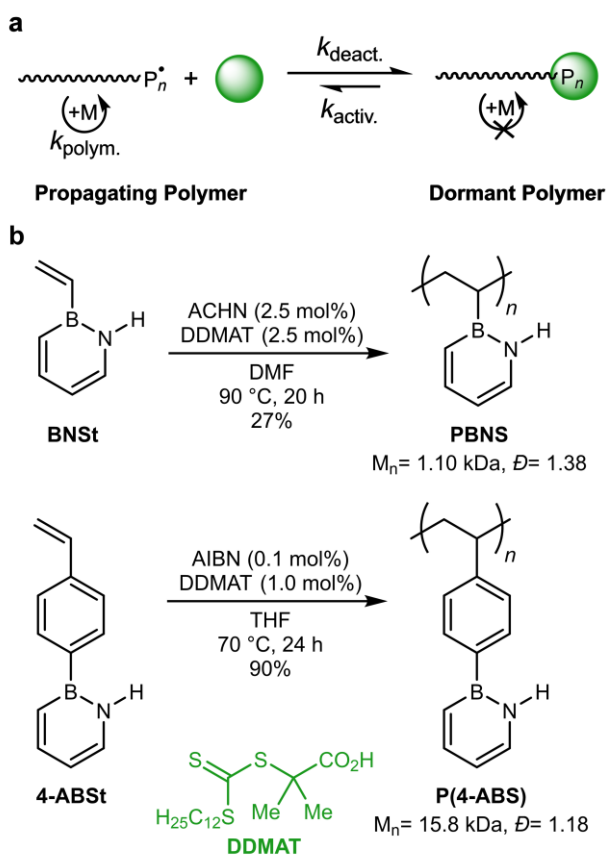
^a % Conversion.

Table 1.2. Selected BN polystyrene photophysical data compared to hydrocarbon polymers.

Entry	BN Aromatic Side Chains			Ref.	Hydrocarbon Aromatic Side Chains			
	Polymer	λ_{\max}^a	λ_{em}^b		Polymer	λ_{\max}^a	λ_{em}^b	Ref.
1	PBNS	277	344	31	PS	261	278	52
2	P(4-ABS)	299	369	31	PVBP	n.d.	313	53
3	PBNMeS	279	n.d.	32	P2MeS	265	n.d.	32
4	PBN2VN	320	398	35	P2VN	277	335, 401	35

^a Longest wavelength absorption in nanometers. ^b Wavelength emitted after excitation at λ_{\max} in nanometers. PVBP = poly(vinyl biphenyl); P2MeS = poly(2-methylstyrene); P2VN = poly(2-vinylnaphthalene).

1.3.2 Controlled Radical Polymerization. Controlled radical polymerization (CRP) introduces a dynamic equilibrium between propagating and dormant polymer chains (Scheme 1.3a).⁵⁴ The low concentration of propagating polymer chain ends suppresses chain recombination and other termination events that contribute to a broad distribution of chain lengths (dispersity, \mathcal{D}) in free radical polymerization. CRP is desirable for advanced applications requiring control of molecular weight, dispersity, and end group structure. Notable examples include atom transfer radical



Scheme 1.3 a) Controlled radical polymerization by reversible deactivation. Green sphere represents a generic deactivating agent. b) Liu & Jäkle: RAFT polymerization of BNSt and BN-VBP.³¹ DDMAT = 2-(dodecylthiocarbonothioylthio)-2-methylpropionic acid; DMF = dimethylformamide; ACHN = 1,1'-azobis(cyanocyclohexane).

polymerization (ATRP), nitroxide mediated polymerization (NMP), and reversible addition-fragmentation chain transfer (RAFT) polymerization. RAFT polymerization is convenient, as typically a chain transfer agent (CTA) is simply added to free radical polymerizations.⁵⁵ Different CTA structures are optimal for styrenes, acrylates, and other monomers.

Liu and Jäkle reported RAFT polymerization of both BNSt and 4-ABSt using the chain transfer agent 2-(dodecylthiocarbonothioylthio)-2-methylpropionic acid (DDMAT) (Scheme 1.3b), a CTA optimized for styrene polymerization. Only P(4-ABS) demonstrated one of the signatures of CRP, chain extension upon introduction of additional monomer. Chain extension indicates end group fidelity, that the chain cap can still be reversibly cleaved to allow further polymerization.

The outlook for BN aromatic vinyl monomer CRP is very promising. Future efforts will undoubtedly continue to explore methods in addition to RAFT, as well as the preparation of block copolymers containing BN aromatic side chains.

1.4 Copolymerization

Copolymerization of two or more monomers is an essential strategy for tuning the physical properties of a polymer. The binary copolymerization behavior of two monomers M_1 and M_2 is described by their reactivity ratios r_1 and r_2 , where r_1 is the ratio of the rate constants for M_1 - M_1 homopolymerization divided by M_1 - M_2 crosspolymerization and r_2 describes the ratio of the rate constants for M_2 - M_2 homopolymerization divided by M_2 - M_1 crosspolymerization. Alternating copolymers arise when $r_1 = r_2 = r_1 \cdot r_2 = 0$, indicating a preference for cross-polymerization. This behavior is seen for structurally dissimilar monomers, such as the radical copolymerization of electron-rich styrene with electron-poor maleic anhydride. Statistical copolymerizations arise when r_1 and r_2 are both close to 1 and is typically only observed with structurally similar monomers.

Examination of the copolymerization of styrene with fluorinated analogs of styrene shine light on the consequences of aromaticity to polymerization. Although structurally similar, it has been shown that styrene and 2,3,4,5,6-pentafluorostyrene (PFS) copolymerize in an alternating fashion,

in contrast to the statistical copolymerization of styrene with *p*-fluorostyrene.⁵⁶ Benzene ($T_m = 5.4$ °C) and hexafluorobenzene ($T_m = 5.0$ °C) form a tightly associated 1:1 charge transfer (Lewis acid–Lewis base) complex with an elevated melting temperature, $T_m = 23.7$ °C.⁵⁷ Quadrupole–quadrupole interactions of benzene and hexafluorobenzene resulting from the dual quadrupole moments (an effect of differing electronegativities within C–F and C–H bonds) describe the mode of complex formation.⁵⁸

Reactivity ratios, especially the product of reactivity ratios ($r_1 \cdot r_2$),^{59,60} are generally independent from concentration, solvent, and temperature effects of the copolymerization reaction.⁶¹ Exception to this rule occurs when comonomer–comonomer complexation occurs, the extent of which is dynamically dependent on solution temperature and/or concentration. Calculation of reactivity ratios for styrene and PFS at several copolymerization temperatures show that with decreasing temperature $r_1 \cdot r_2$ approaches naught ($r_1 \cdot r_2 = 0.17$ at 70 °C; 0.048 at 25 °C).⁵⁶ Deviations in the reactivity ratios show that charge transfer complex formation between styrene and PFS may have some influence on the alternating nature of the comonomers, but the copolymerizations is still highly alternating at elevated temperatures.

It is more likely that the alternating nature is mainly a consequence of frontier molecular orbital overlap of electron poor PFS and electron rich styrene. ¹³C NMR shifts are sensitive to resonant and mesomeric effects of groups bound to the ethylenic double bond. It has been shown that the ¹³C NMR shifts of styrenic β -carbons are predictive of reactivity towards radical polymerization and follow a linear free energy relationship with both Alfrey–Price Q–e values and Hammett's σ constants.⁶² Charge transfer complex formation does however lead to marked increases in the glass transition temperature of alternating copolymers vs. the predicted mole-averaged glass transition temperatures calculated from homopolymers.^{56,63}

Copolymerization of BN aromatic vinyl monomers with styrene and its derivatives therefore presents an opportunity to qualitatively and quantitatively assess the styrene-like reactivity of the organoborane monomer. Copolymerizations with 2-methylstyrene (2MeSt), 2-vinylnaphthalene

(2VN), and styrene have been reported. These studies uniformly suggest that BN aromatic vinyl monomers have comparable, but somewhat lower, reactivity compared to the analogous hydrocarbons.

1.4.1 BNMeSt and 2-Methylstyrene. Sönnichsen and Staubitz contrasted the homopolymerizations of BNMeSt and 2MeSt and also reported the free radical copolymerization of 2MeSt and PBNMeS.³² 2MeSt polymerization proceeded to higher conversion and provided higher molecular weight polymer than observed for free radical polymerization of BNMeSt under similar reaction conditions (P2MeS, $M_n = 46.7$ kDa; PBNMeS, $M_n = 16.5$ kDa). A binary free radical copolymerization (1:1 molar ratio of monomers) provided the atactic statistical copolymer P(2MeS-*co*-BNMeS) ($M_n = 21.8$ kDa) which was determined to be enriched in 2MeSt by NMR spectroscopy. The authors concluded that the relative rates of 2MeSt and BNMeSt homo- and cross-polymerization are of comparable magnitude, but 2MeSt is more reactive. Reactivity ratios were not reported.

The physical properties of the copolymer are intermediate between the parent homopolymers. P2MeS is an indefinitely stable white solid, while PBNMeS decomposes in air from a white to a brown solid within 72 hours. P(2MeS-*co*-BNMeS) discolors more slowly than PBNMeS. A single copolymer glass transition temperature (T_g), the temperature at which the material transforms from a glassy to rubbery state, was observed at 114 °C. This single T_g , intermediate between the homopolymers (P2MeS, $T_g = 132$ °C; PBNMeS, $T_g = 85$ °C), supported microstructural assignment to a statistical copolymer.

1.4.2 BN2VN and 2-Vinylnaphthalene. In 2017, we described the free radical copolymerization of BN2VN and 2VN.³⁵ Gel permeation chromatography (GPC) revealed a unimodal distribution of copolymer molecular weights. A bimodal molecular weight distribution would have suggested formation of two homopolymers instead of a single copolymer. A suite of NMR spectroscopies (^1H , ^{11}B , ^{13}C) aided copolymer characterization. A UV-vis spectroscopic assay based on the different absorption intensities at 320 nm of the BN naphthalene and naphthalene side

chains was developed to quantify BN2VN incorporation. Based on this optical assay, a close agreement between monomer feed ratio and copolymer composition was determined. P(BN2VN-*co*-2VN) was prepared with between 9.2-74 wt% BN2VN. Copolymer molecular weights (M_n) ranged between 6.0-8.4 kDa, with the highest molecular weight copolymers obtained from copolymers enriched in 2VN. Our results again suggested that the vinyl borane has comparable, but lower, reactivity than the hydrocarbon analog. Further details of P(BN2VN-*co*-2VN) copolymers are described in Chapter 4.

1.4.3 BN2VN and Styrene. In early 2018, we reported free radical copolymerization of styrene and BN2VN. An optical assay based on the selective absorption at 320 nm of the BN naphthalene side chain confirmed BN2VN incorporation into the copolymer at levels commensurate with the feed ratio.³⁶ Reactivity ratios for BN2VN and styrene were determined from low conversion free radical copolymerizations using both traditional linearization methods and modern nonlinear least squares statistical analysis (Table 1.3 and Figure 1.2).⁵⁰ The reactivity ratios ($r_1(\text{BN2VN}) = 0.423$ and $r_2(\text{St}) = 2.30$) indicated a statistical copolymerization. Styrene is more reactive than BN2VN and at low conversion styrene-enriched copolymers were obtained. These insights enabled control over copolymer properties, such as the T_g . The T_g 's of copolymers with between 6.0-84 wt% BN2VN varied systematically with BN2VN content. Good agreement between calculated and experimental T_g was observed. Further details of P(BN2VN-*co*-S) copolymers are described in Chapter 5 and the determination of reactivity ratios are described in Chapter 7.

Sneddon reported the radical copolymerization of VB and styrene in 1991.³⁰ The reactivity ratios ($r_1(\text{VB}) = 0.078$ and $r_2(\text{St}) = 4.02$) indicated a greater reactivity mismatch between styrene and VB than between styrene and BN2VN. We attribute this reactivity difference to the increased aromaticity of BN naphthalene compared to borazine.^{28,29,50} BN2VN polymers show exciting potential as a solution to the challenge of preparing hydroxy-functionalized polyolefins via postpolymerization modification. In the following section, we summarize oxidative postfunctionalization of PBN2VN-*stat*-PS yielding statistical styrene-vinyl alcohol copolymers.

Table 1.3. Reactivity Ratios for the Copolymerization of BN Aromatic Vinyl Monomers and Styrene.

M₁	r₁	M₂	r₂	Ref.
VB	0.078	Styrene	4.02	30
BN2VN	0.423	Styrene	2.30	36

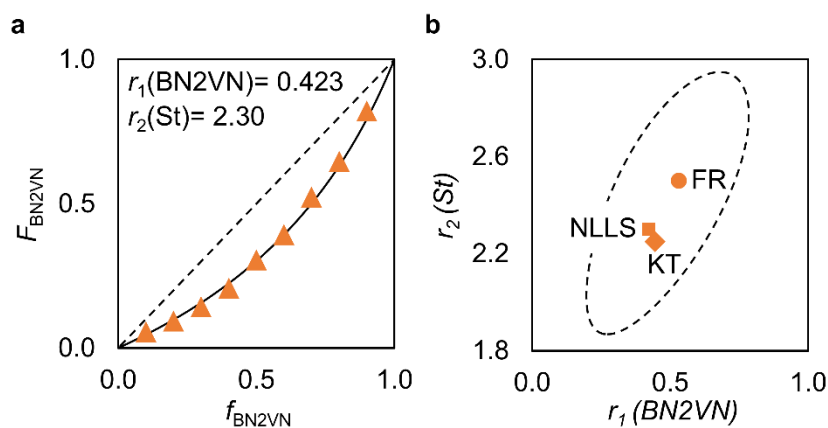


Figure 1.2. Klausen: Styrene-BN2VN reactivity ratios. a) Mayo-Lewis plot for the statistical copolymerization of BN2VN and styrene with AIBN.³³ Dashed line represents a random copolymerization ($r_1 = r_2 = 1$); solid curve is a fit to the experimental data and indicates a statistical copolymerization where $r_1 = 0.423$ and $r_2 = 2.30$. F_{BN2VN} = fractional composition of BN2VN in the copolymer; f_{BN2VN} = fractional composition of BN2VN in the monomer feed. b) Reactivity ratios of statistical copolymerization of BN2VN and styrene with AIBN by Fineman-Ross (FR), Kelen-Tüdös (KT) and non-linear least squares (NLLS) analysis. Dashed ellipsoid represents the 95% confidence interval of NLLS analysis.³³

1.5 Postpolymerization Modification

Postpolymerization modification is another means to alter the physical and chemical properties of polymers. Chemistries performed on polymers differ from that of small molecules due to innate dispersities and non-uniform structures. For example, extent of comonomer incorporation can be determined from bulk polymer, however differences in incorporation cannot be readily

determined macromolecule to macromolecule. Postpolymerization chemistries are used to transform one polymer to another commercial polymer, create highly specialized technical polymers, as well as also being relevant to the degradation and recycling of waste polymers.

Hydrophilic poly(vinyl alcohol) (PVA) is transformed from the hydrophobic homopolymer poly(vinyl acetate) (PVAc) by hydrolysis. Differing degrees of hydrolysis, due to non-quantitative yields, impart a range of materials properties and are separated into two grades, fully (PVA) and partially (PVAc/PVA) hydrolyzed. Commercial PVA is produced by the base-catalyzed alcoholysis of PVAc in ethanol or methanol. PVA may also be produced by the saponification of PVAc with sodium hydroxide in water.

Mechanistic studies have shown that the hydrolysis of PVAc is autocatalytic with increased rates upon reaction progress.⁶⁴ The presence of an adjacent hydroxy group enhances the reactivity of an acetate group towards alcoholysis or saponification.⁶⁵ Increasing the hydrophilicity of PVAc/PVA polymer increases susceptibility towards hydrolysis. This is a non-trivial consequence of the self-aggregation of amphiphilic macromolecules in aqueous solutions, diffusion of reagents into aggregates limiting reactivity. The solution phase conformations of PVAc/PVA polymers are dependent on degrees of polymerization, hydrolysis, and blockiness of the polymer.⁶⁶

Partially hydrolyzed PVAc/PVA have been developed as water soluble packaging for detergents, such as the Tide POD®.⁶⁷ PVAc/PVA is accessed from various routes, either incomplete hydrolysis (alcoholysis or saponification) of PVAc as described above, or by the reacetylation of completely hydrolyzed PVA. Reacetylation to PVAc/PVA is performed by heating PVA with acetic acid and water; reduction in water content leads to high degrees of acetylation.⁶⁵ The polymer architecture of PVAc/PVA is dependent on the preparative method used. Reacetylation of PVA produces a completely random PVAc/PVA, saponification of PVAc creates PVAc/PVA with a blocky sequence distribution, and alcoholysis of PVAc produces PVAc/PVA with an architecture intermediate between random and blocky.^{65,68}

Extent of random vs. blocky sequence distribution can be determined spectroscopically. Infrared spectroscopy offers a convenient and straight-forward analysis of PVAc/PVA architecture.^{65,69,70} PVAc has a C=O carbonyl stretch at $\sim 1734\text{ cm}^{-1}$, which remains unchanged in blocky PVAc/PVA with low degrees of hydrolysis. Upon transition to a more random sequence distribution, the C=O stretch shifts to lower frequency, $\sim 1715\text{ cm}^{-1}$, due to increased hydrogen binding with adjacent hydroxy groups.^{65,69,70} Conversely, PVA has an O–H alcohol stretch at $\sim 3290\text{ cm}^{-1}$, which remains unchanged in random PVAc/PVA with high degrees of reacylation. Upon transition to a more blocky sequence distribution, the O–H stretch shifts to higher frequency, $\sim 3470\text{ cm}^{-1}$.⁶⁹

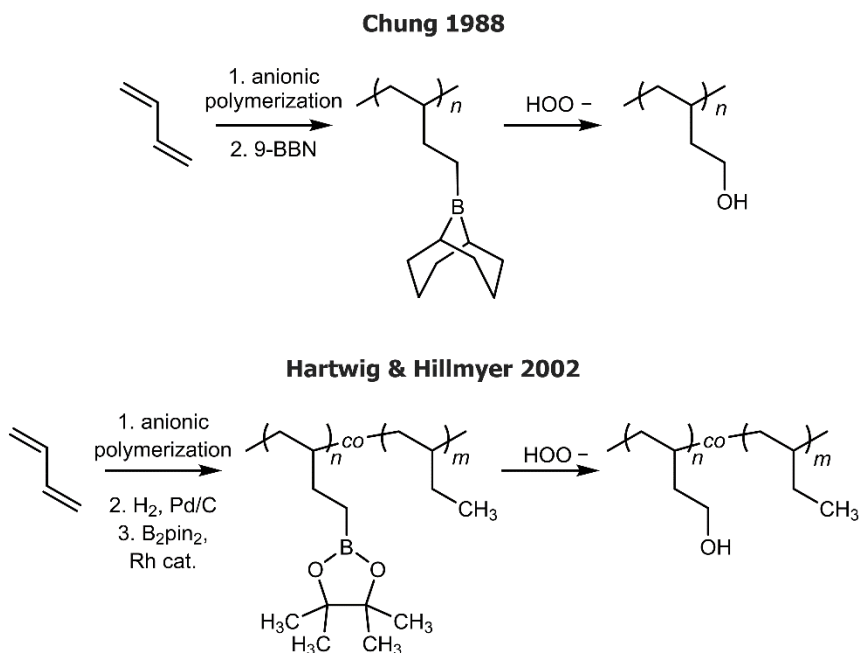
PVA and PVAc can be differentiated by colorimetric assay upon complexation with iodine, developing a blue or red-violet color, respectively.⁷¹ In the presence of boric acid and iodine, PVA forms a blue-green colored complex.^{72,73} PVA and iodine have also been used to quantify borate concentrations.⁷⁴ Unfortunately, complexation with iodine only qualitatively detects PVA or PVAc content in sufficiently blocky polymers with sufficiently long sequences.^{68,71} Spectroscopic polymer architecture determination is most powerful when combined with thermal analysis of PVAc/PVA polymers.^{68,70}

Organoboranes are versatile intermediates in synthetic chemistry, serving as precursors to alcohols, amines, and other functional groups.^{26,27} This versatility highlights the potential for boron-functionalized polymers to serve as a platform to functional materials, but the challenge of introducing boron into the polymer limits the scope of relevant polymer architectures. Chung et al. functionalized alkenyl side chains in high-vinyl polybutadiene via hydroboration-oxidation,⁷⁵ while Hartwig and Hillmyer demonstrated catalytic C–H activation of poly(ethylene) (PEE)⁷⁶ yielding partially hydroxylated polymers (Scheme 1.4). Hillmyer et al. also reported C–H functionalization of the commodity polymers linear low-density polyethylene (LLDPE) and polypropylene.^{77,78}

Challenges in the vinyl polymerization of trialkylboranes include deactivation of the double bond and the oxidative and hydrolytic instability of trialkylboranes. Chung reported Ziegler–Natta

polymerization of the monohydroboration products derived from long chain dienes, which were converted to polyalcohols by hydroperoxide oxidation.⁷⁹ A four-carbon or longer spacer was needed between the double bond and boron to avoid suppressing reactivity. Vinyl boronic ester polymerization has been reported, but polymer sensitivity in air to hydrolysis and cross-linking limited characterization.^{48,49}

Hydroperoxide oxidation occurs with the reactive perhydroxyl anion, HO_2^- , formed by the deprotonation of hydrogen peroxide ($\text{pK}_a = 11.6$) upon mixing with a strong base, such as sodium hydroxide. Controlled oxidation is facilitated by high temperatures ($\geq 50^\circ\text{C}$) and exclusion of transition metals (Fe, Mn, Cu).⁸⁰ Fenton reagent is hydrogen peroxide with catalytic ferrous iron and is a powerful non-selective oxidant by formation of various radical reactive oxygen species (ROSs). Cuprous and cupric copper have also been shown to transform H_2O_2 into various radical ROSs via Fenton-like chemistry.⁸¹

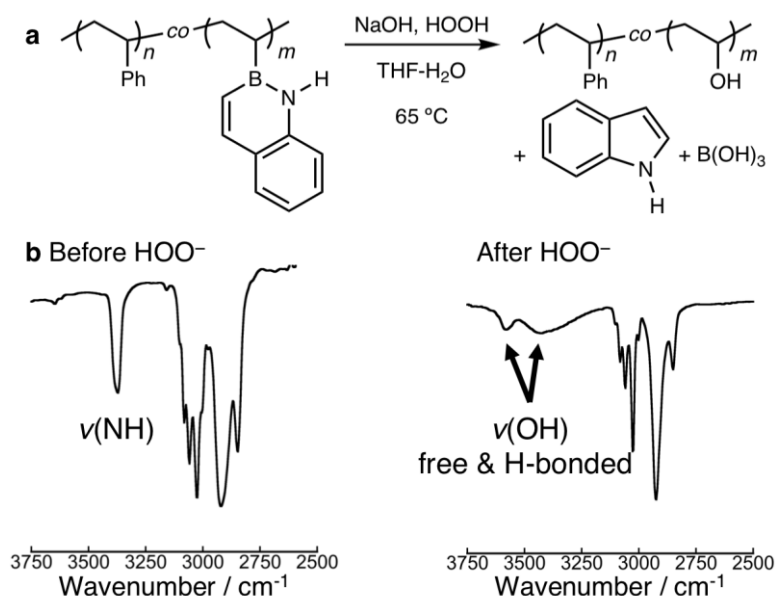


Scheme 1.4. Borane strategy for polyalcohol synthesis.

Nonetheless, the significant commercial interest in the incorporation of a controlled amount of a polar functional group into a nonpolar polymer continues to motivate academic and industrial research into general strategies for polymer functionalization. Polar functional groups play an essential role in modifying a plastic's strength, toughness, melting point, and solvent compatibility.^{82,83} Examples of commercial polar-nonpolar copolymers include acrylonitrile-butadiene-styrene (ABS) and ethylene-vinyl acetate (EVA).^{5,84} Challenges in the direct copolymerization of polar and nonpolar monomers are many, but include the incompatibility of a Lewis basic functional group with the polymerization catalyst and significant mismatch in reactivity ratios.⁸⁵⁻⁸⁷

Styrene (St) and vinyl acetate (VAc) are an example of a comonomer pair with fundamentally incompatible reactivity: St is far more reactive than VAc and no VAc is incorporated in a binary copolymerization ($r_1(\text{St}) = 55$ and $r_2(\text{VAc}) = 0.01$).^{88,89} The reactivity mismatch between VAc and conjugated monomers limits VAc's utility as a precursor to hydroxy-functionalized copolymers, even though poly(vinyl acetate) is a commodity polymer and precursor to poly(vinyl alcohol) (PVA) via side chain saponification.⁹⁰ PVA is a semicrystalline water-soluble polymer, with applications as a coating or adhesive.

The efficient statistical copolymerization of styrene and BN2VN suggested a solution to this challenge via oxidative conversion of the C–B bond into a C–O bond. We showed that alkaline hydrogen peroxide effected the conversion of PBN2VN-*co*-PS to PVA-*co*-PS (Scheme 1.5a). Several different copolymers with variable BN2VN content (13-58 wt%) and molecular weight ($M_n = 12.8$ -39.6 kDa) were investigated. In all cases, complete consumption of the organoborane side chain was observed, as monitored by loss of the unique spectroscopic signatures of the BN naphthalene chromophore. Overoxidation of the BN naphthalene side chain was identified, resulting in formation of indole and boric acid as by-products. A methanol azeotrope removed residual boric acid as trimethyl borate. Infrared spectroscopy provided evidence of the characteristic hydroxyl group stretching frequency above 3000 cm^{-1} (Scheme 1.5b).



Scheme 1.5. Klausen: Postfunctionalization of BN2VN copolymers. a) Typical reaction conditions for oxidation of PBN2VN-*co*-PS to PVA-*co*-PS. b) Cropped IR spectra highlighting the disappearance of BN2VN $\nu(\text{NH})$ feature and appearance of PVA $\nu(\text{OH})$ features after oxidation. Sample shown is P(BN2VN₃₂-*co*-S₉₂). IR spectra reprinted with permission from reference ³⁶. Copyright 2018 Wiley.

The durability and persistence of plastics in the environment has motivated widespread study in the fate of polymeric pollutants and their cradle to grave chemistries, implicit to environmental degradation and polymer recyclability. Biodegradation is the biotic degradation of organic material by fungi, bacteria, and archaea. Degradation leads to the formation of structural inhomogeneities. Metabolism of biodegradable polymers provides a source of energy and carbon for microorganisms. Carbon within the polymer is converted to biomass and ultimately mineralized. Aerobic degradation of organic polymers results in the formation of carbon dioxide and water, whereas the anaerobic degradation of organic polymers results in the formation of methane, a greenhouse gas, and water.

PVA has been known to biodegrade since the early 1930's.⁹¹ A historic use of PVA has been as a paper coating, improving paper strength and resistance to oils and greases.⁹² Specialized PVA

degrading microbiota have been isolated from the sewage sludge of a paper mill wastewater treatment plant.⁹³ Oxidase-type extracellular and intercellular enzymatic systems are responsible for degradation by random scission of the polymer chain followed by terminal, unzipping depolymerization of oligomeric PVA. Degradation of PVA is dependent on the degree of hydrolysis, the most hydrophilic polymers (>72% hydrolyzed) show a marked increase in the rate of degradation.

Microbial degradation is facilitated by microbial adhesion to the surface of plastics, however the hydrophobicity of many polymers inhibit biofilm formation and adhesion. Experimentally, addition of a surfactant (Tween) enhances growth conditions, encouraging biodegradation.⁹⁴ Statistical incorporation of polar comonomers into hydrophobic polymers improve hydrophilicity of the material. This change in surface adhesion properties encourages the biodegradation of inert plastic refuse, especially if the polar segments are susceptible to biodegradation and oxidative backbone scission, as seen for PVA. Although polystyrene has recently been found to be susceptible to biodegradation, hydrophobicity and high molecular weights inhibit utilization of this substrate as a carbon source.⁹⁵ Statistical styrene-vinyl alcohol (SVA) copolymers have the propensity to retain favorable materials properties of polystyrene, while improving the biodegradability of the polymer by statistical backbone scission.

BN2VN enabled the first synthesis of statistical SVA copolymers. SVA copolymers showed tunable variation in physical properties with hydroxy content. Solubility in polar, protic solvents like methanol increased with increasing hydroxy concentration. Differential scanning calorimetry (DSC) also showed systematic variation in the T_g . While PBN2VN-*c*-PS had a T_g intermediate between PS and PBN2VN, after oxidation, the T_g was intermediate between PS and PVA. Further details on the oxidation of P(BN2VN-*c*-S) copolymers to SVA copolymers are described in Chapter 6.

The styrene-like reactivity and versatility of BN2VN suggests a general platform for postfunctionalization chemistry. In the following section, we highlight a different application of postfunctionalization of BN aromatic side chains.

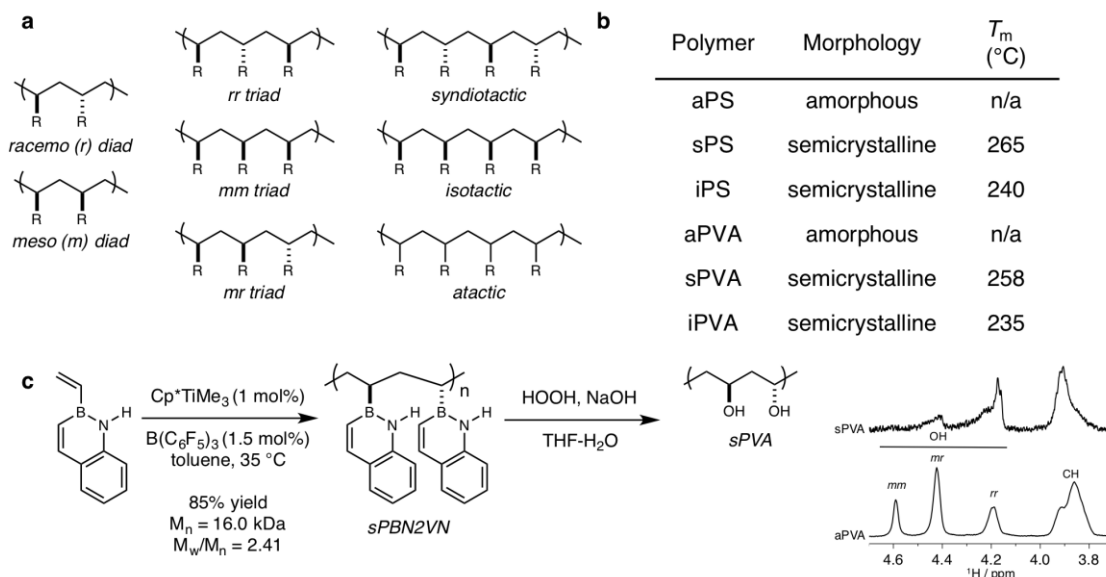
1.6 Stereoregular Polymers and Coordination-Insertion Polymerization

Transition metal complexes catalyze coordination-insertion polymerization of ethylene, propylene and other vinyl monomers, yielding high molecular weight commercial polymers. Rational ligand design in well-defined homogeneous catalysts has yielded highly stereoregular polymers.⁹⁶

Polymer physical properties, including morphology and melting temperature, depend on the stereochemical relationships between adjacent repeat units in a polymer chain (Scheme 1.6). There are three types of tactic, or stereoregular, polymers: atactic, syndiotactic, and isotactic. If the stereochemical configuration of two adjacent repeating units is the same, it is a *meso* (*m*) diad, while in a *racemo* (*r*) diad the configurations are different in the two repeating units. Two adjacent *racemo* diads make a *rr* triad, two adjacent *meso* diads make a *mm* diad, and adjacent *meso* and *racemo* diads make a *mr* triad. A perfectly syndiotactic macromolecular chain consists of exclusively *rr* triads, a perfectly isotactic chain consists exclusively of *mm* triads, and an atactic chain consists of a statistical distribution of *rr*, *mm*, and *mr* triads.

The synthesis of highly stereoregular polar polyolefins is limited by the challenge of identifying coordination polymerization catalysts compatible with polar functional groups.^{83,85} Open coordination sites on the metal interact with carbonyl, amine, and other functional groups, resulting in catalyst and/or polymer decomposition. Nonetheless, stereoregular polar polyolefins have interesting properties and applications. For example, PVA hydrogels have potential therapeutic applications and high molecular weight PVA fibrils exhibit high tensile strength.⁹⁷⁻⁹⁹ Tacticity has a profound effect on both these applications as relative stereochemistry influences the extent of intra- and intermolecular hydrogen bonding between hydroxy groups.^{100,101} Synthetic routes to sPVA include cationic polymerization of vinyl ethers with bulky protecting groups¹⁰²⁻¹⁰⁴ or radical polymerization of vinyl pivalate,^{105,106} followed by protecting group cleavage. Syndiotacticities are typically modest and cationic polymerizations yield low molecular weight materials. The limited substrate scope of cationic polymerization and the poor reactivity of vinyl ester-derived radicals

also impose a limitation on the ability to tune PVA's properties through copolymerization with nonpolar monomers.



Scheme 1.6. Stereoregular polymers. a) Stereoregular polymer nomenclature. b) Variation in physical properties with tacticity. c) Klausen: Synthesis of syndiotactic PBN2VN (sPBN2VN) by coordination-insertion polymerization and postpolymerization oxidation to syndiotactic poly(vinyl alcohol) (sPVA). Inset is cropped ^1H NMR spectra (400 MHz, $\text{DMSO-}d_6$) of sPVA and aPVA highlighting the diagnostic hydroxy triads. Spectrum reprinted with permission from reference ³⁴.

Dr. Shehani Mendis of our group demonstrated that syndioselective coordination-insertion polymerization of BN2VN followed by stereoretentive oxidation provided sPVA by an orthogonal mechanism.³⁴ This exciting result is the first example of BN styrene polymerization with a method other than radical polymerization.

Homogeneous monocyclopentadienyl complexes^{107,108} known to catalyze ethylene and syndioselective styrene polymerization upon Lewis acid activation were also effective BN2VN polymerization catalysts. BN2VN's aromaticity, and the dative interaction between neighboring elements, reduced the Lewis acidity and basicity of boron and nitrogen respectively, resulting in compatibility with the oxophilic Ti catalyst. Additionally, BN2VN's aromaticity suggested

its ability to intercept the mechanism of styrene syndioselective polymerization.¹⁰⁹ Indeed, we found that Cp*TiMe₃ and B(C₆F₅)₃ provided syndiotactic PBN2VN (sPBN2VN) in high yield (Scheme 1.6c). ¹H and ¹³C NMR studies, as well as thermal properties, suggested a highly stereoregular structure. Sodium hydroperoxide oxidation of sPBN2VN yielded sPVA, as confirmed by ¹H NMR (Scheme 1.6c, inset) and IR spectroscopy.

1.7 Outlook

The studies highlighted herein showcase the exciting potential for BN polystyrenes to impact both fundamental and applied polymer science. BN aromatic vinyl monomers exhibit styrene-like reactivity and versatility in several contexts, including facile radical copolymerization with aromatic hydrocarbons and the ability to intercept reaction mechanisms dependent on styrene's aromaticity. The unusual photophysical properties of BN polystyrenes not only point to potential sensing applications, but also facilitate quantitative copolymer characterization. New directions for BN polystyrenes as intermediates in the preparation of long-sought functional copolymers and stereoregular polymers were emphasized. Future work will undoubtedly continue to expand the synthetic potential of these materials, including the preparation of other BN aromatic isomers (e.g. 1,3- or 1,4-azaborines) and the further development of modern polymerization chemistries.

2.1 Introduction

We report the synthesis and characterization of new extended azaborine derivatives and the remarkable structural, optical and electronic similarity of these heterocycles to anthracene.

The unusual stability of some cyclic conjugated organic structures, or aromaticity, is a foundational concept in organic chemistry.¹¹⁰ Main group organometallic compounds containing Hückel's rule number of n electrons were first synthesized by Dewar in 1958.¹¹¹ In recent years,¹¹² new synthetic approaches courtesy of Liu,¹¹³ Ashe,¹¹⁴ and Molander^{115,116} have energized research in the area of BN-heterocycles and both fundamental and applied research have expanded in scope. Most recently Liu described the synthesis of BN tetracene.¹¹⁷

The continued development of these materials depends on predictive structure-function relationships as theoretical accounts have suggested that not all CC to BN bond substitutions are equal.¹¹⁸ In an effort to systematically characterize structure-dependent properties, we target a series of extended azaborine derivatives (BN anthracenes) with aryl

rings exocyclic to the BN heterocycle (**Figure 2.1**). We show that the *B*-aryl anthracenes in which the 1,2-positions are substituted with the BN bond have optical and electronic properties consistent with delocalization. The observed trends closely parallel anthracene itself and point to the remarkable innocence of some CC to BN bond substitutions.

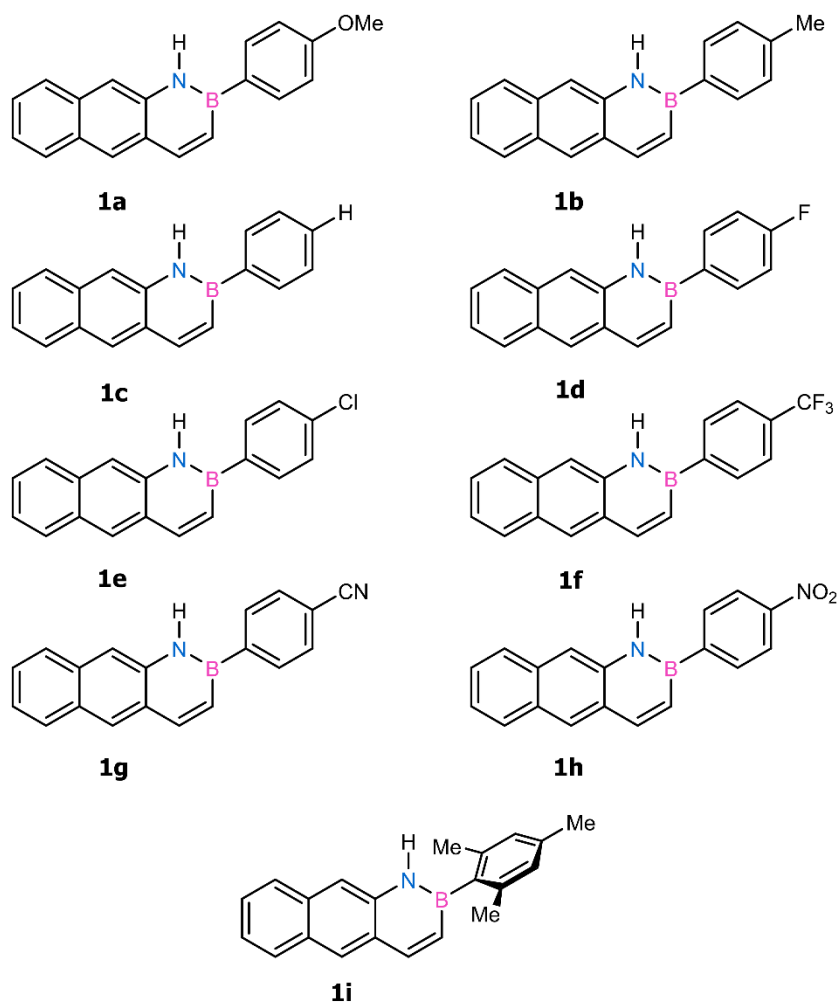


Figure 2.1. Chemical structures of known (**1c**) and new (**1a-b, 1d-i**) BN anthracenes synthesized in this work.

2.2 B-Aryl Anthracene Synthesis

Dewar's pioneering synthesis of BN naphthalene via borylation of 2-vinylniline with trichloroborane (**Figure 2.2**) inspires recent work on extended azaborine derivatives.³⁸ Molander reported the one-pot synthesis of functionalized BN naphthalene derivatives by the *in situ* generation of organodichloroboranes from bench-stable potassium organotrifluoroborate salts.^{115,116} Liu recently reported the first synthesis of BN anthracene by adaptation of Dewar's borylation and reduction sequence (**Figure 2.3a**).¹¹⁹ The Liu synthesis begins with conversion of 2-amino-3-naphthoic acid **2** to iodoarene **3** by a Sandmeyer reaction-Curtius rearrangement sequence. The key intermediate **4** is obtained after a Suzuki vinylation with potassium vinyltrifluoroborate that proceeds in 65% yield.

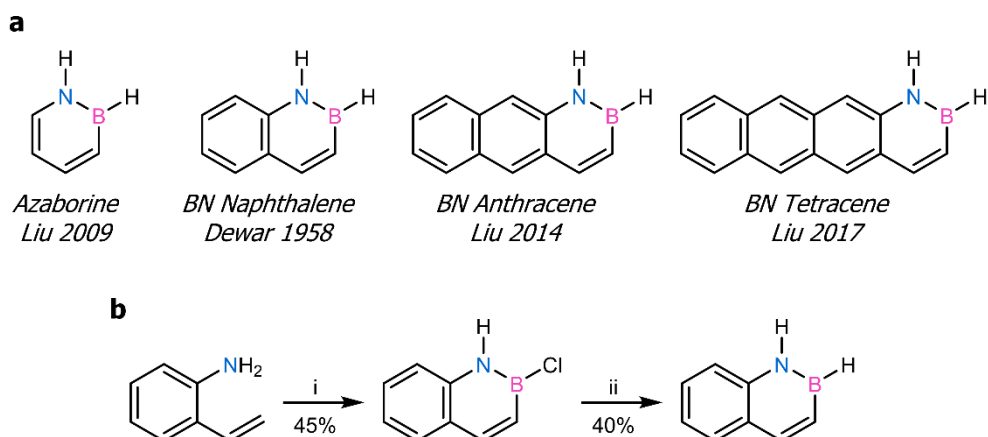


Figure 2.2. a) Linearly fused extended azaborine derivatives. b) Dewar's synthesis of BN naphthalene. i) BCl_3 , PhH, 80 °C, 45%; ii) LAH, Et_2O , 40%. LAH = lithium aluminium hydride.

Towards the synthesis of our target library of compounds, we applied Molander's one-pot reaction conditions to Liu's 2-amino-3-vinylnaphthalene intermediate **4** (**Figure 2.3b**). We also report a higher yielding synthetic route to key intermediate **4**. We subject 2-amino-3-naphthoic acid **2** to the sequence of a Sandmeyer reaction with cuprous

chloride¹²⁰ and a Curtius rearrangement to yield chloroarene **5**. A Suzuki reaction between chloroarene **5** and vinylboronic acid MIDA ester¹²⁰ catalysed by Pd(OAc)₂/SPhos proceeds in 90% yield. The overall yield of **4** from commercially available **2** is 71%. While compound **1c** was recently reported by Liu et al., the other BN anthracenes in this study are unknown.

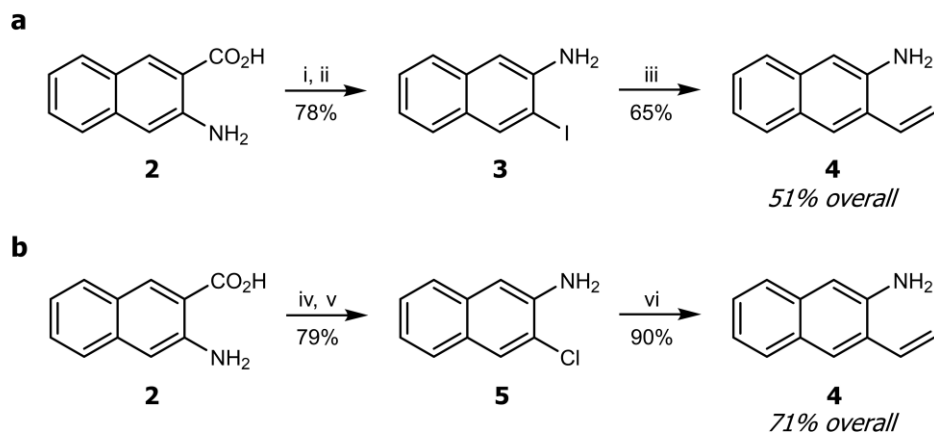


Figure 2.3. Synthesis for BN anthracene starting material. a) Liu synthesis of **4**. i) NaNO₂, KI, HCl, 88%. ii) DPPA, NEt₃, H₂O, 89%. iii) Pd(dppf)Cl₂, NEt₃, potassium vinyl trifluoroborate, 65%. b) Klausen synthesis of **4**. iv) NaNO₂, H₂SO₄; CuCl, HCl, 86%. v) DPPA, NEt₃, H₂O, 92%. vi) vinylboronic acid MIDA ester, SPhos, Pd(OAc)₂, K₃PO₄, 90%. DPPA = diphenylphosphoryl azide; MIDA = N-methyliminodiacetic acid; SPhos = 2-dicyclohexylphosphino-2',6'-dimethoxybiphenyl.

2.3 Single Crystal X-ray Crystallography

Single crystals of *B*-aryl anthracenes were grown from solution at room temperature. Key crystallographic parameters for the structures of **1b**, **1c**, **1d**, **1f**, **1g**, **1h**, and **1i** are summarized in Table 1.

Across the series, the length of the BN bond remains statistically identical at *ca.* 1.42 Å (Table 2.1). This bond length is comparable to the 1.44 Å bond length of borazine (B₃N₃H₆).¹²¹ It is intermediate between the BN single bond length (1.51 Å) and the BN double bond length (1.31 Å).¹²² Intermediate bond lengths and partial bond order are

experimental hallmarks of cyclic delocalization, or aromaticity: the bond lengths in benzene are *ca.* 1.40 Å, intermediate between the carbon-carbon single bond length of *ca.* 1.54 Å and the carbon-carbon double bond length of *ca.* 1.34 Å.

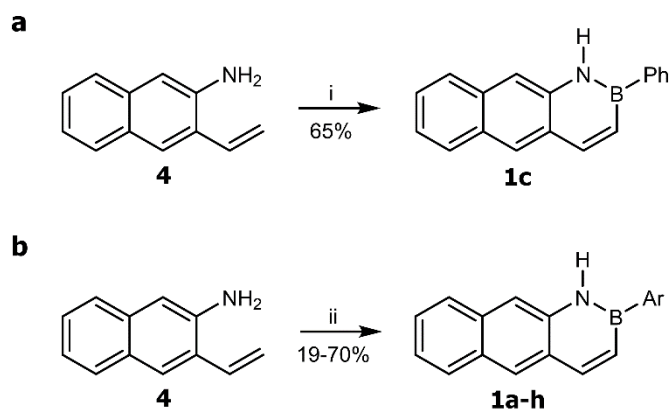


Figure 2.4. BN Anthracene synthesis. a) Liu: **1c**. i) PhBCl₂, toluene, 110 °C, 65%. b) Klausen library: **1a-h**. ii) ArBF₃K, SiCl₄, NEt₃, toluene-CPME, 100 °C, 19-70%. CPME = cyclopentyl methyl ether.

Table 2.1. Selected torsion angles and bond distances for **1b**, **1c**, **1d**, **1f**, **1g**, **1h** and **1i**. The values and esd in Table 2.1 were directly obtained from the experimental cif files.

Compound	Aryl Group	∠N1-B1-C13-C14 (deg) ^a	N1-B1 (Å)
1b*	4-(CH ₃)C ₆ H ₄	-6.6(6), 7.5(5)	1.421(5), 1.418(5)
1c	Ph	-5.0(3)	1.426(3)
1d	4-FC ₆ H ₄	-5.3(2)	1.423(2)
1f	4-(CF ₃)C ₆ H ₄	5.4(2)	1.4175(18)
1g	4-(CN)C ₆ H ₄	5.4(2)	1.419(2)
1h	4-(NO ₂)C ₆ H ₄	-2.7(2)	1.4207(16)
1i	Mes ^b	-84.7(2)	1.418(2)

^a Torsion angle. ^b Mes = mesityl = 2,4,6-trimethylphenyl. * The two values of the torsion angles and bond distances are given for two crystallographically independent molecules.

In all BN anthracenes we have prepared, the crystal packing arrangement is herringbone (**Figure 2.4a-b**), the same arrangement as in anthracene.^{123,124} That the BN anthracenes should have a similar crystal packing structure to anthracene is not obvious. Anthracene is a high symmetry hydrocarbon with zero net molecular dipole. Herringbone packing maximizes quadrupolar interactions between the positively charged aromatic edges and the negatively charged aromatic face. In contrast, the polar BN bond desymmetrizes the BN anthracenes and in principle the bond dipole moment could influence molecular interactions. That it does not again points to the innocence of a single BN bond substitution in the aromatic core. Furthermore, our structures are disordered so that two neighbouring

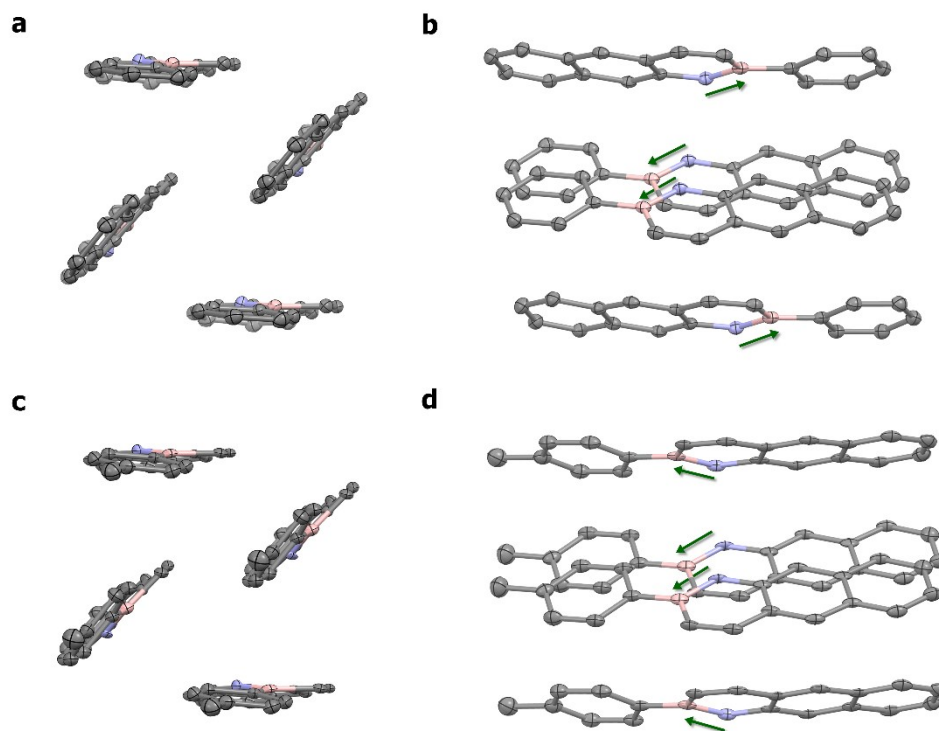


Figure 2.4. Representative crystal packing of BN anthracenes. a) Herringbone packing of *B*-Ph **1c**. b) Herringbone packing of *B*-Tol **1b**. c) Approximately antiparallel orientation of **1c** molecules. d) Approximately parallel orientation of **1b** molecules. The BN dipole is indicated with a green arrow. Displacement ellipsoids are given at 50% probability level. Disorder and hydrogens omitted for clarity. Grey = carbon; blue = nitrogen; pink = boron.

molecules may be either aligned parallel or antiparallel with respect to the BN bond (**Figure 2.4c-d**). That there is no preference between parallel and antiparallel orientations shows the minimal influence of the bond dipole moment on the packing structure.

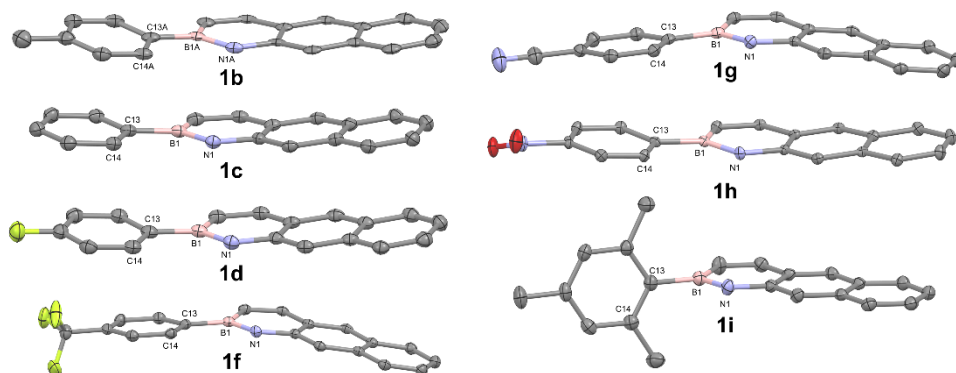


Figure 2.5. Displacement ellipsoid plots (50 % probability level) of BN anthracenes at 110(2) K. Disorder and hydrogens omitted for clarity. Grey = carbon; blue = nitrogen; pink = boron; green = fluorine, red = oxygen.

In both ours and Liu's crystal structures of **1c**, the absolute value of the torsion angle between the exocyclic ring and the extended core is 5°. In fact, all BN anthracene structures but **1i** show that the exocyclic *B*-aryl group is co-planar with the anthracene framework (**Figure 2.5**). The absolute values of the torsion angles vary from 2.7 to 7.5° (Table 1). In contrast, in the crystal structure of the heterocycle **1i**, the mesityl group is almost orthogonal to the plane of the BN anthracene ($\angle = ca. 85^\circ$). The orthogonal mesityl group is expected, as steric hindrance between the ortho methyl groups and the anthracene core prevents a coplanar arrangement.

2.4 2-Arylanthracene Syntheses and X-Ray Structures

We hypothesized that the exocyclic *B*-aryl ring is coplanar with the anthracene core to stabilize the empty p-orbital on boron. As a control, we synthesized 2-phenylanthracene

8a, which has a full octet. We find that Suzuki coupling of commercially available 2-chloroanthroquinone and an arylboronic acid¹²⁵ followed by quinone reduction¹²⁶ yields 2-arylanthracenes **8a-c** (**Figure 2.6**).

The crystal structure of **8a** shows a coplanar arrangement ($\angle C^{20}-C^{15}-C^{13}-C^{14} = -6.7(4)^\circ$) of the anthracene and exocyclic phenyl ring, which does not support the hypothesis that coplanarity is a result of a favourable driving force related to the empty boron orbital. A herringbone crystal packing structure in which individual molecules are antiparallel is observed for compound **8a**. This result again highlights the similarity of BN anthracenes to aromatic hydrocarbons.

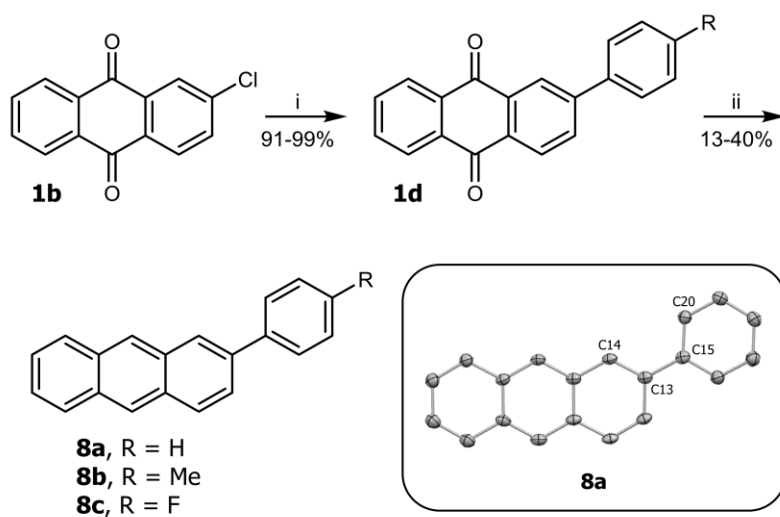


Figure 2.6. Synthesis of 2-arylanthracenes **8a-c**. i) $ArB(OH)_2$, $Pd(PPh_3)_4$, K_2CO_3 , toluene, $110^\circ C$, 91-99%; ii) LAH, HCl, THF (repeat twice), 13-40%. LAH = lithium aluminium hydride. Inset shows molecular structure of **8a** determined by single crystal XRD. Displacement ellipsoid plot (50% probability level) of **8a** at $110(2)$ K. Grey = carbon. Disorder and hydrogens omitted for clarity. Atoms C14, C13, C15, and C20 are labelled. The torsion angle defined by these carbons is $-6.7(4)^\circ$.

2.5 Calculated Structure

For more insight into the coplanar geometry, we compared the optimized geometry of isolated molecules in vacuum to the molecular crystal structures using density functional theory calculations (CAM B3LYP/6-311G(d,p)). At this level of theory, all *B*-aryl anthracenes and 2-arylanthracenes were predicted to have a noncoplanar structure with the key torsion angle varying between 25 and 40°. Calculations also accurately predict a BN bond length of 1.42 Å. The difference between the optimized *in vacuo* structure and the experimentally determined crystal structure suggest crystal packing and intermolecular forces drive coplanarity. We identify short edge-face contacts between the exocyclic ring face and aromatic edges of neighbouring molecules in the crystal packing structure.

2.6 Absorbance Spectroscopy

Solution phase absorbance spectroscopy of BN anthracenes suggests these materials can be divided into two classes.

In the first class are the coplanar derivatives **1a-g**. These materials all have an onset of absorbance around 400 nm, corresponding to an optical bandgap of about 3.10 eV (**Table 2.2**, entries 1-7). In the second class are BN anthracene itself and mesityl derivative **1i** (entries 8-9). These two materials are slightly blue-shifted relative to the coplanar derivatives with an onset of absorbance at 390 nm ($E_g \approx 3.16$ eV).

Clearly, the exocyclic ring positively influences the properties of the entire system when it achieves a coplanar arrangement. The degree of red-shifting achieved in the BN anthracenes is remarkably similar to that observed in the hydrocarbon scaffold as well. We find that 2-arylanthracenes **8a-c** are also about 10 nm red-shifted relative to anthracene itself (entries 10-13) and that the optical band gaps of **8a-c** are similar to their BN analogs.

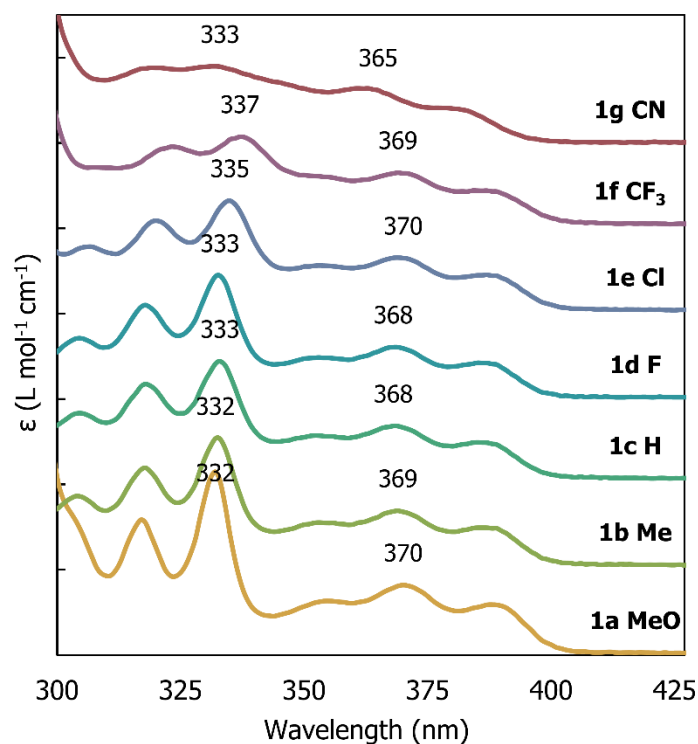


Figure 2.7. Absorbance spectroscopy in THF. The extinction coefficient ϵ in $\text{M}^{-1} \text{cm}^{-1}$ is plotted versus wavelength in nanometers. Spectra are offset for clarity and hash marks represent $10,000 \text{ M}^{-1} \text{cm}^{-1}$.

Table 2.2. Experimental optical properties for compounds synthesized in this study.^a

Entry	Compound	Substituent	λ_{onset} (nm) ^b	E_g (eV) ^c
1	1a	4-MeO	401	3.09
2	1b	4-Me	400	3.10
3	1c	4-H	400	3.10
4	1d	4-F	399	3.10
5	1e	4-Cl	400	3.10
6	1f	4-CF ₃	401	3.09
7	1g	4-CN	396	3.13
8	1i	Mes	393	3.15
9	BN Anthracene	n/a	392	3.17
10	8a	4-H	398	3.12
11	8b	4-Me	399	3.11
12	8c	4-F	398	3.12
13	Anthracene	n/a	383	3.24

^a Spectra recorded in tetrahydrofuran at room temperature. ^b λ_{onset} = wavelength of light corresponding to the onset of absorbance. ^c E_g = optical band gap.

2.7 Electrochemistry

BN anthracene electrochemistry closely parallels anthracene's electrochemistry. In dimethylformamide at room temperature, for BN anthracenes **1a-g**, we observe a reversible or quasireversible reduction peak at about -2.5 V vs. Fc/Fc⁺ (**Table 2.2**, entries 1-7). Reversible anthracene reduction ($E_p \sim -2.0$ V vs. SCE) has been reported in both acetonitrile and dimethylformamide;¹²² under our conditions, anthracene is reduced at -2.46 V vs. Fc/Fc⁺.

Table 2.3. Electrochemical properties for compounds synthesized in this study.^a

Entry	Compound	Substituent	$E_{p,a}$ (V) ^b	$E_{p,c}$ (V) ^b
1	1a	4-MeO	0.82	-2.54
2	1b	4-Me	0.79	-2.54
3	1c	4-H	0.81	-2.52
4	1d	4-F	0.91	-2.53
5	1e	4-Cl	0.74	-2.48
6	1f	4-CF ₃	0.85	-2.41
7	1g	4-CN	0.88	-2.33
8	1i	Mes	0.93	-2.59
9	BN Anthracene	n/a	0.77	-2.53
10	8a	4-H	0.82	-2.37
11	8b	4-Me	0.80	-2.39
12	8c	4-F	0.81	-2.37
13	Anthracene	n/a	0.86	-2.46

^a Data recorded as 3.5 mM solutions in anaerobic, anhydrous dimethylformamide at room temperature with tetrabutylammonium hexafluorophosphate ($[Bu_4NPF_6] = 0.1$ M) supporting electrolyte under argon. Working electrode = platinum button; counter electrode = platinum wire; reference electrode = Ag/Ag⁺NO₃⁻ in acetonitrile; scan rate = 0.1 V s⁻¹. ^b Relative to Fc/Fc⁺ internal standard. Fc = ferrocene; $E_{p,a}$ = peak anodic potential; $E_{p,c}$ = peak cathodic potential.

BN anthracenes **1a-g** are irreversibly oxidized at room temperature in dimethylformamide ($E_{p,a} \sim 0.8$ V vs. Fc/Fc^+) and anthracene undergoes rapid oxidative decomposition at even cryogenic temperatures.¹²⁷ The short-lived radical cation intermediates are thought to react with solvent, as stable electrochemically generated anthracene cations are observed only at very low temperatures and in very nonnucleophilic solvents.¹²⁸ Indeed, we observe additional electrochemically active species in the voltammogram on repeated scans of **1a-g**. As the nitro group is itself redox active, the cyclic voltammogram of compound **1h** is complex.

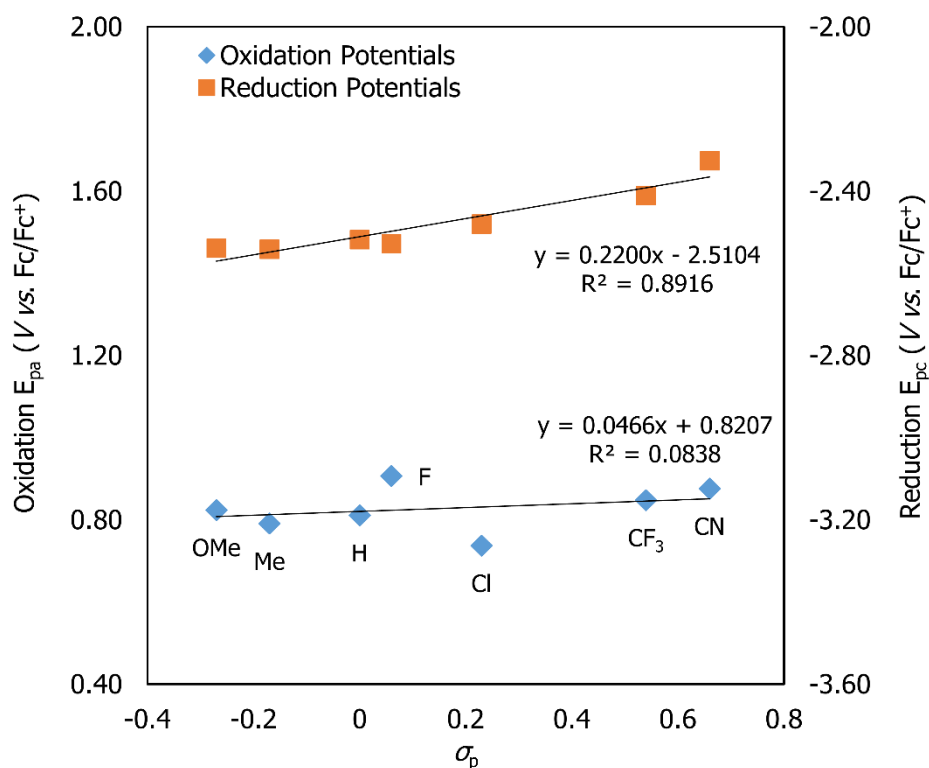


Figure 2.8. Potential dependence on BN anthracene electronic properties. Plot of experimentally determined peak reduction potential (red squares) and peak oxidation potential (blue diamonds) versus σ_p for BN anthracenes **1a-g**. The black lines represent least squares fits to $f(x) = a + \rho x$.

While the optical spectroscopy of BN anthracenes shows the same onset of absorbance regardless of electron-donating or electron-withdrawing substituents (**Figure 2.7**), and therefore the same HOMO-LUMO gap, electrochemistry can separately probe the HOMO and LUMO energies. We find that the reduction potential becomes less negative with increasing electron-withdrawing character in the series **1a-g**, reflecting a lower lying LUMO level in BN anthracenes with electron-withdrawing substituents. A least-squares fit of the $E_{p,c}$ to the Hammett parameter σ_p is linear ($R^2 = 0.89$, $\rho = -0.22$, Figure 8). The small rho value suggests a modest overall influence of the substituent on the LUMO energy.

The influence of the exocyclic substituent on the peak oxidation potential is less clear-cut. A Hammett analysis shows considerable scatter and a least-squares fit of the $E_{p,a}$ to the Hammett parameter σ_p is not linear (**Figure 2.8**). Given that these materials have the same optical band gap, but a tunable reduction potential, we predicted that the exocyclic substituent should have an equal effect on the frontier orbitals, lowering the HOMO by an amount equal to the amount by which it lowers the LUMO. Similar results have been observed in triazaborine heterocycles.¹²⁹ That we don't observe a linear free energy relationship between substituent and the peak oxidation potential may reflect the rapid decomposition of the BN anthracene radical cation, which results in a broad and unstable peak oxidation potential and contributing to the scatter in the Hammett analysis.

2.8 Electronic Structure Calculations

To further explore substituent effects absent any decomposition, we turned to DFT calculations. As described earlier, ground state geometry optimization of **1a-g** (CAM B3LYP/6-311G(d,p)) converges on structures in which the exocyclic ring is not coplanar with the anthracene core. This level of theory was selected to allow for direct comparison to Liu's calculations on BN anthracene.¹¹⁹

Comparison of the calculated HOMO and LUMO energies of **1c** and the orbital densities in the optimized geometry ($\angle = 25^\circ$) and using the crystallographic coordinates ($\angle = 7.52^\circ$) shows that electronic structure is not strongly conformation dependent. Since we are not able to isolate diffraction quality crystals for **1a** and **1e**, we carried out the remaining electronic structure calculations using the calculated geometries.

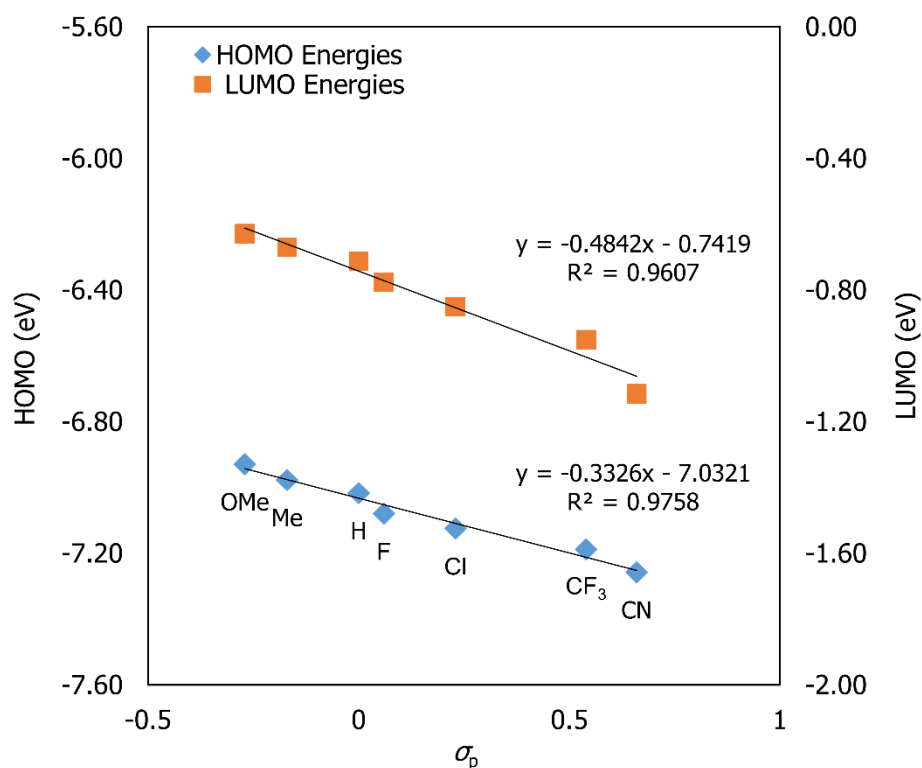


Figure 2.9. Frontier molecular orbital energy dependence on BN anthracene electronic properties. Plot of calculated (CAM B3LYP/6-311G(d,p)) LUMO (red squares) and HOMO (blue diamonds) energies versus σ_p for BN anthracenes **1a-g**. The black lines represent least squares fits to $f(x) = a + \rho x$.

We find a linear free energy relationship between both the calculated HOMO and LUMO energies and the Hammett parameter σ_p (Figure 9). The slope ρ of the two lines are similar (HOMO: -0.33; LUMO: -0.48) consistent with an equal magnitude substituent effect.

The calculated band gaps across the series are also constant, in agreement with the absorbance spectroscopy.

2.9 Conclusion

Our results show that the properties of BN anthracenes closely parallel anthracene and its derivatives. Substituents at the equivalent of the 2-position of anthracene have a small but measurable influence on electronic properties, without perturbing bulk structure. These conclusions enable predictions about structure-function relationships in azaborine derivatives. For example, given that in anthracene peripheral functionalization at the 9,10 positions is of particular interest for materials applications, our results highlight the desirability of more synthetic methods increasing the chemical and structural diversity of extended BN materials.

3.1 Introduction

Polystyrene (PS) is an essential commodity chemical produced annually on a million-tonne scale.⁴ PS derivatives arising from chemical modification of the benzene ring represent important materials in their own right, such as polystyrene sulfonate, the ion exchange resin Dowex.⁸ The incorporation of boron into organic materials for functional purposes is an active area of synthetic innovation.^{11,112,130} BN for CC bond substitution (e.g. 1,2-dihydro-1,2-azaborine (C₄H₆BN) is a BN analog of benzene) is a particularly attractive approach to developing stable organoboranes. A number of 1,2-azaborine-containing conjugated polymers and small molecules have been investigated as electronic materials.^{23,131–134} Polymerization of vinyl borazine is reported.³⁰ Liu and Jäckle¹³⁵ and Staubitz¹³⁶ have reported the synthesis and free radical polymerization of azaborine-containing vinyl monomers (Scheme 1a). These elegant synthetic studies of BN-polystyrene (PBNS) support the viability of achieving azaborine incorporation without heterocycle decomposition.

Elucidation of the bulk properties of these exciting polymers requires scalable synthetic approaches. While the synthesis of monocyclic 1,2-azaborine derivatives is a significant challenge, major progress has been achieved in the last several years.⁴⁰ Ashe

reported the first synthesis of BN-styrene in 2009 via a ring expansion strategy.⁴³ The five-step synthesis from *N*-(trimethylsilyl)allylamine proceeds in 5.6% overall yield, however the repeated use of toxic and pyrophoric reagents including organostannanes and alkyllithiums poses a limitation with respect to scale and atom economy. Liu has reported a protecting group free synthetic approach to 1,2-azaborine derivatives, including BN-styrene, featuring a ring closing metathesis reaction promoted by Schrock's catalyst (15% overall yield).⁴⁴ Liu's synthetic route has been adapted in both Jäkle's and Staubitz's syntheses of PBNS.^{135,136} The polymerizations are conducted on millimolar scale.

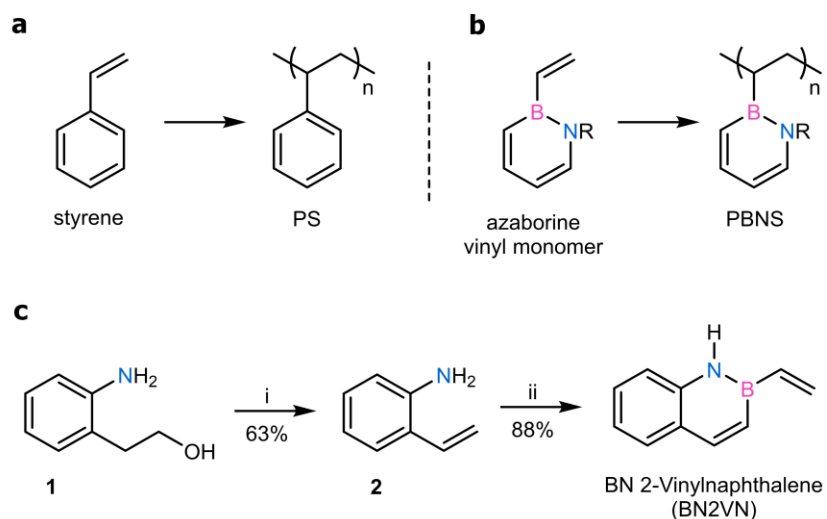
The synthesis of bicyclic extended azaborines is considerably more straightforward than monocyclic structures. Dewar synthesized BN naphthalene in 1959 by reaction of 2-aminostyrene with trichloroborane followed by reduction.^{38,119} Molander has reported a convenient one-pot approach to BN naphthalenes via *in situ* generation of chloroboranes from potassium organotrifluoroborate salts.^{115,137} An attractive feature of Molander's report is the use of cyclopentyl methyl ether (CPME), a green solvent alternative to THF.^{138,139} In earlier work, we described the synthesis and optoelectronic characterization of BN anthracenes using Molander's conditions.⁵¹

3.2 Azaborine Monomer Development

We hypothesized that the BN variant of 2-vinylnaphthalene (BN2VN) could serve as a readily accessible vinyl monomer. Here we report the two-step synthesis of BN2VN, two gram-scale free radical polymerization of this novel monomer, and comparison of the properties of azaborine and hydrocarbon polymers (PBN2VN and P2VN), as well as random copolymers.

The synthesis minimizes the use of toxic reagents and solvents (**Scheme 3.1b**). Commercially available **1** is converted to 2-aminostyrene **2** in 63% yield by water elimination under solvent-free conditions.¹⁴⁰ Borylation with potassium vinyltrifluoroborate in toluene-CPME using Molander's conditions¹¹⁵ yields BN2VN in 88% yield. Purification of

intermediates is straightforward: we obtain **2** by distillation directly from the reaction medium and BN2VN can be isolated either by column chromatography or sublimation. The only stoichiometric by-products in the synthesis are water, halosilanes (e.g. ClSiF_3), and triethylamine hydrochloride. The yield over two steps is 55%.



Scheme 3.1. Vinyl borane monomer strategy. a) Preparation of polystyrene (PS) and BN polystyrene (PBNS) from vinyl monomers, R = H or Me. b) Scalable synthesis of BN2VN in two steps from commercially available starting material. i) KOH, 180 °C, 63%; ii) potassium vinyltrifluoroborate, SiCl_4 , NEt_3 , toluene-CPME, 60 °C, 88%. Me = methyl; Et = ethyl; CPME = cyclopentyl methyl ether.

The CC to BN bond substitution results in significant changes in the ^1H NMR spectrum of monomer BN2VN compared with 2VN, particularly with respect to the vinylic protons (**Figure 3.1**). The terminal beta-styryl protons (labelled with diamond (◆) and star (★)) shift to lower field ($|\Delta| = 0.37\text{-}0.71$ ppm), consistent with electron-withdrawing substitution. The alpha-styryl proton shifts to higher field ($|\Delta| = 0.39$ ppm). The N-H proton is also apparent at δ 7.91.

BN bond substitution also results in significant changes in chemical environment in the aromatic ring. 2VN and BN2VN formally have the same symmetry but the ^1H NMR spectrum of BN2VN shows six distinct and well-resolved aryl multiplets spanning from 7.0 to 8.0 ppm while the 2VN spectrum shows 3-4 multiplets within a more condensed range (7.4-8.0) due to overlapping signals.

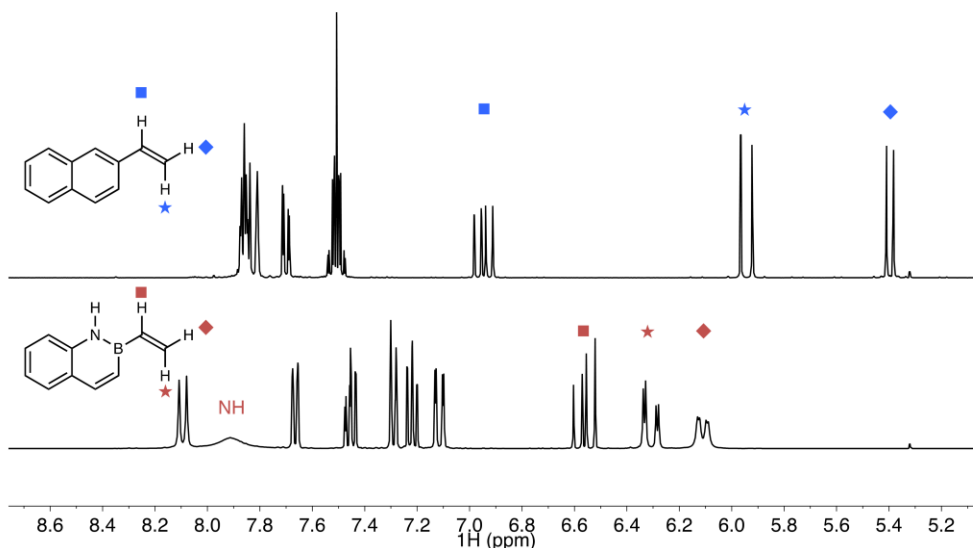


Figure 3.1. Comparison of ^1H NMR spectra of 2VN and BN2VN in CD_2Cl_2 . Vinyllic protons are labelled with ■, ◆, and ★ (blue = 2VN; red = BN2VN).

3.3 Free Radical Polymerization

We next examined the free radical polymerization of BN2VN. With 3 mol% of 2,2'-azobis(2-methylpropionitrile) (AIBN) as initiator, the BN2VN homopolymer (PBN2VN) was isolated in 58% yield after methanol precipitation and drying in a vacuum oven for 36 hours. Gel permeation chromatography (GPC) analysis of PBN2VN revealed a low molecular weight polymer of moderate dispersity ($M_n = 6.0$ kDa, $\mathcal{D} = M_w/M_n = 1.43$) (**Table 3.1**, entry 1). Higher molecular weight material is obtained under solvent-free conditions ($M_n = 8.9$ kDa, $\mathcal{D} = M_w/M_n = 1.54$) (**Table 3.1**, entry 5).

Table 3.1. PBN2VN molecular weight characteristics. Influence of initiator concentration, temperature, and solvent.

Entry	AIBN (mol%)	Time (h)	Temperature (°C)	Monomer Conc. (M)	M _n (kDa) ^a	Đ ^a
1	3	24	70	3.33	6.0	1.43
2	3	48	70	3.33	4.6	1.26
3	1	24	70	3.33	5.6	1.25
4	1	48	70	3.33	5.5	1.24
5	1	72	85	n/a	8.9	1.54

^a Measured by gel permeation chromatography (GPC) at 254 nm relative to polystyrene standard (THF, 0.35 mL min⁻¹, 40 °C).

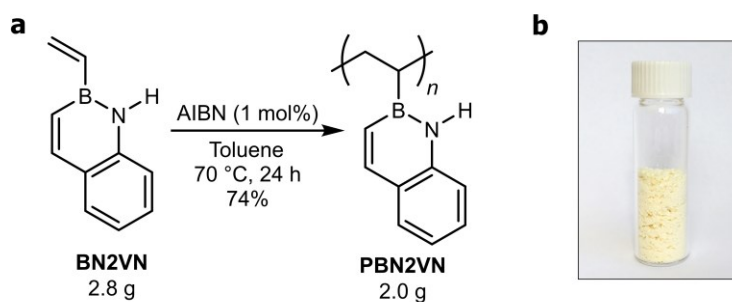
Under the same reaction conditions as BN2VN, the hydrocarbon monomer 2VN yields a polymer of similar, although slightly higher, molecular weight and dispersity. This is in contrast to Liu and Jäkle who found significant differences in reactivity between *B*-vinyl and *C*-vinyl monomers with only *C*-vinyl monomers yielding high molecular weight polymers.¹³⁵ No background auto-polymerization was observed: heating BN2VN to 60-100 °C in the absence of AIBN, either neat or with toluene, did not lead to polymer formation (**Table 3.2**).

Table 3.2. Absence of thermal auto-polymerization upon heating BN2VN without radical initiator.

Entry	Solvent	Temperature (°C)	Time (h)	Polymer Formed ^a
1	Neat	60	24	No
2	Toluene ^b	60	24	No
3	Neat	70	24	No
4	Toluene ^b	70	24	No
5	Neat	100	24	No
6	Toluene ^b	100	24	No

^a Measured by gel permeation chromatography (GPC) at 254 nm relative to polystyrene standard (THF, 0.35 mL min⁻¹, 40 °C). If no product of molecular weight higher than that of BN2VN was detected, polymer was determined to not be formed. ^b [BN2VN]= 6.6 M.

Our synthetic approach enables the first multigram synthesis of an azaborine-derived polymer (**Scheme 3.2a**). Free radical polymerization according to the standard conditions provides PBN2VN in 74% yield. After precipitation from methanol and drying in a vacuum oven for 36 hours, we obtain more than two grams of PBN2VN ($M_n = 3890$ Da, $\bar{D} = M_w/M_n = 1.84$) as a pale yellow, free-flowing powder (**Scheme 3.2b**).



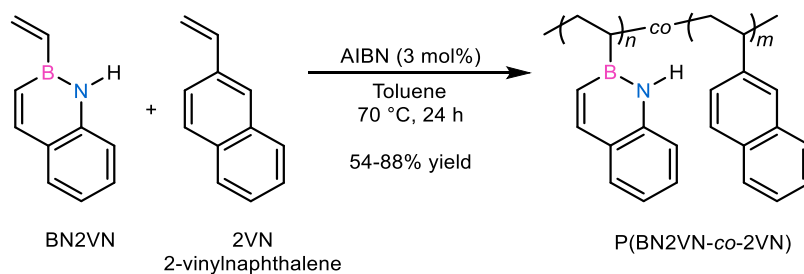
Scheme 3.2. PBN2VN. a) Multi-gram scale polymerization of BN2VN. b) PBN2VN is a pale yellow powder. AIBN = 2,2'-azobis(2-methylpropionitrile).

3.4 Conclusion

In summary, we describe a high-yielding and efficient synthesis of BN 2-vinylnaphthalene that enables the study of vinyl azaborine polymer properties. We report the preparation of homopolymers of BN2VN, including large-scale multigram polymerization. The scalable synthesis will enable studies on the materials properties and applications of azaborine polymers.

4.1 Introduction

Encouraged by results suggesting that 2VN and BN2VN have comparable reactivity in free radical polymerization, statistical co-polymers were targeted by varying the feed ratio of BN2VN and 2VN (**Scheme 4.1**). The molecular weight of the isolated copolymers increases modestly with higher 2VN content in the feed ratio, consistent with slightly greater 2VN reactivity (**Table 4.1** and **Figure 4.1d**).



Scheme 4.1. Free radical co-polymerization of BN2VN and 2VN. AIBN = 2,2'-azobis(2-methylpropionitrile).

4.2 Determination of Copolymer Composition

We quantify % BN2VN incorporation with a spectroscopic assay. UV-vis absorbance spectra are shown in **Figure 4.2**. The onsets of absorbance in BN2VN and 2VN are similar, but the intensities of individual transitions vary significantly (**Figure 4.2a**), with BN2VN absorbing more strongly at 326 nm than 2VN. The same trend is observed in the homopolymers and at 320 nm, PBN2VN absorbance is much stronger than P2VN absorbance (**Figure 4.2b**). The spectra of both homopolymers are slightly blue-shifted relative to monomers, consistent with a decrease in conjugation occurring as the vinyl group is polymerized.

Table 4.1. Optical and molecular weight properties of polymers and co-polymers.

Entry	Sample Name ^a	Feed Ratio BN2VN:2VN	ϵ_{320} ^b	BN2VN Conc. (wt%) ^c	M_n (kDa) ^d	\bar{D} ^d
1	PBN2VN	100:0	30.7	100%	6.0	1.43
2	P(BN2VN ₇₄ -co-2VN ₂₆)	80:20	23.4	74%	6.5	1.34
3	P(BN2VN ₄₉ -co-2VN ₅₁)	50:50	16.6	49%	6.2	1.48
4	P(BN2VN ₉ -co-2VN ₉₁)	20:80	5.38	9.2%	7.1	1.54
5	P2VN	0:100	2.86	0%	8.4	1.68
6	PBN2VN ^e	100:0	n.d.	100%	8.9	1.54

^a Samples named according to copolymer composition determined by UV-vis spectroscopy. ^b Extinction coefficient at 320 nm (ϵ_{320}) in L g⁻¹ cm⁻¹. ^c Determined by UV-vis spectroscopy using Equation 3.1. ^d Measured by gel permeation chromatography (GPC) at 254 nm relative to polystyrene standard (THF, 0.35 mL min⁻¹, 40 °C). ^e Polymerization conditions: solvent-free, 85 °C, 1 mol% AIBN, 72 h. n.d. = not determined.

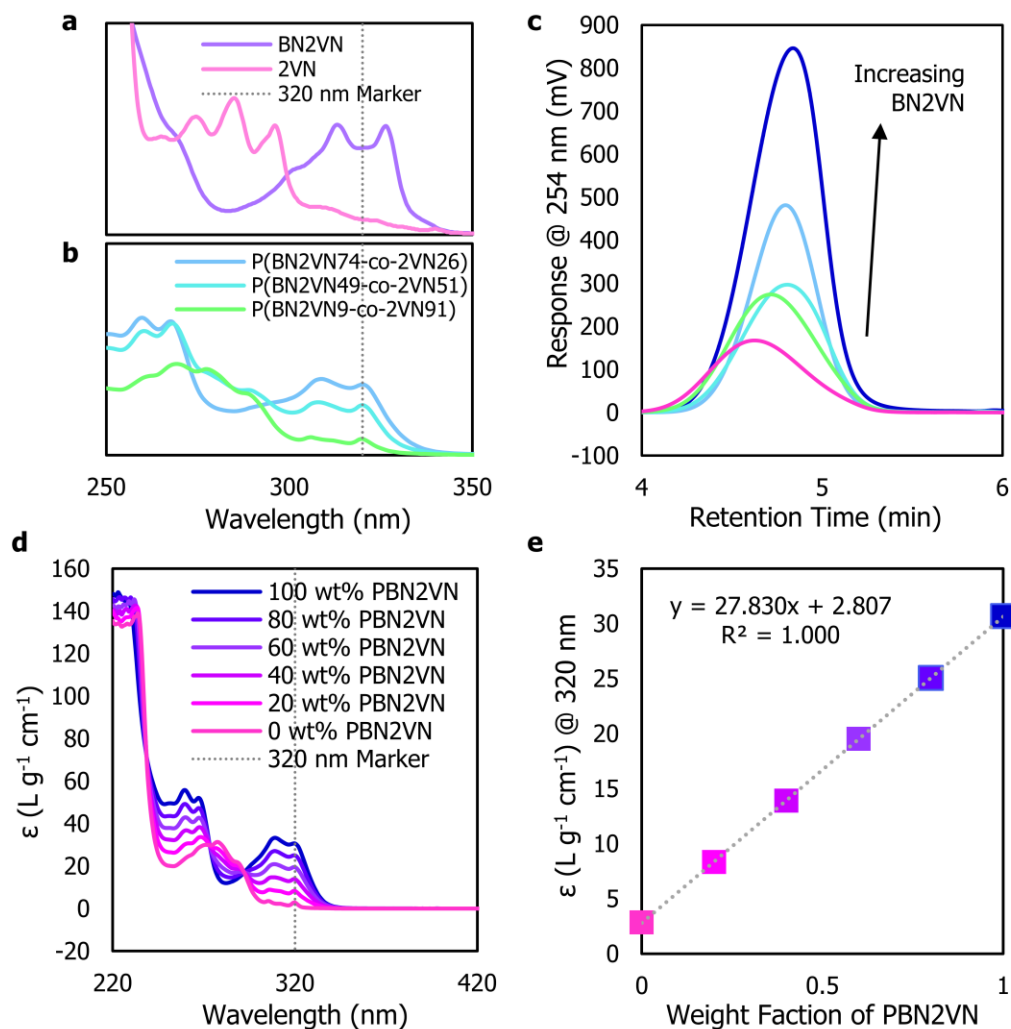


Figure 4.1. Absorbance spectroscopy in THF. a) UV-vis absorption spectra of BN2VN and 2VN. b) UV-vis absorption spectra of P(BN2VN₉-*co*-2VN₉₁), P(BN2VN₄₉-*co*-2VN₅₁), and P(BN2VN₇₄-*co*-2VN₂₆). c) GPC traces of homo- and co-polymers detected at 254 nm. Increasing BN content indicated with black arrow; P2VN, P(BN2VN₉-*co*-2VN₉₁), P(BN2VN₄₉-*co*-2VN₅₁), P(BN2VN₇₄-*co*-2VN₂₆), and PBN2VN. d) UV-vis absorption spectra of PBN2VN, P2VN, and blends with absorption at 320 nm indicated. e) Calibration curve for compositional analysis of P(BN2VN-*co*-2VN). Plot of weight fraction of PBN2VN in binary PBN2VN:P2VN blends versus absorption at 320 nm. Linear fit to data yields equation 4.1.

We exploit the differential light absorption at 320 nm to construct a calibration curve for BN2VN incorporation (**Figure 4.1d-e**).¹⁴¹ A plot of extinction coefficient at 320 nm versus the weight fraction of PBN2VN in different mixtures of the homopolymers yields a straight line. A linear regression analysis of the data provides **Equation 4.1**, in which X = the weight fraction of BN2VN. Using copolymer absorption at 320 nm and **Equation 4.1**, we calculate the % BN2VN incorporation. **Table 4.1** summarizes the feed ratio of the random co-polymers, measured % incorporation, and co-polymer molecular weight characteristics. The close agreement of feed ratio and % BN2VN incorporation further supports the observation that 2VN and BN2VN have comparable reactivity in free radical polymerization. Elemental analysis of homopolymers and copolymers are consistent with the weight percent incorporation of 2BNVN estimated by UV-vis absorbance spectroscopy.

$$\varepsilon = (27.8)X + 2.81 \quad \text{(Equation 4.1)}$$

4.3 Structural Characterization of Copolymers

The ¹H NMR spectrum of the PBN2VN homopolymer shows the disappearance of vinylic protons and the development of aliphatic peaks in the 0.5-3.0 ppm region (**Figure 4.2**), consistent with vinyl polymerization. A broad multiplet is observed in the aromatic region as well (6.0-8.0 ppm). The signals in P2VN are significantly sharper than observed in PBN2VN. We attribute the peak width to the polarizing effect of BN bond substitution: as the ¹H NMR spectrum of monomer BN2VN has more signals than the ¹H NMR spectrum of monomer 2VN despite similar symmetry, the overlap of these signals is expected to result in a broader aromatic massif in the PBN2VN homopolymer. Five features can be identified in the PBN2VN aromatic massif, which we attribute to the five aromatic C-H signals. The NH broad singlet is not identifiable. Copolymers with higher % BN2VN incorporation have fewer distinct features, reflecting the greater number of isomeric states and stereochemical configurations.

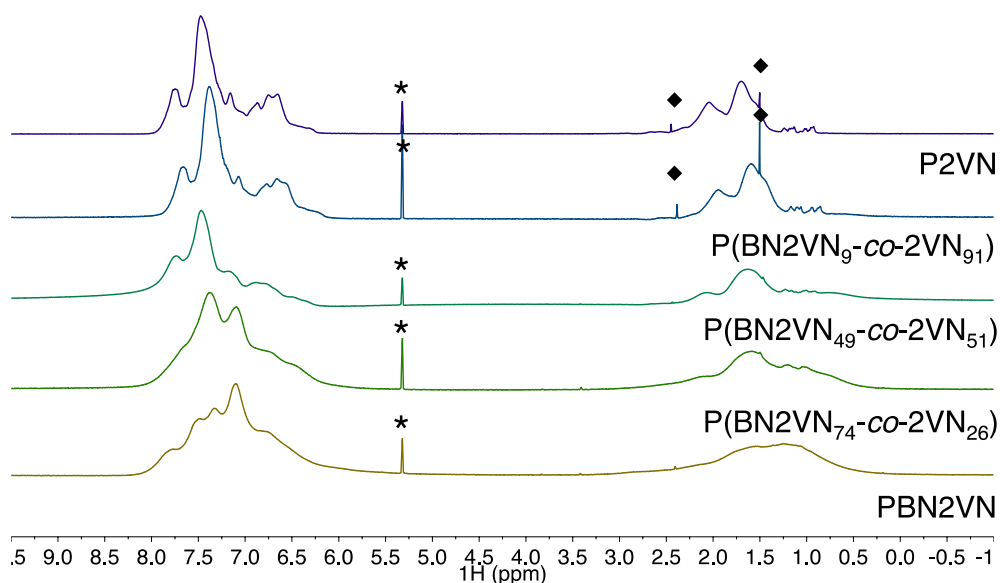


Figure 4.2. Comparison of ¹H NMR spectra of (top to bottom) P2VN, P(BN2VN₉-co-2VN₉₁), P(BN2VN₄₉-co-2VN₅₁), P(BN2VN₇₄-co-2VN₂₆), and PBN2VN in CD₂Cl₂. Peaks labelled with an asterisk correspond to residual CH₂Cl₂. Peaks labelled with a diamond correspond to residual methanol and are observed in P2VN and P(BN2VN₉-co-2VN₉₁).

¹¹B NMR spectroscopy provides further insight into PBN2VN structure. BN2VN has a single sharp peak at δ 32.4, while homopolymer PBN2VN has a broad singlet with a midpoint at δ 32.8. The ¹¹B NMR chemical shifts reported by Liu and Jäkle for PBNS (δ 40)¹³⁵ and Staubitz for P(4-ABS) (δ 44)¹³⁶ are more deshielded than the naphthyl polymer and show a greater difference between *B*-vinyl monomer and *B*-alkyl polymer (Δ 8-12 ppm). The modest change in chemical shift upon polymerization could reflect an intrinsic difference between the systems, as molecular BN naphthalene materials show a small difference (Δ <5 ppm) in ¹¹B NMR chemical shift when comparing *B*-vinyl and *B*-alkyl substituents (see *B*-(*E*)-propene, δ 33.0 versus *B*-methyl, δ 37.7).^{115,116} The downfield shift may also be attenuated by shielding from neighbouring aromatic groups.¹⁴² The broad signal is present in all copolymer ¹¹B NMR spectra, but diminishes in intensity relative to the background signal

arising from boron in probe components as the %BN2VN incorporation decreases (see **Figure 4.3**).

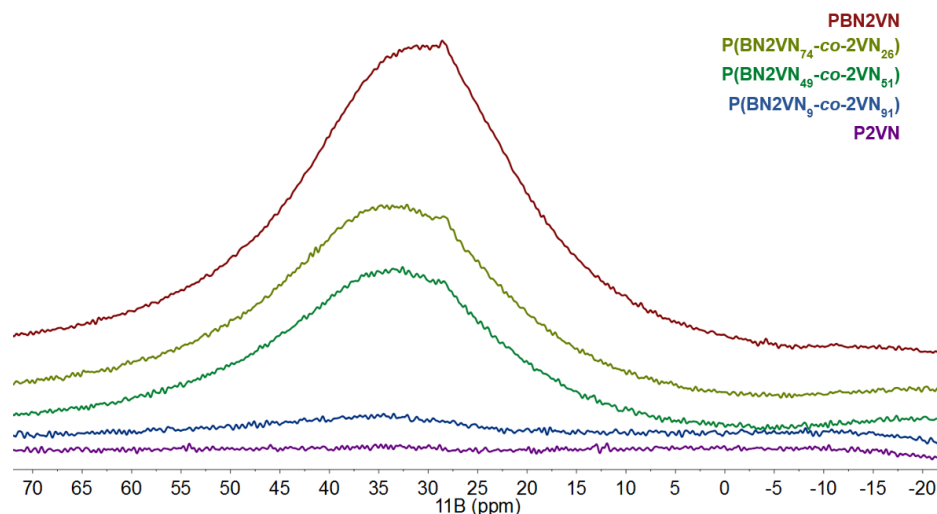


Figure 4.3. Comparison of background subtracted ^{11}B NMR spectra of (top to bottom) PBN2VN, P(BN2VN₇₄-co-2VN₂₆), P(BN2VN₄₉-co-2VN₅₁), P(BN2VN₉-co-2VN₉₁), and P2VN in CD_2Cl_2 .

4.4 Conclusion

In summary, we describe a high-yielding and efficient synthesis of BN 2-vinylnaphthalene that enables the study of vinyl azaborine polymer properties. We report the preparation of copolymers of BN2VN and 2VN, as well as quantitative characterization of BN2VN incorporation via absorbance spectroscopy and elemental analysis. Structural characterization by NMR is reported.

5.1 Introduction

Polymerization of azaborine vinyl monomers is promising given their increased stability relative to other boranes.^{43,44} Building on Sneddon's description of the polymerization of vinyl borazine,³⁰ several groups have recently reported free radical polymerization of azaborine vinyl monomers.^{135,136,143} This complements progress on inorganic main chain BN polymers and azaborine-derived conjugated polymers.^{18,19,133,134,144,145} We described the synthesis and gram-scale free radical polymerization of BN 2-vinylnaphthalene (BN2VN), as well as the preparation of copolymers with 2-vinylnaphthalene (2VN).¹⁴³

BN2VN-styrene copolymers are attractive candidates for investigating the vinylborane copolymerization with commercially ubiquitous styrene due to the scalable monomer synthesis.^{51,143,146} We prepare BN2VN in high overall yield and in two steps from commercially available starting materials. The multistep syntheses of monocyclic azaborine vinyl monomers limit polymerizations to milligram scale.^{135,136} The successful copolymerization of BN2VN and 2VN suggests the feasibility of copolymerization of styrene and BN2VN (PBN2VN-*co*-PS).

5.2 Theoretical Considerations for Monomer Coreactivity

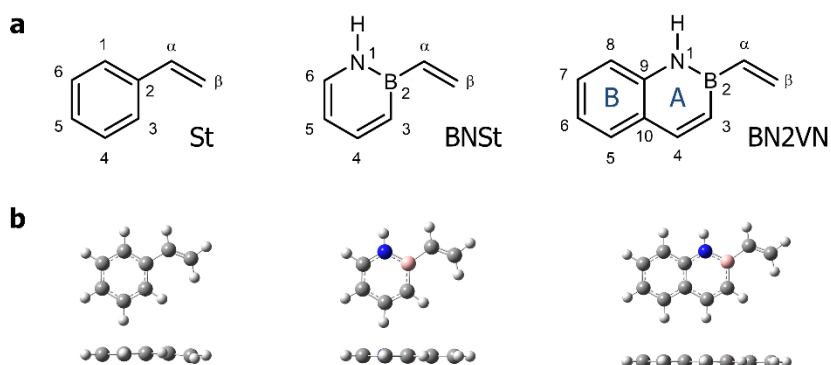


Figure 5.1. Aromatic vinyl borane monomers. a) Chemical structures of St, BNSt, and BN2VN with atom and ring numbering indicated. BN naphthalene numbering adapted from Dewar and Liu.^{147,148} b) Geometry optimized structures (CAM-B3LYP/6-311G(d,p)). Top down and side on views highlight planarity.

5.2.1 Molecular Geometries. Calculations on BN2VN reveal structural signatures of aromaticity including ring planarity and bond lengths intermediate between single and double bonds. Geometries were optimized using the restricted or unrestricted CAM-B3LYP¹⁴⁹ hybrid exchange-correlation functional with the 6-311G(d,p) basis set. CAM-B3LYP is known to reliably describe radicals and extended conjugated systems.^{150,151} Geometry optimization of St and BN styrene (BNSt) as control structures was performed at the same level of theory.

All three geometry optimized structures are planar, as seen in top down and side on views (**Figure 5.1**). In BN2VN, the sum of the bond angles within both the A and B rings of BN2VN is 720° and the average bond angle is 120° (**Table 5.1**). The same is observed in St and BNSt. The BN rings have a wider range of bond angles than the all carbon systems, reflecting the lower aromaticity of BN benzene (1,2-azaborine) analogs.

Table 5.1. Range of endocyclic bond angles (deg) in St, BNSt, and BN2VN. From geometry optimized structures.

	St	BNSt	BN2VN
Minimum	118.1	114.0	114.7 (A ring) 118.6 (B ring)
Maximum	121.2	123.9	125.0 (A ring) 121.4 (B ring)
Average	120.0	120.0	120.0 (A ring) 120.0 (B ring)
Sum of Ring Bond Angles	720.0	720.0	720.0 (A ring) 720.0 (B ring)

Optimized bond lengths are shown in Table 2. The BN bond in BN2VN is 1.422 Å. This value is consistent with the calculated BN bond length in BNSt (1.434 Å), 1,2-azaborine (1.438 Å)²⁸ and other previous theoretical work.^{152,153} The calculated BN bond length in BN2VN and BNSt is intermediate between BN single (1.582 Å)¹⁵⁴ and double bonds (1.396 Å).^{130,155,156} The CC bonds are also intermediate between single and double bonds in length. A wider range of bond lengths is observed in BN aromatic rings than in all carbon rings.

Table 5.2. Selected bond lengths (Å) in St, BNSt, and BN2VN. From geometry optimized structures. See **Figure 5.1** for atom numbering.

St		BNSt		BN2VN	
Bond	Length (Å)	Bond	Length (Å)	Bond	Length (Å)
C(1)–C(2)	1.395	B–N	1.434	B–N	1.422
C(2)–C(3)	1.397	B–C(3)	1.516	B–C(3)	1.530
C(3)–C(4)	1.384	C(3)–C(4)	1.363	C(3)–C(4)	1.350
C(4)–C(5)	1.390	C(4)–C(5)	1.424	C(4)–C(10)	1.442
C(5)–C(6)	1.386	C(5)–C(6)	1.356	C(10)–C(9)	1.408
C(6)–C(1)	1.387	C(6)–N	1.363	C(9)–N	1.380
C(α)–C(β)	1.328	C(α)–C(β)	1.331	C(α)–C(β)	1.331

The C(α)–C(β) bond lengths in BNSt and BN2VN are both predicted to be 1.331 Å long, on par with a typical C–C double bond (1.34 Å). Vinyl bond lengths between 1.317–1.326 Å are

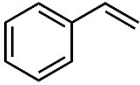
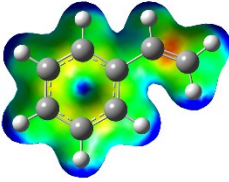
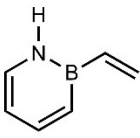
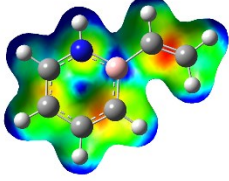
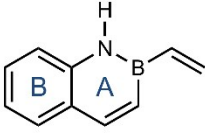
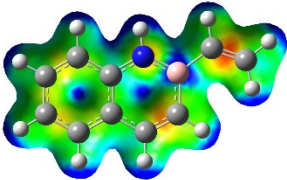
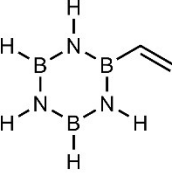
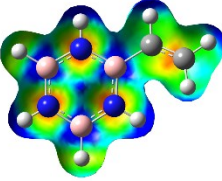
reported in crystal structures of related neutral *B*-vinyl compounds, supporting the validity of the predicted bond lengths.^{157,158}

Crystal structures of the vinyl monomers are not available to confirm the predicted bond lengths. BNSt is a volatile liquid. While we successfully grew large colorless plate-like crystals of BN2VN, diffraction was surprisingly poor as crystals barely diffracted beyond 1 Å (using both Mo and Cu K α radiation). Several attempts to collect data at different temperatures (110, 200 and 293 K) were carried out, but all lead to poor quality diffraction patterns. Strong decay of intensities at higher resolution may be explained by poor long-range order in the crystal.

5.2.2 NICS Calculations. Nucleus independent chemical shift (NICS) calculations^{159,160} are routinely used as a magnetic index of local aromaticity. NICS values give a quantitative correlation of aromaticity by computing magnetic shielding or deshielding of a ghost atom (Bq) at ring centers or any location of interest. The location of Bq influences the magnitude of the shielding or deshielding effect arising from ring current. Significantly negative NICS values denote aromaticity and diatropic ring currents, while significantly positive NICS values denote antiaromaticity and paratropic ring currents. NICS values close to 0 indicate a non-aromatic structure.

NICS values for BN2VN and several control structures were calculated as the negative value of the nuclear magnetic shielding computed at the geometric center of a ring (NICS(0)), by the gauge-independent atomic orbital (GIAO) method (Table 1.3).^{161–165} St exhibits the largest negative NICS values, while vinyl borazine (VB) has the least negative NICS values. BNSt and BN2VN, in which only one CC bond is substituted with a BN bond, are intermediate between these structures. The A-ring of BN2VN is less aromatic than the B-ring, but comparable to BNSt. Our results are consistent with prior computational work showing decreasing aromaticity with increasing BN substitution.^{28,153,166–169} Borazine (B₃N₃H₆)'s weak aromaticity is attributed to the greater polarity of the BN bond compared to the CC bond, which localizes electron density on the more electronegative N atom.^{121,170}

Table 5.3. Electrostatic potential (ESP) maps and NICS comparisons (ppm) of vinyl monomers. -10 kcal mol⁻¹ (red) to 70 kcal mol⁻¹ (blue).

Structure	ESP Map	NICS(0) A ring	NICS(1) A ring	NICS(0) B ring	NICS(1) B ring
		-8.24	-10.78	-	-
		-4.53	-6.56	-	-
		-3.22	-5.83	-9.62	-11.25
		-1.68	-2.63	-	-

Electrostatic potential (ESP) maps support our conclusions about relative aromaticity. The poor delocalization of electrons in VB is readily apparent from its ESP map: electron density is highly localized to the electronegative nitrogen atoms. BN2VN exhibits the characteristic polarization of aromatic compounds, with an electron deficient C–H edge and electron-rich surface above the plane of the ring. Electron-density is less uniformly distributed above the π face in BNSt and BN2VN than in St.

5.2.3 Bond Dissociation Energies. Relative trends in hydrocarbon C–H bond dissociation energies correlate with radical stability.¹⁷¹ The weakest C–H bond in toluene accurately predicts

that the most stable radical is formed at the benzylic position (**Figure 5.2a**).¹⁷² We investigated if BN aromatic rings exert a similar influence on bond dissociation energies as phenyl rings.

We selected BN 2-ethynaphthalene (BN2EtN) as a model system. Ethylbenzene (EtB) and BN 2-ethylbenzene (BNEtB) are included for comparison. Vibrational frequencies of fully geometry optimized closed-shell and radical structures were computed using the CAM-B3LYP functional with the 6-311G(d,p) basis set. From these data, theoretical gas phase bond dissociation enthalpies (BDEs, $\Delta_{\text{rxn}}H_{298}$) were calculated at 298.15 K from homolytic cleavage of various C–H and N–H bonds from enthalpy corrected energies (**Figure 5.2a**).^{173,174}

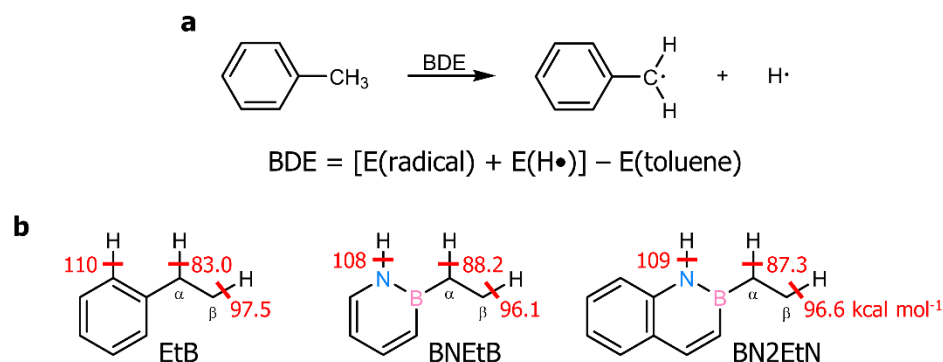


Figure 5.2. Reactive radical computations. a) BDE calculation, shown for the homolytic abstraction of a benzylic hydrogen atom from toluene. Energies used are the “Sum of electronic and thermal enthalpies” terms from vibrational frequency job outputs. b) Calculated BDEs for each indicated C–H or N–H bond for ethylbenzene (EtB), BN ethylbenzene (BNEtB), and BN 2-ethylnaphthalene (BN2EtN) (CAM-B3LYP/6-311G(d,p)).

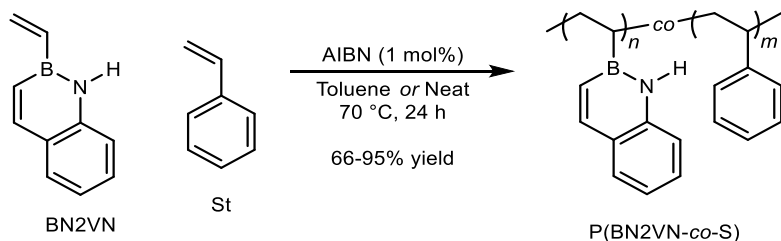
The calculated C–H BDEs of BN2EtN follow the trends consistent with our intuitive understanding of radical stabilization effects in hydrocarbons (**Figure 5.2b**). The C(α)–H bond has the lowest BDE (87.3 kcal mol⁻¹), followed by the C(β)–H bond (96.6 kcal mol⁻¹). The aryl C–H bonds are significantly stronger (106–111 kcal mol⁻¹) than alkyl C–H bonds, as is the N–H bond (109 kcal mol⁻¹). Qualitatively similar trends are observed with EtB and BNEtB where the BDE decreases in the order $\alpha < \beta < \text{aryl}$ (**Figure 5.2b**).

Carbon-centered alkyl radicals such as the α -cyanoisopropyl radical derived from AIBN or benzylic radicals arising from toluene (PhCH_2^\bullet) exclusively add to the tail position of styrene.¹⁷⁵ The calculated BDE's suggest that there is no energetic reason to expect an increase in head-addition or aromatic substitution with BN2VN.

5.3 BN2VN and Styrene Copolymerization

We investigated the free radical copolymerization of BN2VN and styrene with a focus on quantifying the incorporation of BN2VN. Polymerizations were conducted with azoisobutyronitrile (AIBN, 1 mol%) in toluene or in neat styrene (**Table 5.1**). Copolymerizations were conducted with feed ratios of 60 wt. %, 33 wt. %, or 14 wt. % BN2VN.

All polymerizations proceeded to >75% conversion. The use of toluene resulted in polymers of moderate molecular weight and dispersity (12.8-14.6 kDa, $\mathcal{D} = 1.72$ -1.88; **Table 5.4**). Similar results are obtained in a control reaction with styrene alone (PS_{129}). Gel permeation chromatography (GPC) curves of the polymers are unimodal, consistent with formation of a single copolymer instead of two homopolymers (**Figure 5.3**).



Scheme 5.1. Free radical co-polymerization of BN2VN and styrene (St). AIBN = 2,2'-azobis(2-methylpropionitrile).

Neat reaction conditions provided high molecular weight polymers with high molecular weight distributions (32.6-39.6 kDa, $\mathcal{D} = 4.23$ -5.40, Table 1). GPC curves show a shoulder at high molecular weight that contributes to the high dispersity (**Figure 5.3b**, shoulder indicated with a

black arrow). Homopolymerization of each monomer is unlikely as the shoulder is also observed in the PS control reaction. Additionally, the molecular weight distribution is unchanged when the absorbance wavelength is changed from 254 nm to 310 nm. Since PS is transparent at 310 nm, if two homopolymers were present, only one peak should be observed at 310 nm. Instead, we suggest that the shoulder is a consequence of the gel effect in which at high molecular weight, the slow diffusion of the viscous polymer results in accelerated chain growth.⁶¹

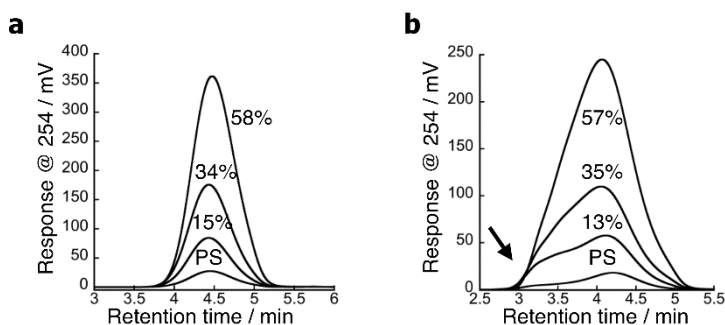


Figure 5.3. GPC curves of copolymers. a) Polymerization in toluene. Labels refer to the wt. % of BN2VN. b) Polymerization in neat styrene. Arrow indicates a high molecular weight shoulder.

Table 5.4. Optical and molecular weight properties of PBN2VN-*co*-PS and PS.

Entry	Sample Name ^a	Feed Ratio wt.% BN2VN	ϵ_{320} ^b	Experimental wt.% BN2VN ^c	M_n (kDa) ^d	\bar{D} ^d
1	P(BN2VN ₄₈ - <i>co</i> -S ₅₁) ^e	60	16.8	58	12.8	1.72
2	P(BN2VN ₃₂ - <i>co</i> -S ₉₂) ^e	33	9.74	34	14.5	1.75
3	P(BN2VN ₁₄ - <i>co</i> -S ₁₁₉) ^e	14	4.50	15	14.6	1.78
4	PS ₁₂₉ ^e	0	n.d.	n.d.	13.5	1.88
5	P(BN2VN ₁₂₇ - <i>co</i> -S ₁₄₁) ^f	60	16.4	57	34.4	4.23
6	P(BN2VN ₈₇ - <i>co</i> -S ₂₃₆) ^f	33	10.2	35	38.1	4.91
7	P(BN2VN ₃₂ - <i>co</i> -S ₃₃₂) ^f	14	3.79	13	39.6	5.40
8	PS ₃₁₃ ^f	0	n.d.	n.d.	32.6	5.03

^a Samples named according to copolymer composition determined by UV-vis spectroscopy. ^b Extinction coefficient at 320 nm (ϵ_{320}) in L g⁻¹ cm⁻¹. ^c Determined by UV-vis spectroscopy using Equation 5.1. ^d Measured by gel permeation chromatography (GPC) at 254 nm relative to polystyrene standard (THF, 0.35 mL min⁻¹, 40 °C). ^e Polymerization conditions: AIBN (1 mol%), toluene ([monomers]=10 M). ^f Polymerization conditions: AIBN (1 mol%), neat.

5.4 Determination of Copolymer Composition

In our prior work on BN2VN-2VN copolymerization, we described a UV-vis absorbance spectroscopy assay for BN2VN incorporation based on the differential absorption of naphthalene and BN-naphthalene at 320 nm.¹⁴³ A similar calibration curve was constructed for BN2VN and styrene (**Figure 5.4b**). A plot of extinction coefficient at 320 nm (ϵ_{320}) versus the wt. % PBN2VN in binary mixtures of the homopolymers yields a straight line. A linear regression analysis of the data yields eq. 1 in which X = the weight percent of BN2VN incorporation. Using the experimentally determined copolymer ϵ_{320} and eq. 5.1, the PBN2VN-*co*-PS samples were analysed for wt.% BN2VN incorporation. The experimentally determined incorporation closely matched the feed ratio (**Table 5.4**). Elemental analysis is consistent as well.

$$\epsilon_{320} = 28.2X + 0.208 \quad (\text{Eq. 5.1})$$

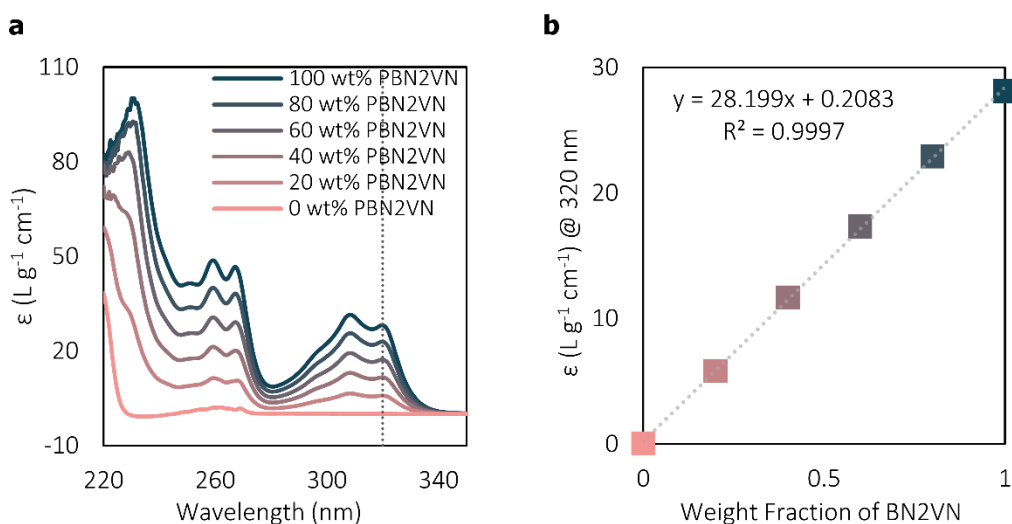


Figure 5.4. P(BN2VN-*co*-S) composition calibration. a) UV-Vis spectra of PBN2VN and PS homopolymers and blends. b) Calibration curve for BN2VN and styrene for determination of wt. % PBN2VN from extinction coefficient at 320 nm (ϵ_{320}).

5.5 Conclusion

Computational characterization of BN2VN aromaticity, including both structural parameters and NICS values give support for BN2VN and styrene coreactivity with radical copolymerization. The BN naphthalene side chain influences radical stabilities in a manner similar to the phenyl side chain in styrene. We report the preparation of BN2VN and styrene copolymers, as well as quantitative characterization of BN2VN incorporation via absorbance spectroscopy and elemental analysis.

A BN Aromatic Ring Strategy for Tunable Hydroxy Content in Polystyrene

6.1 Introduction

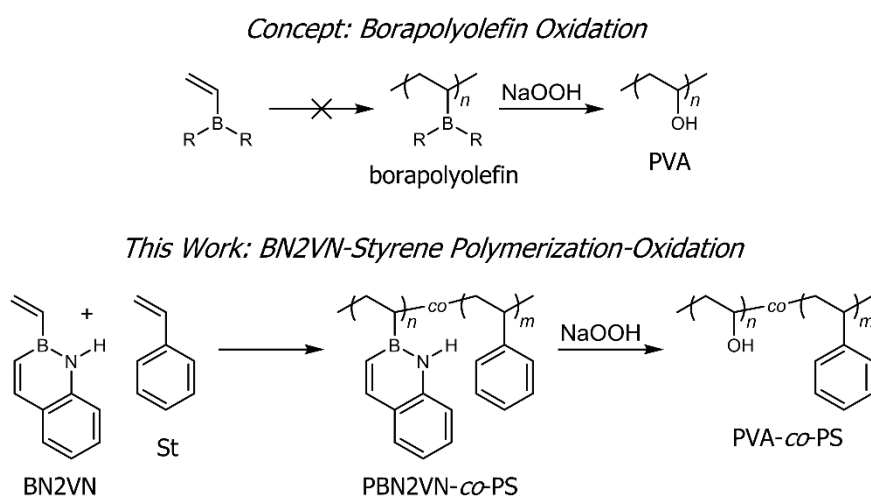
The incorporation of polar functional groups into nonpolar polymers is an essential strategy for modifying the strength, toughness, and solvent resistance of a polymeric material.^{82,83,176,177} Industrial examples include acrylonitrile-butadiene-styrene (ABS) and ethylene-vinyl acetate (EVA).^{5,84} Challenges in the copolymerization of nonpolar and polar monomers include phase separation,¹⁷⁸ significant differences in reactivity (reactivity ratios),^{61,179} and the limited compatibility of polar functional groups with polymerization catalysts.^{83,85-87}

6.2 Oxidative Strategy

Here we describe a synthetic strategy that converts a nonpolar BN aromatic group into a polar hydroxy substituent. This strategy ensures comonomer miscibility and compatible reactivity, while caging the potent reactivity of organoboranes within in a stable aromatic core, and accesses structures that are a challenge for existing technology. Our solution is based on the unique properties of 1,2-azaborines, aromatic rings in which one CC bond is replaced with the BN bond.^{112,113,133} Recognizing the versatility of organoboranes in synthesis,^{180,181} we hypothesized that sodium hydroperoxide (NaOOH) oxidation¹⁸² of a vinylborane polymer would yield derivatives of water-soluble poly(vinyl alcohol) (PVA) (Scheme 1). However, concerns about the hydrolytic and

oxidative stability of boron reagents, as well as the propensity of vinyl boronic acids to undergo protodeboronation,¹⁸³ have contributed to limited investigation of vinyl boronate polymerization.⁴⁹

BN2VN polymers are attractive candidates for investigating the proposed borapolyolefin oxidation due to the scalable monomer synthesis.^{51,143,146} Oxidative cleavage of the C-B bonds in PBN2VN-*co*-PS yields PVA-*co*-PS, a copolymer of nonpolar styrene and polar vinyl alcohol, in which the hydroxy content is tuned by the BN2VN content in the starting copolymer. The styrene-vinyl alcohol (SVA) statistical copolymer is not directly accessible from free radical copolymerization of styrene and vinyl acetate; styrene-enriched polymer is obtained due to the reactivity of the styrene radical relative to the vinyl acetate radical.⁸⁹



Scheme 6.1. Preparation of PVA derivatives via organoborane oxidation. St = styrene; BN2VN = BN 2-vinylnaphthalene; PVA = poly(vinyl alcohol).

6.3 Model Oxidation

The proposed oxidation was probed with model compound **1** (Figure 6.1). Upon treatment with NaOOH, complete conversion of **1** to two products of was observed within 10 minutes at 0 °C. ¹H NMR spectroscopic analysis of the unpurified reaction mixture and comparison to authentic samples supports the assignment of these products as indole **2** and phenethyl alcohol **3** (Figure 6.1). Indole is suggested to arise from oxidation of both C-B bonds of **1** to an intermediate

enol that tautomerizes and cyclizes. Liu *et al.* recently described oxidative functionalization of the exocyclic C-B bond of azaborines in which the alkyl fragment dimerizes.¹⁸⁴

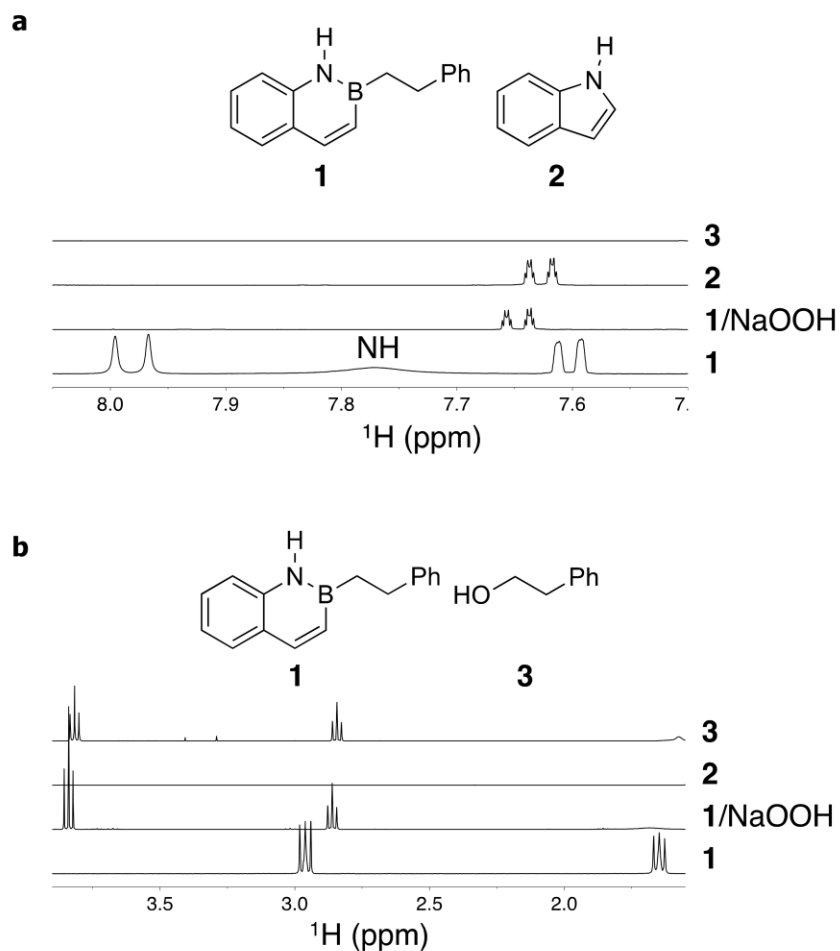


Figure 6.1. ¹H NMR analysis of NaOOH-mediated oxidation of compound **1** (CD₂Cl₂). Top to bottom: Phenethyl alcohol (**3**), indole (**2**), unpurified reaction mixture, **1**. a) Aromatic region. b) Aliphatic region.

6.4 BN2VN-Styrene Copolymer Oxidation

NaOOH oxidation of PBN2VN-*co*-PS copolymers was conducted. Data for P(BN2VN₃₂-*co*-S₉₂) are described here as a representative example (see published supplementary information for other copolymers). Reaction progress is monitored by GPC analysis at 310 nm. The loss of absorption at 310 nm before and after oxidation (**Figure 6.2c**) is consistent with cleavage of the BN2VN chromophore from the polymer. Extended reaction times and heating (15 h/65 °C) are required to observe >90% loss of signal at 310 nm. The need for forcing conditions is attributed to *in situ* cross-linking of the polymer with boric acid formed from oxidation of the azaborine (indole is also observed in crude reaction mixtures). During isolation, a methanol azeotrope removes boric acid as trimethyl borate.

Comparing GPC traces of oxidized P(BN2VN₃₂-*co*-S₉₂) measured by optical response at 310 nm versus refractive index (RI) provides compelling evidence that the polymer chains are intact. While no absorbance at 310 nm is observed after oxidation (**Figure 6.2c**), the RI data show a unimodal distribution and a modest decrease in molecular weight consistent with loss of the large BN naphthalene group (**Figure 6.2d**). Control reactions with PS₁₂₉ and PS₃₁₃ do not show a decrease in molecular weight. If unselective oxidation leading to backbone fragmentation were

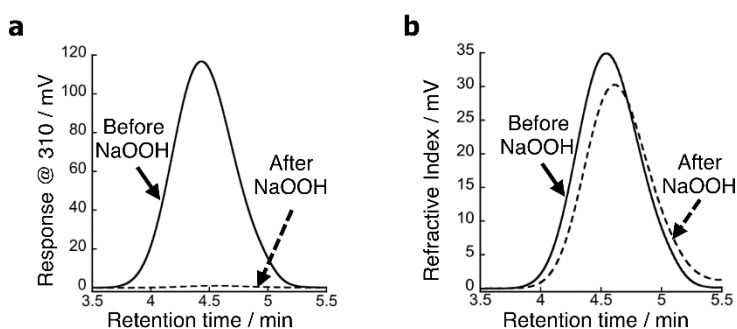


Figure 6.2. GPC curves of copolymers. a) Response by absorbance at 310 nm. GPC curves of PBN2VN₃₂-*co*-PS₉₂ before (solid) and after (dashed) NaOOH treatment. b) Response by refractive index. GPC curves of PBN2VN₃₂-*co*-PS₉₂ before (solid) and after (dashed) NaOOH treatment.

occurring, the GPC traces of the borapolyolefins and PS samples would no longer be unimodal. The intact macromolecular backbone is consistent with prior work by Chung and others on functionalization of polyethylene and polypropylene by hydroboration-oxidation of vinyl end groups^{82,185} or internal unsaturation arising from copolymerization with dienes.^{186–188} Table 1 summarizes the molecular weight characteristics of all polymers in this study before and after oxidation. Polymer fractionation during reisolation may be occurring, as the polymers exhibiting a high molecular weight shoulder (**Figure 6.2c**) show a narrower and more unimodal dispersity after reisolation.

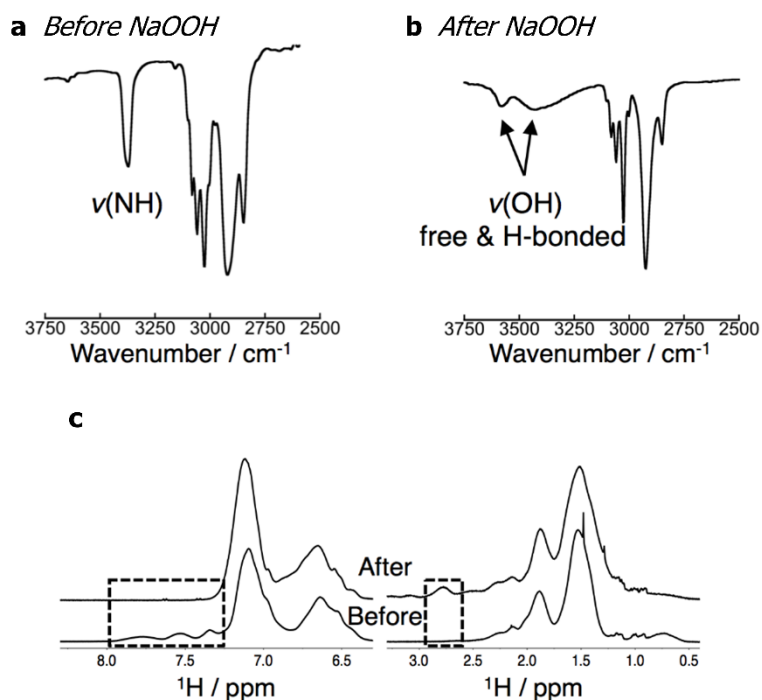


Figure 6.3. a) FTIR spectrum of P(BN2VN₃₂-co-S₉₂). b) FTIR spectrum of oxidized P(BN2VN₃₂-co-S₉₂). c) ¹H NMR spectra of P(BN2VN₃₂-co-S₉₂) before (bottom) and after (top) NaOOH treatment. The dashed box (left) highlights changes in the aromatic region. The dashed box (right) highlights the appearance of new signals at higher field after oxidation.

Infrared (IR) spectroscopy of the oxidized copolymers is consistent with a PVA-*co*-PS structure. PVA has several characteristic features in its IR spectrum, including a strong, broad OH stretching frequency at 3340 cm^{-1} .¹⁸⁹ Hydrogen-bonding is well known to broaden and shift the OH resonance to lower frequencies¹⁹⁰ and the unusually low frequency hydroxy resonance in PVA is attributed to strong hydrogen-bonding networks.¹⁸⁹ FTIR spectroscopic analysis of P(BN2VN₃₂-*co*-S₉₂) before and after NaOOH treatment shows significant changes (**Figure 6.3a-b**), including the loss of the NH stretching frequency, but retention of aromatic CH stretching frequencies consistent with polystyrene.¹⁹¹ After oxidation, two features consistent with an OH stretch are observed, a comparatively sharp resonance at 3570 cm^{-1} and a broader resonance at 3430 cm^{-1} (**Figure 6.3b**). These resonances are assigned to free OH and hydrogen-bonded OH groups, respectively. As the BN2VN content of the original copolymers increases, the resonance assigned to the hydrogen-bonded OH group broadens, intensifies, and shifts to even lower frequency, consistent with increased hydroxy content and increased hydrogen-bonding. There is no evidence of hydroxy groups in NaOOH-treated PS control samples.

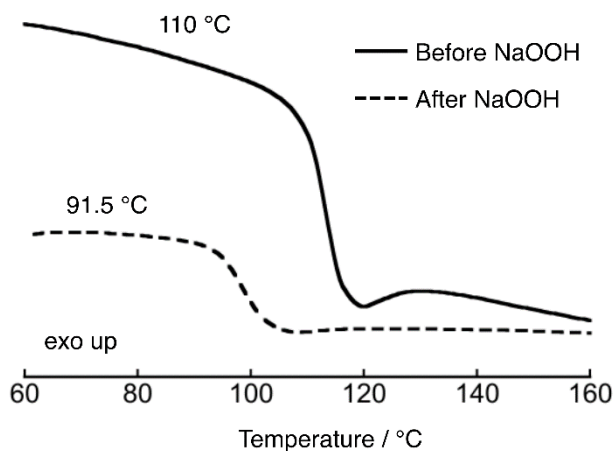


Figure 6.4. DSC curves of P(BN2VN₈₇-*co*-S₂₃₆) before (solid) and after (dashed) NaOOH treatment. The onset T_g is indicated.

^1H NMR spectra of P(BN2VN₃₂-*co*-S₉₂) before and after NaOOH treatment show disappearance of the BN2VN peaks in the aromatic region, but not the loss of styrenic signals in the aromatic region (left box, **Figure 6.3c**). In the aliphatic region, after NaOOH treatments new peaks are observed at 2.5-3.0 ppm that are not observed in the borapolyolefin (right box, **Figure 6.3c**). These peaks are assigned to protons adjacent to hydroxy functionality. This assignment is consistent with the greater than 2.0 ppm change in chemical shift of the protons adjacent to the boron atom upon oxidation to phenethyl alcohol observed in model system **1** (**Figure 6.1**).

The white powdery SVA copolymers exhibit physical properties that vary with hydroxy content, including miscibility with polar, protic solvents and glass transition temperature (T_g). While low hydroxy content polymers like P(BN2VN₁₄-*co*-S₁₁₉) are purified by precipitation into methanol, polymers with higher hydroxy content are soluble in methanol and must be isolated by precipitation into water. Glass transition temperatures (T_g 's) were determined by differential scanning calorimetry (DSC). Borapolyolefin P(BN2VN₈₇-*co*-S₂₃₆) has a single glass transition with an onset at 110 °C. The observation of a single T_g intermediate between PS (104 °C) and PBN2VN (129 °C) is consistent with a statistical copolymer. After NaOOH treatment, a single T_g is observed intermediate between PS (104 °C) and PVA (85 °C) and significantly lower than PBN2VN (Figure 6.4).

6.5 Conclusion

BN2VN, a BN aromatic vinyl monomer, exhibits styrene-like reactivity and forms statistical St-BN2VN copolymers under free radical conditions. Chemoselective organoborane oxidation providing novel SVA statistical copolymers is demonstrated. The hydroxy content is tuned by the starting BN2VN content. This synthetic strategy opens up a pathway for modulating the properties of two industrially relevant polymers, PS and PVA. The concept of oxidizing a protected borane is not limited to the statistical copolymers described herein and BN2VN copolymers represent a platform for the preparation of diverse polymeric architectures via the remarkable chemistry of C-B bonds.

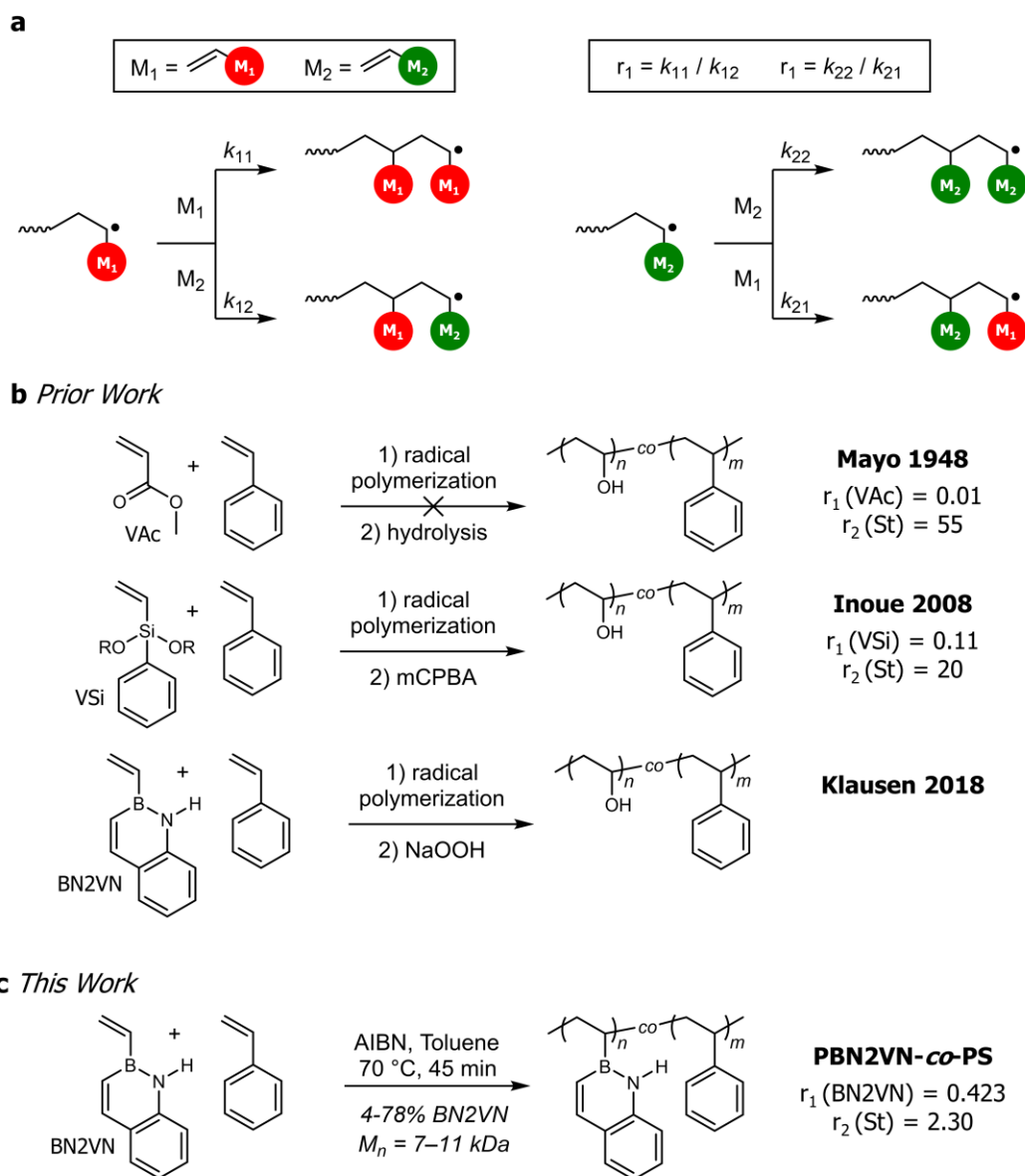
7.1 Introduction

We show in Chapter 5 that the unusual aromaticity of the BN heterocycle leads to styrene-like reactivity. Computational data including structural parameters and nucleus independent chemical shift (NICS) values support the aromaticity of the BN naphthalene side chain of BN2VN. This work outlines design principles for the synthesis of tailored polymeric styrene-vinyl alcohol architectures.

Poly(vinyl alcohol) (PVA) is a widely used water-soluble coating and adhesive via cross-linking with boric acid.⁹⁰ It is commercially synthesized by free radical polymerization of vinyl acetate (VAc), followed by hydrolysis. While PVA's physical properties such as solvent resistance, crystallinity, and toughness are in principle modulated by incorporation of nonpolar groups, the reactivity mismatch between VAc and conjugated monomers complicates the synthesis of hydroxy-functionalized polymers by direct radical copolymerization.^{82,88,89}

The copolymerization behavior of two monomers M_1 and M_2 is described by their reactivity ratios r_1 and r_2 , which indicate the propagation preference of each monomer (**Scheme 7.1a**).¹⁷⁹ The reactivity ratio r_1 is the ratio of the rate constants (k_{11}/k_{12}) for addition of M_1 or M_2 to an M_1 -terminated polymer. Likewise, the reactivity ratio r_2 is the ratio of the rate constants (k_{22}/k_{21}) for addition of M_2 or M_1 to an M_2 -terminated polymer. A large reactivity ratio r_1 indicates a strong

preference for homopolymerization, while a reactivity ratio r_1 significantly less than 1 indicates a strong preference for cross-polymerization. Ideal copolymerization is observed when the product of the reactivity ratios is 1.⁶¹



Scheme 7.1. Reactivity ratios in vinyl comonomers. a) Reactivity ratios for a comonomer pair M_1 and M_2 . b) Prior work on the synthesis of styrene-vinyl alcohol copolymers: extreme reactivity mismatch between vinyl acetate (VAc) and styrene (St) or vinyl silanes (VSi) results in zero or low hydroxy content, while BN2VN leads to high hydroxy content. c) This work: determination of the reactivity ratios of BN2VN and St.

VAc and St are an example of an extremely mismatched comonomer pair in which the rate of cross-polymerization is essentially zero (**Scheme 7.1b**). The reactivity ratios $r_1(\text{VAc}) = 0.01$ and $r_2(\text{St}) = 55$ indicate that both St- and VAc-terminated polymers strongly prefer to add St.⁸⁹ Instead of copolymerization, consecutive homopolymerization is observed: St is polymerized first and when consumed, VAc homopolymerization is initiated. Low concentrations of St, initiator concentration inhibit VAc polymerization by consuming all initiator.⁸⁸ The structural dissimilarity of St and VAc contributes to the reactivity mismatch: while the St-terminated polymeric radical is significantly resonance stabilized, the VAc-terminated polymer is not.

We recently reported a solution to the challenging St-VAc radical copolymerization. The free radical copolymerization of St and BN 2-vinylnaphthalene (BN2VN), followed by sodium hydroperoxide (NaOOH) oxidation, provided statistical styrene-vinyl alcohol copolymers (**Scheme 7.1c**).^{36,192} Evidence for a statistical copolymer includes the observation of a single glass transition temperature (T_g) intermediate between PBN2VN and polystyrene (PS), as well as a single T_g intermediate between PVA and PS in oxidized samples.

BN2VN is a unique vinylborane due to the aromaticity of the 10 π electron BN naphthalene ring system (**Scheme 7.1c**). The Hückel aromaticity of cyclic conjugated BN materials^{112,193} is well-established on the basis of resonance stabilization energy,¹⁹⁴ electronic structure,¹¹⁹ and magnetic properties.^{28,119,169,195} Building on Sneddon's early work on vinyl borazine (VB) polymerization,¹⁹⁶⁻¹⁹⁸ several groups have recently explored BN for CC bond substitution in polymer backbones,¹⁷⁻²² conjugated polymers,^{23,24,199} or in aromatic side chains.^{31,32,36,192}

While in principle any organoborane is a precursor to PVA via oxidation, BN2VN is attractive in several respects. BN2VN is stable to bench-top handling, whereas many organoboranes are air- and water-sensitive and prone to cross-linking.^{48,49} We attribute BN2VN's increased stability to the aromatic cage surrounding the central boron atom. A high-throughput two-step synthesis of BN2VN makes multigram scale polymerization possible.¹⁹² Monocyclic BN aromatic heterocycles currently require multistep syntheses,^{43,44,113,193,200} which limits polymerizations to the milligram scale.^{31,32} VB

polymerization is hampered by polymer crosslinking arising from thermal dehydrogenative coupling of the inorganic side chain and hydrolytic instability.^{46,196,197}

BN2VN's aromaticity enables compatible reactivity with St and high copolymer hydroxy content. For example, while vinylsilanes are typically more bench stable than vinylboronates, these lack aromatic character. Inoue et al. reported an alkoxyvinylsilane monomer (VSi) for styrene copolymerization that yields vinyl alcohol derivatives after Tamao–Fleming oxidation.²⁰¹ VSi incorporation is limited by mismatched reactivity ratios [$r_1(\text{VSi}) = 0.11$, $r_2(\text{St}) = 20$] (Scheme 1b).²⁰²

Herein we characterize BN2VN's aromaticity and measure well-matched St and BN2VN reactivity ratios by traditional linearization methods and modern nonlinear least squares methods (NLLS: $r_1(\text{BN2VN}) = 0.423$, $r_2(\text{St}) = 2.30$; $r_1r_2 = 0.97$). Quantitative assessment of BN2VN and St reactivities enables fine control of copolymerization and the design of tailored styrene-vinyl alcohol copolymers.

7.2 Determination by Linearization Methods

Reactivity ratios for radical copolymerizations following the terminal model are traditionally calculated by linearization of the copolymer equation (**Equation 7.1**) where f_1 is the mole fraction of M_1 in the feed, $f_2 = 1 - f_1$, F_1 is the mole fraction of M_1 in the copolymer and F_2 is the mole fraction of M_2 in the copolymer.

$$F_1 = \frac{r_1 f_1^2 + f_1 f_2}{r_1 f_1^2 + 2 f_1 f_2 + r_2 f_2^2} \quad (\text{Eq. 7.1})$$

However, several assumptions underlying the linearization methods introduce significant systemic error, resulting in highly variable estimates of copolymerization reactivity ratios.^{203,204} Nonlinear least squares (NLLS) fitting is the most statistically accurate method for estimating reactivity ratios.²⁰⁵ We describe initial estimation of St and BN2VN reactivity ratios based on the Fineman–Ross and Kelen–Tüdös linearization methods and then a NLLS analysis of the copolymerization data. Good agreement is observed between the three methods.

In the Fineman–Ross²⁰⁶ method (**Equation 7.2**) for linearization of the copolymer equation, several copolymerizations with different ratios of the two monomers are carried out to low conversion and the composition of the copolymers is determined.

$$\frac{f_1(2F_1-1)}{(1-f_1)F_1} = \frac{f_1^2(1-F_1)}{(1-f_1)^2F_1} r_1 - r_2 \quad (\text{Eq. 7.2})$$

A plot of G versus H yields a straight line with slope r_1 and y-intercept $-r_2$, where G and H are

$$G = \frac{f_1(2F_1-1)}{F_1(1-f_1)} \quad H = \frac{f_1^2(1-F_1)}{(1-f_1)^2F_1}$$

A disadvantage of the Fineman–Ross method is that low or high values of f_1 disproportionately influence the analysis. The Kelen–Tüdös method addresses this limitation by adding an arbitrary correction factor α that uniformly distributes data points.²⁰⁷ The reactivity ratios r_1 and r_2 are determined by a fit of the experimental data to equation 3

$$\eta = [r_1 + (r_2/\alpha)]\xi - (r_2/\alpha) \quad (\text{Eq. 7.3})$$

where η , ξ and α are:

$$\eta = \frac{G}{\alpha + H} \quad \xi = \frac{H}{\alpha + H} \quad \alpha = \sqrt{H_{\min}H_{\max}}$$

The plot of η versus ξ gives a straight line with intercepts $-r_2/\alpha$ and r_1 when $\xi = 0$ and $\xi = 1$ respectively.

Copolymerization of BN2VN and St ($\frac{f_1}{f_2} = 0.111-9.00$) was performed with 2,2'-azobis(2-methylpropionitrile) (AIBN) as the radical initiator at 70 °C in toluene for 45 minutes. Polymerizations were quenched at low conversion (3-7%) by precipitation into methanol. Copolymer composition was analyzed by two independent techniques, absorbance spectroscopy and elemental analysis.

As previously reported, the unique absorbance at 320 nm of the BN naphthalene chromophore enables a UV-vis assay for quantitative determination of BN2VN content in a copolymer.^{36,192} The absorption at 320 nm is measured for a series of different blends of PS and PBN2VN. A plot of the extinction coefficient at 320 nm (ϵ_{320}) versus the weight fraction of PBN2VN in the blend (X_{BN2VN}) is a straight line and linear regression provides equation 4 (Figure 5.5b).

$$\chi_{BN2VN} = \frac{\epsilon_{320}-0.208}{28.2} \quad (\text{Eq. 7.4})$$

The fractional composition of BN2VN in a copolymer is calculated using equation 4 from the copolymer's extinction coefficient at 320 nm (ϵ_{320}). UV-vis spectra of copolymer solutions were recorded in THF at room temperature.

BN2VN composition can also be determined by elemental analysis. **Equation 7.5** describes the relationship between weight percent of carbon (wt% C) in a copolymer and the weight fraction BN2VN.

$$\chi_{BN2VN} = -\frac{\text{wt\% C} - 92.3}{14.8} \quad (\text{Eq. 7.5})$$

Table 7.1 summarizes copolymer characteristics. Good agreement is observed between both analytical methods with respect to determination of F_{BN2VN} , the fractional composition of BN2VN in the copolymer. Reactivity ratios determined using the Fineman–Ross method (**Figure 7.1a**) and the Kelen–Tüdös method (**Figure 7.1b**) support an ideal radical copolymerization ($r_1 r_2 = 1$) in which St is somewhat more reactive than BN2VN. Four separate estimates of the reactivity ratios are obtained by analysis of each set of experimental data by both linearization methods (**Table 7.2**). In all cases, r_1 (BN2VN) is close to 0.5 (0.390-0.531), r_2 (St) is close to 2 (2.09-2.50), and the product of the reactivity ratios ($r_1 r_2$) is close to 1.0 (0.815–1.33).

Table 7.1. Low conversion P(BN2VN-*co*-S) molecular weight characteristics.

Entry	Sample Name ^a	Yield	M _n (kDa) ^b	Đ ^b	ε ₃₂₀ ^c
1	P(BN2VN ₄ - <i>co</i> -S ₁₀₃)	6.2%	11.4	1.48	1.90
2	P(BN2VN ₁₀ - <i>co</i> -S ₈₆)	6.5%	10.4	1.50	4.26
3	P(BN2VN ₁₅ - <i>co</i> -S ₈₁)	5.2%	10.8	1.53	6.44
4	P(BN2VN ₂₀ - <i>co</i> -S ₇₀)	5.3%	10.4	1.48	8.59
5	P(BN2VN ₂₅ - <i>co</i> -S ₆₁)	4.9%	10.3	1.48	10.9
6	P(BN2VN ₃₂ - <i>co</i> -S ₄₆)	4.7%	9.63	1.46	14.5
7	P(BN2VN ₃₈ - <i>co</i> -S ₃₅)	3.4%	9.53	1.44	17.5
8	P(BN2VN ₄₁ - <i>co</i> -S ₂₀)	3.8%	8.39	1.38	21.5
9	P(BN2VN ₃₉ - <i>co</i> -S ₁₁)	3.9%	7.22	1.34	23.9

^a Samples are named according to average degree of polymerization (\overline{DP}) of each monomer.

^b Determined by GPC analysis at 254 nm relative to a polystyrene standard. ^c In L g⁻¹ cm⁻¹.

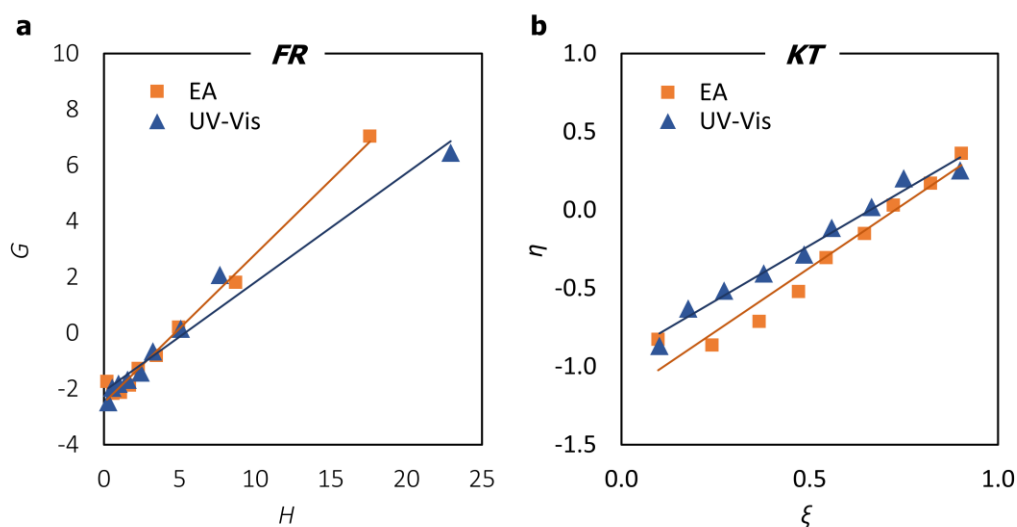


Figure 7.1. Determination of reactivity ratios for the copolymerization of BN2VN and St by the a) Fineman-Ross (FR) method and b) Kelen–Tüdös (KT) method.

Table 7.2. Copolymer Parameters for Linear Determination of Reactivity Ratios.

Entry	Sample Name	f_{BN2VN}	$F_{BN2VN}(UV-Vis)^a$	$F_{BN2VN}(EA)^b$
1	P(BN2VN ₄ -co-S ₁₀₃)	0.100	0.0411	0.0568
2	P(BN2VN ₁₀ -co-S ₈₆)	0.200	0.101	0.0965
3	P(BN2VN ₁₅ -co-S ₈₁)	0.300	0.160	0.148
4	P(BN2VN ₂₀ -co-S ₇₀)	0.400	0.221	0.213
5	P(BN2VN ₂₅ -co-S ₆₁)	0.500	0.292	0.309
6	P(BN2VN ₃₂ -co-S ₄₆)	0.600	0.409	0.395
7	P(BN2VN ₃₈ -co-S ₃₅)	0.700	0.516	0.521
8	P(BN2VN ₄₁ -co-S ₂₀)	0.800	0.675	0.643
9	P(BN2VN ₃₉ -co-S ₁₁)	0.900	0.779	0.819

^a Determined by UV-vis from ϵ_{320} according to **Equation 7.4**. ^b Determined by elemental analysis (EA) from wt% C according to **Equation 7.5**.

Table 7.2. Reactivity ratios BN2VN and styrene via linearization methods.

	Fineman–Ross		Kelen–Tüdös	
	UV-Vis	EA	UV-Vis	EA
r_1 (BN2VN)	0.390	0.531	0.477	0.445
r_2 (St)	2.09	2.50	2.39	2.25
$r_1 \cdot r_2$	0.815	1.33	1.14	1.00

7.3 Determination by NLLS Method

The Mayo–Lewis plots of the fractional composition of BN2VN in the copolymer (F_{BN2VN}) versus the fractional composition of BN2VN in the monomer feed (f_{BN2VN}) for both analytical methods are shown in Figures 4a-b. The dashed line indicates the linear behavior expected from a random (Bernoullian) copolymerization in which both monomers are equally reactive ($r_1 = r_2 = 1$). Data analysis by van Herk’s NLLS method²⁰⁵ yielded estimates of the reactivity ratios r_1 (BN2VN) and r_2 (St) and a 95% joint confidence interval (JCI, **Figure 7.5c-d**). Point estimates of the reactivity ratios derived from linearization methods are included and fall within the confidence interval, with the exception of Fineman–Ross reactivity ratios derived from UV-vis spectroscopy.

Based on the NLLS data analysis, we report r_1 (BN2VN) = 0.517 and r_2 (St) = 2.46 (UV-vis) and r_1 (BN2VN) = 0.423 and r_2 (St) = 2.30 (EA). This is a dramatic narrowing of the difference in reactivity between styrene and a vinyl alcohol precursor compared to prior state of the art (**Table 7.3**).

Table 7.3. Comparison of reactivity ratios in vinyl alcohol precursor and styrene copolymerization.

Vinyl Alcohol Precursor	r_1 (Precursor)	r_2 (St)	Reference
VAc	0.01	55	89
VSi	0.11	20	202
BN2VN	0.52, UV-vis 0.42, EA	2.5, UV-vis 2.3, EA	This work

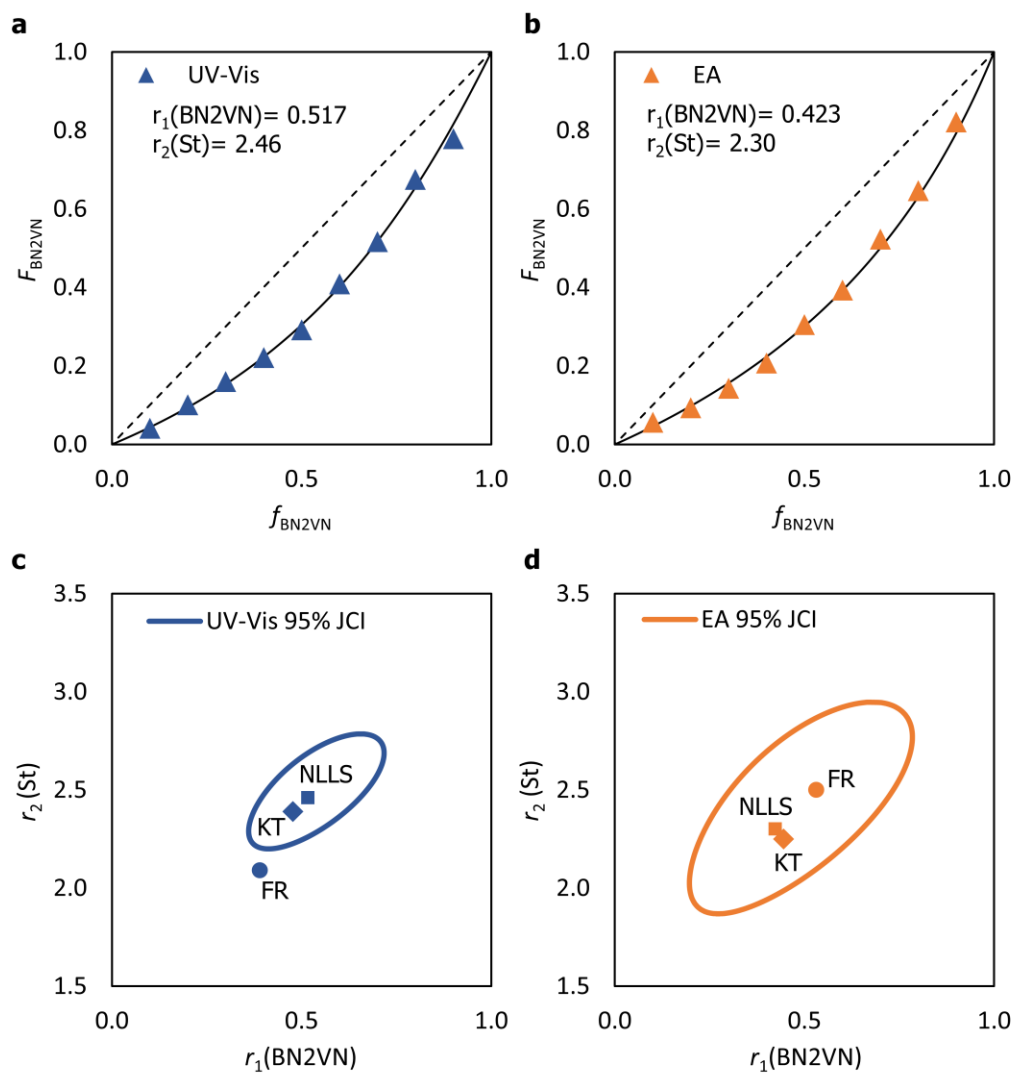


Figure 7.5. Mayo–Lewis plots of the fractional composition of BN2VN in the copolymer (F_{BN2VN}) versus the fractional composition of BN2VN in the monomer feed (f_{BN2VN}) determined by a) UV-vis spectroscopy and b) elemental analysis. The dashed line indicates the linear behavior expected from a random copolymerization ($r_1 = r_2 = 1$); the solid line indicates behavior for the respectively labeled reactivity ratios. NLLS determined 95% joint confidence intervals (JCI's) and point estimates of the reactivity ratios derived by NLLS and linearization methods from c) UV-vis and d) elemental analysis data.

7.4 Insights into Polymer Microstructure

The BN2VN and St reactivity ratios ($r_1 < 1 < r_2$; $r_1 r_2 = 1$) belong to the special case of an ideal copolymerization in which the monomers do not have equal reactivities. An ideal copolymerization occurs when the propagating species has no preference for one monomer over another and implies that the product of the reactivity ratios $r_1 r_2$ must be 1 ($k_{11} = k_{21}$ and $k_{22} = k_{12}$).

$$r_1 r_2 = \frac{k_{11}}{k_{12}} \times \frac{k_{22}}{k_{21}} = 1$$

A subset of ideal copolymerizations occurs when $r_1 = r_2 = 1$ (both monomers are equally reactive) and a random copolymer with an equal distribution of monomers results. An ideal copolymerization is still possible with monomers with unequal reactivities ($r_1 < 1 < r_2$). In this case, at low conversion, a statistical copolymer is expected that is enriched in the more reactive monomer (e.g. St).

The glass transition temperature (T_g) is a probe of copolymer microstructure. A diblock copolymer has two T_g 's corresponding to the homopolymer T_g , while a statistical copolymer has a single T_g intermediate between the homopolymers. A gradient copolymer has a single T_g , typically wider than the homopolymers. While ^{13}C NMR spectroscopy is typically used for copolymer sequence analysis, the relaxation rate of the quadrupolar boron-11 nucleus ($I = 3/2$) negatively influences the ^{13}C NMR signals of boron-adjacent carbon atoms, resulting in a drastic reduction in signal height.²⁰⁸

T_g 's of the St-BN2VN copolymers were determined by differential scanning calorimetry (DSC) under nitrogen (Figure 5a). All copolymers show a single narrow T_g intermediate between PS₁₅₉ ($T_g = 96$ °C, $M_n = 16.5$ kDa)²⁰⁹ and PBN2VN₁₃₂ ($T_g = 135.2$ °C, $M_n = 20.4$ kDa),³⁶ which increases with increasing BN2VN content (**Figure 7.5a**). Good agreement is observed between experimental T_g 's (triangles) and predicted T_g (dashed line, Figure 5b and Table 7).²¹⁰ Minor deviations from prediction (± 7 °C) may reflect the lower molecular weights of the samples in this study ($M_n = 7.22 - 11.4$ kDa) compared to the PBN2VN reference and instrumental error (3-10 °C at a heating rate of 10 °C min⁻¹).²¹¹

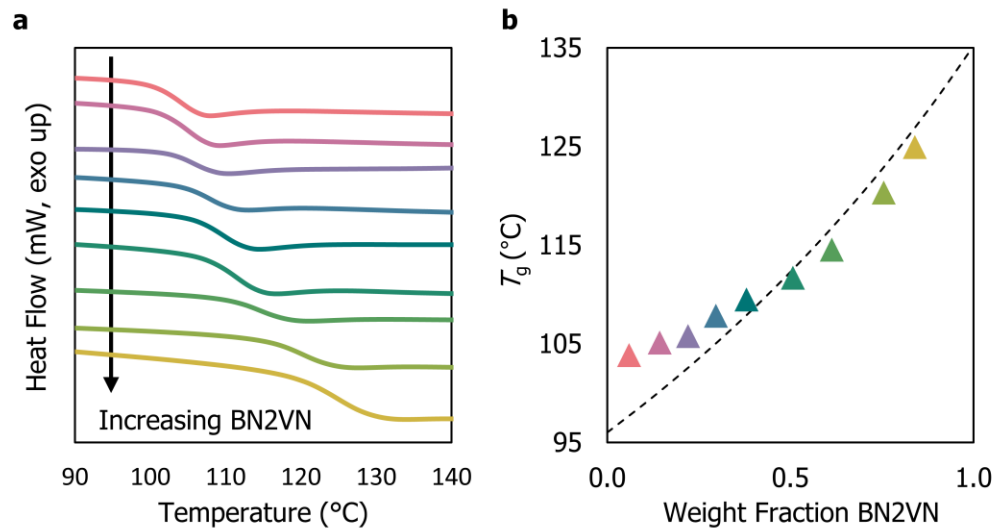


Figure 7.6. Low conversion P(BN2VN-*co*-S) thermal properties. a) Differential scanning calorimetry (DSC) thermograms of P(BN2VN₄-*co*-S₁₀₃), P(BN2VN₁₀-*co*-S₈₆), P(BN2VN₁₅-*co*-S₈₁), P(BN2VN₂₀-*co*-S₇₀), P(BN2VN₂₅-*co*-S₆₁), P(BN2VN₃₂-*co*-S₄₆), P(BN2VN₃₈-*co*-S₃₅), P(BN2VN₄₁-*co*-S₂₀), and P(BN2VN₃₉-*co*-S₁₁). b) Dependence of glass transition temperature (T_g , point of inflection) on the weight fraction BN2VN in the copolymers. Predicted T_g (dashed line) calculated using the Fox equation.²¹⁰

Table 7.4. Comparison of experimental and predicted T_g 's.

Entry	Polymer	wt% BN2VN ^a	Experimental T_g (°C) ^b	Predicted T_g (°C) ^c
1	P(BN2VN ₄ - <i>co</i> -S ₁₀₃)	6.0	104	97
2	P(BN2VN ₁₀ - <i>co</i> -S ₈₆)	14	105	100
3	P(BN2VN ₁₅ - <i>co</i> -S ₈₁)	22	106	102
4	P(BN2VN ₂₀ - <i>co</i> -S ₇₀)	30	108	104
5	P(BN2VN ₂₅ - <i>co</i> -S ₆₁)	38	109	106
6	P(BN2VN ₃₂ - <i>co</i> -S ₄₆)	51	112	110
7	P(BN2VN ₃₈ - <i>co</i> -S ₃₅)	61	115	114
8	P(BN2VN ₄₁ - <i>co</i> -S ₂₀)	76	120	119
9	P(BN2VN ₃₉ - <i>co</i> -S ₁₁)	84	125	122

^a Determined by UV-vis from ϵ_{320} according to **Equation 7.4**. ^b Point of inflection of the glass transition. ^c Predicted T_g calculated using the Fox equation.²¹⁰

Characterization is consistent with the predicted St-enriched statistical copolymer. Bulk composition data show St-enrichment compared to the feed ratio in all samples (see **Table 7.4**), while the observation of a narrow glass transition intermediate between PS and PBN2VN is consistent with a statistical sequence distribution.

7.5 Conclusion

The data presented in this paper show that aromaticity results in well-matched reactivity ratios between styrene and a vinyl alcohol precursor. The reactivity ratios $r_1(\text{BN2VN})$ and $r_2(\text{St})$ were determined by traditional linearization and modern NLLS statistical methods using two independent analytical techniques, elemental analysis and UV-vis spectroscopy. Compared to other comonomer pairs (e.g. St-VAc or St-VSi), St and BN2VN have the reactivity ratios closest to a random copolymerization.

Our results support the development of tailored styrene-vinyl alcohol copolymer architectures, while minimizing the use of excess monomer. The relationship between organoborane structure and reactivity suggests design principles for well-matched reactivity between hybrid and organic vinyl monomers.

I.1. General Methods

- I.1.1 Instrumentation
- I.1.2 Statistical Methods
- I.1.3 Computational Methods
- I.1.4 Materials

I.2. Experimental Details for Chapter 2: BN Anthracenes

- I.2.1 Synthesis of BN Anthracenes 1a-h
 - General Procedure A*
 - 2-(4-Methoxyphenyl)-1,2-Dihydronaphtho[2,3-e][1,2]-Azaborinine (1a)
 - 2-(p-Tolyl)-1,2-Dihydronaphtho[2,3-e][1,2]-Azaborinine (1b)
 - 2-Phenyl-1,2-Dihydronaphtho[2,3-e][1,2]-Azaborinine (1c)
 - 2-(4-Fluorophenyl)-1,2-Dihydronaphtho[2,3-e][1,2]-Azaborinine (1d)
 - 2-(4-Chlorophenyl)-1,2-Dihydronaphtho[2,3-e][1,2]-Azaborinine (1e)
 - 2-(4-(Trifluoromethyl)Phenyl)-1,2-Dihydronaphtho[2,3-e][1,2]-Azaborinine (1f)
 - 4-(Naphtho[2,3-e][1,2]Azaborinin-2(1H)-yl)Benzonitrile (1g)
 - 2-(4-Nitrophenyl)-1,2-Dihydronaphtho[2,3-e][1,2]-Azaborinine (1h)
- I.2.2 Synthesis of Mes BN Anthracene 1i
 - 2-Mesityl-1,2-Dihydronaphtho[2,3-e][1,2]Azaborinine (Mes BN Anthracene, 1i)
- I.2.3 Synthesis of BN Anthracene
 - 1,2-Dihydronaphtho[2,3-e][1,2]Azaborinine (BN Anthracene)
- I.2.4 Synthesis of 2-Arylanthracenes 8a-c
 - General Procedure B*
 - 2-Phenylanthracene-9,10-Dione (7a)
 - 2-(p-Tolyl)Anthracene-9,10-Dione (7b)
 - 2-(4-Fluorophenyl)Anthracene-9,10-Dione (7c)
 - General Procedure C*
 - 2-Phenylanthracene (4-H Ph Anthracene, 8a)
 - 2-(p-Tolyl)Anthracene (4-Me Ph Anthracene, 8b)
 - 2-(4-Fluorophenyl)Anthracene (4-F Ph Anthracene, 8c)

I.3. Experimental Details for Chapter 3: BN 2-Vinylnaphthalene (BN2VN) and Polymers

- I.3.1 BN2VN Monomer Synthesis
 - 2-Aminostyrene (2)
 - Small Scale: 2-Vinyl-1,2-Dihydrobenzo[e][1,2]Azaborinine (BN2VN)
 - Large Scale: 2-Vinyl-1,2-Dihydrobenzo[e][1,2]Azaborinine (BN2VN)

- I.3.2 BN2VN Polymerization
 - PBN2VN₃₉ (Toluene Polymerization)
 - PBN2VN₅₇ (Neat Polymerization)

I.4. Experimental Details for Chapter 4: BN2VN and 2-Vinylnaphthalene (2VN) Copolymers

- I.4.1 Copolymerization of BN2VN and 2VN
 - General Procedure D*
 - PBN2VN₃₉
 - P(BN2VN₇₄-CO-2VN₂₆)
 - P(BN2VN₄₉-CO-2VN₅₁)
 - P(BN2VN₉-CO-2VN₉₁)
 - P2VN₅₄

I.5. Experimental Details for Chapter 5: BN2VN and Styrene Copolymers

- I.5.1 Copolymerization of BN2VN and Styrene
 - General Procedure E*
 - PBN2VN₁₃₂
 - P(BN2VN₁₂₇-CO-S₁₄₁)
 - P(BN2VN₈₇-CO-S₂₃₆)
 - P(BN2VN₃₂-CO-S₃₃₂)
 - PS₃₁₃
 - General Procedure F*
 - P(BN2VN₄₈-CO-S₅₁)
 - P(BN2VN₃₂-CO-S₉₂)
 - P(BN2VN₁₄-CO-S₁₁₉)
 - PS₁₂₉

I.6. Experimental Details for Chapter 6: Polymer Side Chain BN Oxidation

- I.6.1 Small Molecule Oxidation Study
 - Potassium Phenethyltrifluoroborate
 - 2-Phenethyl-1,2-Dihydrobenzo[e][1,2]Azaborinine (1)
 - Oxidation of 2-Phenethyl-1,2-Dihydrobenzo[e][1,2]Azaborinine (1)
- I.6.2 Polymer Oxidation Study
 - General Procedure G*
 - Oxy. P(BN2VN₁₂₇-CO-S₁₄₁)
 - Oxy. P(BN2VN₈₇-CO-S₂₃₆)
 - Oxy. P(BN2VN₃₂-CO-S₃₃₂)
 - Oxy. PS₃₁₃
 - Oxy. P(BN2VN₄₈-CO-S₅₁)
 - Oxy. P(BN2VN₃₂-CO-S₉₂)
 - Oxy. P(BN2VN₁₄-CO-S₁₁₉)
 - Oxy. PS₁₂₉

I.7. Experimental Details for Chapter 7: Reactivity Ratios of BN2VN and Styrene

- I.7.1 Low Conversion BN2VN and Styrene Copolymerization

General Procedure H

P(BN2VN₄-CO-S₁₀₃)

P(BN2VN₁₀-CO-S₈₆)

P(BN2VN₁₅-CO-S₈₁)

P(BN2VN₂₀-CO-S₇₀)

P(BN2VN₂₅-CO-S₆₁)

P(BN2VN₃₂-CO-S₄₆)

P(BN2VN₃₈-CO-S₃₅)

P(BN2VN₄₁-CO-S₂₀)

P(BN2VN₃₉-CO-S₁₁)

I.1 General Methods

I.1.1 Instrumentation: ¹H NMR, ¹¹B NMR, and ¹³C {¹H} NMR spectra were recorded on a Bruker UltraShield Avance I 400 MHz spectrometer, the ¹⁹F NMR spectrum was recorded on a Bruker UltraShield Avance I 300 MHz spectrometer, and chemical shifts are reported in parts per million (ppm). Spectra were recorded in dichloromethane-*d*₂ or acetonitrile-*d*₃ with the residual solvent peak as the internal standard (¹H NMR: CH₂Cl₂, δ = 5.32 ppm; CH₃CN, δ = 1.94 ppm. ¹³C NMR: CH₂Cl₂, δ = 53.84 ppm; CH₃CN, δ = 1.39 ppm). ¹¹B NMR spectra are externally referenced to boron trifluoride diethyl etherate (BF₃•Et₂O, δ = 0 ppm). Carbons bound to boron are not observed due to the quadrupolar relaxation of boron. Broad signals at ~ δ = 2.7 ppm in the ¹¹B NMR spectrum are due to boron contained in probe components; all polymer spectra were acquired using quartz NMR tubes from Norell or Wilmad. Multiplicities are as indicated: s (singlet), d (doublet), t (triplet), q (quartet), p (pentet), m (multiplet), and br (broad). Coupling constants, *J*, are reported in hertz (Hz) and integration is provided, along with assignments, as indicated. Mass spectrometry and high resolution mass spectrometry were performed in the Department of Chemistry at Johns Hopkins University using a VG Instruments VG70S/E magnetic sector mass spectrometer with electron ionization (EI) (70 eV). The UNILab Plus Glove Box by MBRAUN was maintained under nitrogen atmosphere. All column chromatography was performed on a Teledyne ISCO Combiflash Rf+ using Redisep Rf silica columns. Polymer molecular weights were measured by gel permeation

chromatography (GPC) on a Tosoh Bioscience EcoSEC GPC workstation using butylated hydroxytoluene stabilized tetrahydrofuran (THF) as the eluent (0.35 mL min^{-1} , $40 \text{ }^\circ\text{C}$) through TSKgel SuperMultipore HZ-M guard column (4.6 mm ID x 2.0 cm, $4 \text{ }\mu\text{m}$, Tosoh Bioscience) and a TSKgel SuperMultipore HZ-M column (4.6 mm ID x 15 cm, $4 \text{ }\mu\text{m}$, Tosoh Bioscience). Polystyrene standards (EasiVial PS-M, Agilent) were used to build a calibration curve. Processing was performed using EcoSEC Data Analysis software (Version 1.14, Tosoh Bioscience). Polymers were dissolved in THF (1 mg mL^{-1}), filtered (Millex-FG Syringe Filter Unit, $0.20 \text{ }\mu\text{m}$, PTFE, EMD Millipore), and injected using an auto-sampler ($10 \text{ }\mu\text{L}$). UV-Vis spectroscopy was performed on a Shimadzu UV-1800 UV-Vis spectrophotometer. The spectra were measured at room temperature in non-stabilized THF in a quartz cuvette (10 mm). Fluorescence spectroscopy was performed on a Photon Technology International, Inc. QuantaMaster 40 spectrofluorometer equipped with an Ushio short-arc xenon gas discharge lamp. The spectra were measured at room temperature in non-stabilized THF in a quartz cuvette (10 mm) and all solutions were dilute ($\lambda_{\text{max}} < 0.1 \text{ abu}$) to minimize re-absorption effects. Processing was done using Felix32 Analysis (Version 1.2, Build 56, Photon Technology International, Inc.). Fourier-transformed infrared (FTIR) spectroscopy was performed on a ThermoNicolet Nexus 670 FTIR spectrometer. The Polymers were dissolved in dichloromethane (6 mg mL^{-1}), drop cast onto a polished KBr window (International Crystal Labs), and spectra were obtained at room temperature in transmission mode. Differential scanning calorimetry (DSC) was carried out on a TA Instruments DSC Q20 V24.11 Build 124 and processing was performed using Universal Analysis V4.5A (TA Instruments). Polymer samples ($2.5 - 5.0 \text{ mg}$) were sealed in hermetic aluminum pans, heated from 30 to $170 \text{ }^\circ\text{C}$ ($10 \text{ }^\circ\text{C min}^{-1}$), and cooled from 170 to $30 \text{ }^\circ\text{C}$, for three cycles under a purge gas of nitrogen (25 mL min^{-1}). Glass transition temperatures (T_g) were calculated from the third heating cycle (all second and third heating cycles traced, respectively) and the T_g onset is reported. Elemental analysis was performed by Robertson Microlit Laboratories.

I.1.2 Statistical Methods. Experimental data derived from UV-vis spectroscopy and elemental analysis were fit using the NLLS method with Contour version 1.8 with 3% and 1% relative estimated error, respectively. Point estimates of the reactivity ratios and a 95% joint confidence interval were calculated.

I.1.3 Computational Methods. Density Functional Theory (DFT) calculations were performed using the Gaussian 09 program package. Geometries were optimized using the restricted or unrestricted CAM-B3LYP¹⁴⁹ hybrid exchange-correlation functional with the 6-311G(d,p) basis set. CAM-B3LYP is known to reliably describe radicals and extended conjugated systems.^{150,151} Frequency calculations carried out at the same level of theory on fully optimized geometries showed no imaginary frequencies, confirming optimized geometries as local minima on their potential surfaces. Energies reported are the sum of electronic and thermal enthalpies at 298.15 K and are converted to kcal mol⁻¹ from Hartrees (1 E_h = 627.509608 kcal mol⁻¹). Visualization of optimized geometries and electrostatic potential (ESP) maps were performed using GaussView 5.0.9.

Nucleus independent chemical shifts (NICS) were calculated as the negative value of the nuclear magnetic shielding computed at the geometric center of the rings (NICS(0)) and 1.0 Å above the geometric center of the rings (NICS(1)), by the gauge-independent atomic orbital (GIAO) method.^{161–165}

Homolytic bond dissociation energies (BDEs) are calculated as follows: $BDE = (E_{rs} + E_{Ha}) - E_{cs}$ where E_{rs} = enthalpy corrected energy of the radical species; E_{Ha} = energy of a hydrogen atom; E_{cs} = enthalpy corrected energy of the closed shell species.

I.1.4 Materials: Unless otherwise specified, all chemicals were used as purchased without further purification. Solvents used for column chromatography and polymer workup were reagent grade and used as received. Reaction solvent toluene (Fisher, certified ACS) was dried on a J. C. Meyer Solvent Dispensing System (SDS) using stainless steel columns packed with neutral alumina and Q5 reactant, a copper(II) oxide oxygen scavenger, following the manufacturer's recommendations for solvent preparation and dispensation. Acetone (PHARMCO-AAPER) was dried over magnesium

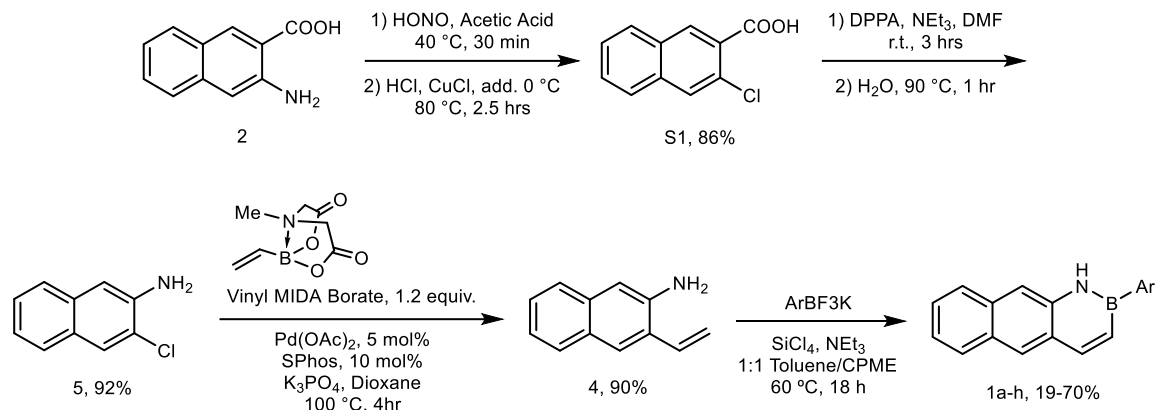
sulfate overnight. Ethanol (PHARMCO-AAPER) was dried over 3 Å molecular sieves. Triethylamine (Sigma Aldrich, >99%) was dried over potassium hydroxide overnight and distilled under argon just prior to use. 2-Vinylnaphthalene (2VN) (Sigma Aldrich, 95%) was sublimed at room temperature and 1.3 Torr, then stored in a glove box freezer (-20 °C) until future use. Styrene (Sigma Aldrich, ReagentPlus, 4-tert-butylcatechol stabilized) was purified by removal of stabilizer by washing twice with an equal volume of 1 N sodium hydroxide solution, then three times with deionized water, dried over anhydrous magnesium sulfate for three hours, decanted into an oven dried round bottom flask, vacuum distilled at room temperature, then freeze-pump-thawed until completely degassed. UV-Vis studies, fluorescence studies, and oxidations were performed in non-stabilized THF from EMD Millipore. GPC studies were performed in butylated hydroxytoluene stabilized THF from EMD Millipore.

2,2'-Azobis(2-methylpropionitrile) (AIBN) (recrystallized, 99%), cyclopentyl methyl ether (CPME) (anhydrous, 99.9%), dichloromethane, hexanes, methanol, phenethylboronic acid, polyvinyl alcohol (98% hydrolyzed, average MW 13000-23000), potassium hydrogen fluoride (99%), potassium hydroxide, potassium vinyltrifluoroborate (95%), sodium chloride (>99%), sodium hydroxide (>97%), potassium vinyltrifluoroborate (95%), and silicon tetrachloride (SureSeal, 99%) were purchased from Sigma Aldrich.

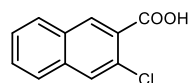
Acetonitrile- d_3 (D, 99.8%), chloroform- d (D, 99.8%), and dichloromethane- d_2 (D, 99.8%) were purchased from Cambridge Isotope Laboratories, Inc. Hydrogen peroxide (30% solution, stabilized) and toluene (for polymer elution) were purchased from EMD Milipore. Diethyl ether (anhydrous) and magnesium sulfate (anhydrous) were purchased from Fisher Chemical. Quinine hemisulfate monohydrate (purum for fluorescence, $\geq 98\%$) was purchased from Fluka. 2-Aminophenethyl alcohol (**1**, 97% or 95%) was purchased from Sigma Aldrich (or TCI America).

I.2 Experimental Details for Chapter 2: BN Anthracenes

I.2.1 Synthesis of BN Anthracenes 1a-h

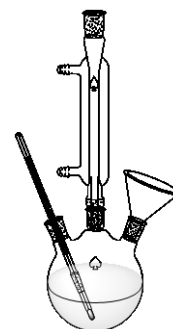


3-Chloro-2-Naphthoic Acid (S1)



This synthesis was adapted from van Koten *et al.*²¹² and Tucker *et al.*²¹³

In air, a 1000 mL 3-neck round bottom flask equipped with a thermometer, unsealed reflux condenser (no water was used to cool), a powder funnel and a stir bar was charged with concentrated sulfuric acid (86 mL). Sodium nitrite (1.1 equiv., 117.7 mmol, 8.12 g) was slowly added to the sulfuric acid over 20 minutes through the powder funnel. The heterogeneous, colorless mixture was heated to 70 °C for 20 minutes, or until all of sodium nitrite dissolved, then was cooled to room temperature then to 0 °C in an ice-water bath. A slurry of 2-amino-3-naphthoic acid (1 equiv., 107.0 mmol, 20.02 g) in glacial acetic acid (214 mL) was poured in portions through the powder funnel into the cooled HONO solution, ensuring the temperature did not exceed 40 °C.¹ The viscous mixture was warmed to room temperature then heated to 40 °C, and stirred at 40 °C for 30 minutes.

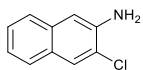


¹ The Sandmeyer reaction is mildly exothermic and Tucker *et al.*²¹³ "The temperature of diazotization is critical. Lower yields are obtained if the temperature rises above 40 °C."

Separately, in air, a 1000 mL round bottom flask equipped with a stir bar and a 125 mL addition funnel was charged with copper(I) chloride (2.2 equiv., 235.4 mmol, 23.38 g) and the copper salt was dissolved in concentrated hydrochloric acid (214 mL). The copper solution was cooled to 0 °C with an ice water bath. The thick, brown solution of diazonium ion, which had been cooled to room temperature, was transferred to the addition funnel and added in a slow stream to the cooled solution of copper salt. Following the complete addition of diazonium salt, the ice water bath was removed and the reaction mixture was warmed to room temperature. The addition funnel was replaced with an unsealed reflux condenser (no cooling). The solution was slowly warmed to 80 °C. At 50 °C effervescence began and heating continued until effervescence ceased, about 2.5 hours. The flocculent reaction mixture was cooled to room temperature, water was slowly added (357 mL), and the mixture was allowed to slowly stir for 5 minutes causing more solids to form. The reaction mixture was filtered through a coarse fritted funnel, washing with water (500 mL) which was collected and subsequently properly disposed of. The solid product was dissolved in ethyl acetate (850 mL), passed through the fritted funnel, and separately collected. The dissolved mixture of **S1** was washed with a saturated sodium chloride solution, and dried over anhydrous sodium sulfate. Solvent was removed by rotary evaporation under reduced pressure and dried on high vacuum overnight. 3-Chloro-2-naphthoic acid (**S1**) was used without further purification (unpurified yield 19.05 g, 86%).

δ_{H} (400 MHz, CDCl ₃)	8.62 (1 H, s), 7.97 (1 H, s), 7.87 (2 H, dd, <i>J</i> 52.3, 8.3), 7.61 (2 H, dt, <i>J</i> 28.9, 7.3).
δ_{C} (101 MHz, DMSO- <i>d</i> ₆)	166.73, 134.25, 131.56, 130.59, 128.94, 128.90, 128.83, 128.61, 127.82, 127.26, 126.84.
HRMS (EI)	[M] ⁺ Calcd for C ₁₁ H ₇ ClO ₂ 206.0135; Found 206.01373.

3-Chloronaphthalen-2-Amine (5)



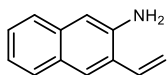
This reaction is adapted from Liu *et al.*¹¹⁹

*CAUTION: This reaction was performed behind a blast shield due to the potential explosion risk associated with acyl azides.*²¹⁴

An oven-dried 1000 mL Schlenk flask equipped with a stir bar was cooled under vacuum and backfilled with nitrogen. To the flask was added **S1** (1 equiv., 50 mmol, 10.33 g). The flask was purged and backfilled three times with nitrogen. Dimethylformamide (DMF) (400 mL) was added via cannula transfer and triethylamine (1.5 equiv., 75 mmol, 10.5 mL) and diphenyl phosphoryl azide (DPPA) (1.5 equiv., 75 mmol, 16.2 mL) were added via syringe. The brown solution was allowed to stir for 3 hours at room temperature under a positive pressure of nitrogen. Nitrogen-sparged water (33.3 mL) was added via cannula transfer and the reaction mixture was heated to 90 °C with stirring for 1 hour. The reaction mixture was cooled to room temperature, opened to atmosphere, and water (350 mL) was added. The biphasic mixture was poured into a 1000 mL separatory funnel and the aqueous layer was washed with diethyl ether (3 x 150 mL). The combined organic layers were washed sequentially with saturated sodium bicarbonate (2 x 175 mL) then saturated sodium chloride solutions (2 x 175 mL) and dried over sodium sulfate. The organic solvent was removed by rotary evaporation under reduced pressure. The brown solid was dissolved in 150 mL warm toluene and hot filtered through a fritted funnel to remove insoluble materials. The organic solvent was removed by rotary evaporation under reduced pressure. This product was used without further purification (unpurified yield 8.13 g, 92%).

δ_{H} (400 MHz, CDCl_3)	7.97 (1 H, s), 7.78 (2 H, dd, J 12.1, 8.3), 7.60 – 7.39 (2 H, m), 7.18 (1 H, s), 4.27 (2 H, s).
δ_{C} (101 MHz, CDCl_3)	140.89, 133.52, 127.99, 127.92, 126.86, 126.49, 125.58, 123.21, 122.25, 109.72.
HRMS (EI)	$[\text{M}]^+$ Calcd for $\text{C}_{10}\text{H}_8\text{ClN}$ 177.0345; Found 177.03418.

3-Vinylnaphthalen-2-Amine (4)



This procedure was adapted from Burke *et al.*¹²⁰

An oven dried 250 mL Schlenk flask equipped with a condenser and stir bar was cooled under vacuum. The flask was charged with **5** (1 equiv., 10 mmol, 1.78 g), palladium(II) acetate (5 mol%, 0.5 mmol, 112.3 mg), SPhos (10 mol%, 1 mmol, 410.5 mg), and vinylboronic acid MIDA ester (1.2 equiv., 12 mmol, 2.05 g). The reaction vessel was purged and backfilled three times with nitrogen. The solids were dissolved in dioxane (100 mL) and a nitrogen-sparged aqueous solution of tribasic potassium phosphate (3 M, 20 mL) was added. The reaction was heated to 100 °C with stirring under a positive pressure of nitrogen for 4 hours. The reaction was cooled to room temperature, transferred to a 250 mL round bottom flask, and concentrated by rotary evaporation under reduced pressure. The solids were dissolved in ethyl acetate (50 mL) and added to a separatory funnel, along with an aqueous solution of sodium hydroxide (1 M, 40 mL). The aqueous layer was extracted with ethyl acetate (3 x 50 mL) and the combined organic layers were dried over sodium sulfate. After filtration, the organic solvents were removed by rotary evaporation under reduced pressure. **4** was purified by automated silica gel column chromatography (40 g column) eluting with 10% ethyl acetate in hexanes (yield 1.52 g, 90%).

δ_{H} (400 MHz, CDCl_3) 7.76 (1 H, s), 7.70 (1 H, dd, J 8.2, 1.1), 7.58 (1 H, dd, J 8.2, 1.1), 7.35 (1 H, ddd, J 8.2, 6.8, 1.3), 7.28 – 7.19 (1 H, m), 7.02 (1 H, s), 6.92 (1 H, ddd, J 17.4, 11.0, 0.8), 5.80 (1 H, dd, J 17.3, 1.5), 5.45 (1 H, dd, J 11.0, 1.5), 4.042 (2 H, s).

δ_{C} (101 MHz, CDCl_3) 142.29, 134.58, 133.05, 128.26, 127.89, 127.54, 126.62, 126.33, 125.50, 122.82, 117.57, 109.67.

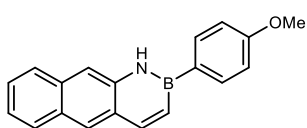
HRMS (EI) $[\text{M}]^+$ Calcd for $\text{C}_{12}\text{H}_{11}\text{N}$ 169.0891; Found 169.08868.

General Procedure A: This procedure was adapted from Molander *et al.*¹¹⁶

An oven dried 15 mL heavy walled cylindrical pressure vessel equipped with a stir bar was charged with **4** (1 equiv., 1.8 mmol, 304 mg) and the appropriate potassium aryltrifluoroborate (0.8 equiv., 1.5 mmol). The vessel and contents were brought into a nitrogen atmosphere glove box. Toluene

(6 mL), cyclopentyl methyl ether (CPME) (6 mL), triethylamine (1.5 equiv., 2.3 mmol, 0.32 mL), and silicon tetrachloride (1 equiv., 1.5 mmol, 175 μ L) were added to the reaction vessel. The vessel was sealed with a PTFE screw cap, brought out of the glove box and heated to 100 $^{\circ}$ C for 18 hours with stirring. The reaction mixture was cooled to room temperature, added to a separatory funnel, and diluted with an aqueous hydrochloric acid solution (1M, 30 mL) and ethyl acetate (25 mL). The organic layer was collected and the aqueous layer was washed with ethyl acetate (3 x 25 mL). The combined organic layers were washed with a saturated aqueous sodium bicarbonate solution (1 x 50 mL) then a saturated aqueous sodium chloride solution (1 x 50 mL), dried over anhydrous sodium sulfate, and concentrated by rotary evaporation under reduced pressure. The products were recrystallized from hot chlorobenzene. (In exception to this procedure was the work-up of **1h**, as detailed below)

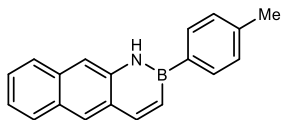
2-(4-Methoxyphenyl)-1,2-Dihydronaphtho[2,3-*e*][1,2]-Azaborinine (4-MeO Ph BN Anthracene, **1a)**



Synthesized according to General Procedure A using potassium 4-methoxyphenyltrifluoroborate (0.8 equiv., 1.5 mmol, 0.32 g). Yield 0.11 g, 25%.

δ_{H} (400 MHz, CDCl_3)	8.24 (1 H, d, J 11.7), 8.17 (1 H, s), 8.05 (1 H, s), 7.99 – 7.92 (3 H, m), 7.88 (1 H, d, J 8.4), 7.73 (1 H, s), 7.50 (1 H, ddd, J 8.3, 6.7, 1.3), 7.41 (1 H, ddd, J 8.0, 6.7, 1.2), 7.10 – 7.04 (2 H, m), 3.92 (3 H, s).
δ_{C} (101 MHz, $\text{DMSO-}d_6$)	160.99, 144.90, 139.20, 135.33, 132.98, 127.99, 127.97, 126.50, 126.27, 126.13, 123.45, 113.59, 113.25, 54.97.
δ_{B} (128 MHz, CDCl_3)	34.10.
HRMS (EI)	$[\text{M}]^+$ Calcd for $\text{C}_{19}\text{H}_{16}\text{BNO}$ 285.1325; Found 285.13217.
Melting Point	263.8 $^{\circ}$ C

2-(p-Tolyl)-1,2-Dihydronaphtho[2,3-*e*][1,2]Azaborinine (4-Me Ph BN Anthracene, 1b)



Synthesized according to General Procedure A using potassium p-tolyltrifluoroborate (0.8 equiv., 1.5 mmol, 0.30 g). Yield 0.077 g, 19%.

δ_{H} (400 MHz, CDCl_3) 8.23 (1 H, d, J 11.6), 8.16 (1 H, s), 8.09 (1 H, s), 7.94 (1 H, d, J 8.2), 7.88 (2 H, d, J 7.9), 7.89 – 7.82 (1 H, m), 7.72 (1 H, s), 7.48 (1 H, ddd, J 8.2, 6.7, 1.3), 7.39 (1 H, ddd, J 8.1, 6.7, 1.2), 7.35 – 7.27 (3 H, m), 2.43 (3 H, s).

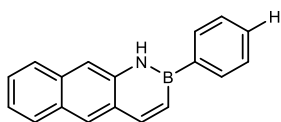
δ_{C} (101 MHz, $\text{DMSO-}d_6$) 145.14, 139.45, 139.10, 133.69, 132.97, 128.68, 128.05, 128.03, 128.02, 126.56, 126.31, 126.19, 123.54, 113.45, 21.22.

δ_{B} (128 MHz, CDCl_3) 34.84.

HRMS (EI) $[\text{M}]^+$ Calcd for $\text{C}_{19}\text{H}_{16}\text{BN}$ 269.1376; Found 269.13806.

Melting Point 252.6 °C

2-Phenyl-1,2-Dihydronaphtho[2,3-*e*][1,2]Azaborinine (4-H Ph BN Anthracene, 1c)



Synthesized according to General Procedure A using potassium phenyltrifluoroborate (0.8 equiv., 1.5 mmol, 0.28 g). Yield 0.17 g, 44%.

δ_{H} (400 MHz, CDCl_3) 8.26 (1 H, d, J 11.6), 8.18 (1 H, s), 8.13 (1 H, s), 8.01 – 7.84 (4 H, m), 7.74 (1 H, s), 7.55 – 7.46 (4 H, m), 7.40 (1 H, ddd, J 8.1, 6.7, 1.2), 7.29 (1 H, dd, J 11.7, 1.9).

δ_{C} (101 MHz, $\text{DMSO-}d_6$) 145.34, 139.02, 133.59, 133.59, 130.28, 129.89, 128.11, 128.09, 128.03, 127.96, 126.591, 126.35, 126.19, 123.60, 113.60.

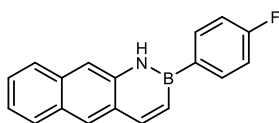
δ_{B} (128 MHz, CDCl_3) 34.62.

HRMS (EI) $[\text{M}]^+$ Calcd for $\text{C}_{18}\text{H}_{14}\text{BN}$ 255.1219; Found 255.12272.

Melting Point 232.5 °C

2-(4-Fluorophenyl)-1,2-Dihydronaphtho[2,3-*e*][1,2]Azaborinine (4-F Ph BN

Anthracene, 1d)

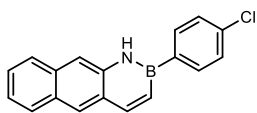


Synthesized according to General Procedure A using potassium 4-fluorophenyltrifluoroborate (0.8 equiv., 1.5 mmol, 0.30 g). Yield 0.22 g, 54%.

δ_{H} (400 MHz, CDCl_3)	8.25 (1 H, d, J 11.6), 8.17 (1 H, s), 8.06 (1 H, s), 7.98 – 7.91 (3 H, m), 7.89 – 7.84 (1 H, m), 7.73 (1 H, s), 7.50 (1 H, ddd, J 8.2, 6.7, 1.3), 7.40 (1 H, ddd, J 8.1, 6.7, 1.2), 7.26 – 7.16 (3 H, m).
δ_{C} (101 MHz, $\text{DMSO-}d_6$)	164.20 (d, J 246.9), 145.88, 139.42, 136.50, 136.42, 133.46, 128.62, 128.57, 128.50, 127.07, 126.85, 126.57, 124.11, 115.49, 115.29, 114.02.
δ_{B} (128 MHz, CDCl_3)	34.42.
δ_{F} (376 MHz, CDCl_3)	-110.75.
HRMS (EI)	$[\text{M}]^+$ Calcd for $\text{C}_{18}\text{H}_{13}\text{BFN}$ 273.1125; Found 273.11224.
Melting Point	247.1 °C

2-(4-Chlorophenyl)-1,2-Dihydronaphtho[2,3-*e*][1,2]Azaborinine (4-Cl Ph BN

Anthracene, 1e)

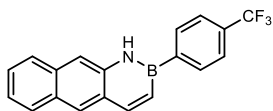


Synthesized according to General Procedure A using potassium 4-chlorophenyltrifluoroborate (0.8 equiv., 1.5 mmol, 0.33 g). Yield 0.30 g, 70%.

δ_{H} (400 MHz, CDCl_3)	8.26 (1 H, d, J 11.7), 8.18 (1 H, s), 8.09 (1 H, s), 7.95 (1 H, ddd, J 8.3, 1.4, 0.7), 7.91 – 7.84 (3 H, m), 7.74 (1 H, s), 7.54 – 7.45 (3 H, m), 7.41 (1 H, ddd, J 8.1, 6.7, 1.2), 7.23 (1 H, dd, J 11.6, 2.0).
δ_{C} (101 MHz, $\text{DMSO-}d_6$)	145.59, 138.85, 135.46, 134.98, 132.99, 128.25, 128.15, 128.05, 128.02, 126.64, 126.42, 126.14, 123.71, 113.68, 113.64.
δ_{B} (128 MHz, CDCl_3)	34.31.
HRMS (EI)	$[\text{M}]^+$ Calcd for $\text{C}_{18}\text{H}_{13}\text{BClN}$ 289.083; Found 289.08337.

Melting Point 254.7 °C

2-(4-(Trifluoromethyl)Phenyl)-1,2-Dihydronaphtho[2,3-*e*][1,2]Azaborinine (4-CF₃ Ph BN Anthracene, 1f)



Synthesized according to General Procedure A using potassium 4-(trifluoromethyl)phenyltrifluoroborate (0.8 equiv., 1.5 mmol, 0.38 g). Yield 0.22 g, 46%.

δ_{H} (400 MHz, CDCl₃) 8.31 (1 H, d, *J* 11.6), 8.21 (1 H, d, *J* 1.0), 8.17 (1 H, s), 8.08 – 8.02 (2 H, m), 7.99 – 7.94 (1 H, m), 7.92 – 7.86 (1 H, m), 7.78 (1 H, s), 7.77 – 7.71 (2 H, m), 7.54 – 7.48 (1 H, m), 7.42 (1 H, ddd, *J* 8.1, 6.7, 1.2), 7.26 (1 H, dd, *J* 11.6, 2.0).

δ_{C} (101 MHz, DMSO-*d*₆) 146.39, 139.17, 134.67, 133.47, 130.48, 130.16, 128.77, 128.72, 128.54, 127.16, 126.95, 126.65, 126.28, 124.92, 124.88, 124.30, 123.57, 114.37.

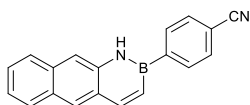
δ_{B} (128 MHz, CDCl₃) 34.53.

δ_{F} (376 MHz, CDCl₃) –62.76.

HRMS (EI) [M]⁺ Calcd for C₁₉H₁₃BF₃N 323.1093; Found 323.10941.

Melting Point 256.3 °C

4-(Naphtho[2,3-*e*][1,2]Azaborinin-2(1H)-yl)Benzonitrile (4-CN Ph BN Anthracene, 1g)



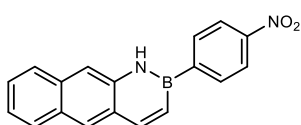
Synthesized according to General Procedure A using potassium 4-cyanophenyltrifluoroborate (0.8 equiv., 1.5 mmol, 0.31 g). Yield 0.062 g, 15%.

δ_{H} (400 MHz, CDCl₃) δ 8.36 – 8.28 (1 H, m), 8.21 (1 H, s), 8.16 (1 H, s), 8.04 – 7.99 (2 H, m), 7.92 (2 H, dtd, *J* 32.0, 8.4, 1.3, 0.8), 7.80 – 7.73 (3 H, m), 7.48 (2 H, dddd, *J* 34.5, 8.1, 6.7, 1.2), 7.22 (1 H, dd, *J* 11.6, 2.0).

δ_c (101 MHz, DMSO- <i>d</i> ₆)	146.01, 138.61, 134.18, 132.99, 131.44, 128.32, 128.28, 128.06, 126.70, 126.50, 126.17, 123.88, 119.09, 113.95, 112.05.
δ_B (128 MHz, CDCl ₃)	34.06.
HRMS (EI)	[M] ⁺ Calcd for C ₁₉ H ₁₃ BN ₂ 280.1172; Found 280.11689.
Melting Point	239.2 °C

2-(4-Nitrophenyl)-1,2-Dihydronaphtho[2,3-e][1,2]Azaborinine (4-NO₂ Ph BN

Anthracene, 1h)

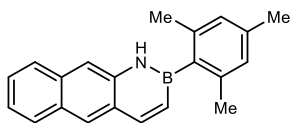


Synthesized according to General Procedure A using potassium 4-nitrophenyltrifluoroborate (0.8 equiv., 1.5 mmol, 0.34 g) and an alternative workup procedure. Once the reaction was cooled to room temperature the reaction mixture was diluted with hexanes (100 mL) then filtered through a fritted funnel and washed with hexanes (10 mL). The product was eluted with dichloromethane (200 mL), washed with a saturated aqueous sodium chloride solution (1 x 50 mL), dried over magnesium sulfate, and concentrated by rotary evaporation under reduced pressure. The product was recrystallized from hot chlorobenzene. Yield 0.27 g, 59%.

δ_H (400 MHz, CDCl ₃)	8.37 – 8.30 (3 H, m), 8.23 (1 H, s), 8.21 (1 H, s), 8.12 – 8.07 (2 H, m), 8.00 – 7.86 (2 H, m), 7.80 (1 H, s), 7.48 (2 H, dddd, <i>J</i> 34.4, 8.1, 6.7, 1.2), 7.25 (1 H, dd, <i>J</i> 11.8, 1.8).
δ_c (101 MHz, DMSO- <i>d</i> ₆)	148.38, 146.07, 138.58, 134.70, 133.00, 130.25, 128.36, 128.34, 128.31, 128.06, 126.98, 126.71, 126.51, 126.16, 123.90, 122.50, 122.48, 114.05.
δ_B (128 MHz, CDCl ₃)	34.26.
HRMS (EI)	[M] ⁺ Calcd for C ₁₈ H ₁₃ BN ₂ O ₂ 300.107; Found 300.10714.
Melting Point	256.3 °C

I.2.2 Synthesis of Mes BN Anthracene 1i

2-Mesityl-1,2-Dihydronaphtho[2,3-*e*][1,2]Azaborinine (Mes BN Anthracene, 1i)



This procedure was adapted from Liu *et al.*¹¹⁹

An oven dried 250 mL Schlenk flask equipped with a condenser and stir bar was cooled under vacuum and purged with argon. The flask was charged with **4** (1 equiv., 1.9 mmol, 0.32 g). The reaction flask was purged and backfilled three times with argon. The solid was dissolved in toluene (40 mL) and the brown solution was cooled to $-40\text{ }^{\circ}\text{C}$ in an acetonitrile/dry ice bath.

Separately, an oven dried 5 mL heart-shaped flask, purged and backfilled with argon three times, was cooled to $-78\text{ }^{\circ}\text{C}$ in an isopropanol/dry ice bath. The flask was charged with boron trichloride (1M in hexanes, 4 mL). The chilled boron trichloride (1 M in hexanes, 2 equiv., 3.8 mmol, 3.8 mL) was added dropwise, via syringe in two portions, to the chilled and stirred solution of **4**. The reaction mixture stirred for 1 hour at $-40\text{ }^{\circ}\text{C}$. While under a high positive pressure of argon and still cool, an oven-dried condenser was fit to the reaction flask, then the reaction mixture was brought to reflux ($120\text{ }^{\circ}\text{C}$) for 18 hours.

The reaction was cooled to room temperature and solvent removed under reduced pressure with stirring. Once dried, the flask was backfilled with argon and the condenser was replaced with a septum. The reaction mixture was redissolved in diethyl ether (40 mL) and cooled to $-40\text{ }^{\circ}\text{C}$ in an acetonitrile/dry ice bath. 2-Mesitylmagnesium bromide (1M in THF, 2 equiv., 3.8 mmol, 3.8 mL) was added dropwise via syringe to the cooled reaction mixture with stirring. Following addition, the solution was warmed to room temperature and allowed to stir under argon for 18 hours.

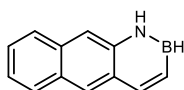
The reaction was cooled to $0\text{ }^{\circ}\text{C}$ in an ice water bath and water (10 mL) was added dropwise by syringe to quench excess Grignard reagent then the biphasic mixture was warmed to room temperature for 30 minutes. Ethyl acetate (15 mL) and water (10 mL) were added and the biphasic mixture transferred to a separatory funnel. The organic layer was collected. The aqueous layer was

extracted with ethyl acetate (3 x 15 mL) and the combined organic layers were washed with a saturated aqueous solution of sodium chloride and dried over sodium sulfate. Organic solvents were removed by rotary evaporation under reduced pressure then passed through a silica gel column, eluting with 50% dichloromethane in hexanes. The product fractions were collected, concentrated by rotary evaporation, and dried on vacuum overnight (yield 0.25 g, 46%).

δ_{H} (400 MHz, CDCl_3)	8.22 (2 H, d, J 11.8), 7.97 (1 H, d, J 8.3), 7.86 (1 H, d, J 8.4), 7.82 (1 H, s), 7.62 (1 H, s), 7.50 (1 H, ddd, J 8.2, 6.7, 1.3), 7.42 (1 H, ddd, J 8.1, 6.7, 1.2), 6.97 (1 H, dd, J 11.5, 1.8), 6.94 (2 H, s), 2.36 (3 H, s), 2.26 (6 H, s).
δ_{C} (101 MHz, $\text{DMSO}-d_6$)	144.42, 139.08, 138.95, 137.980, 136.33, 132.77, 131.00, 128.15, 128.02, 126.85, 126.44, 126.33, 125.80, 123.51, 113.24, 40.15, 39.94, 39.86, 39.73, 39.52, 39.40, 39.31, 39.10, 38.90, 22.62, 20.83.
δ_{B} (128 MHz, CDCl_3)	37.71.
HRMS (EI)	$[\text{M}]^+$ Calcd for $\text{C}_{21}\text{H}_{20}\text{BN}$ 297.1689; Found 297.1689.

1.2.3 Synthesis of BN Anthracene

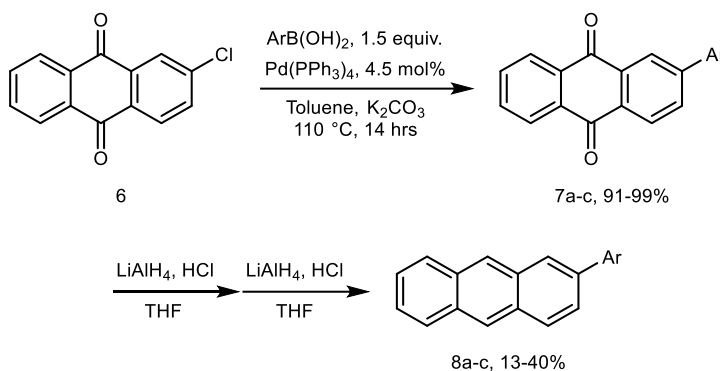
1,2-Dihydronaphtho[2,3-*e*][1,2]Azaborinine (BN Anthracene)



BN anthracene was synthesized as reported by Liu *et al.*¹¹⁹ on a 2.0 mmol scale (yield 0.096 g, 27%). Characterization data matched the reported spectra.

δ_{H} (400 MHz, CDCl_3)	8.25 – 8.12 (3 H, m), 7.94 (1 H, ddt, J 8.3, 1.4, 0.7), 7.89 – 7.84 (1 H, m), 7.68 (1 H, s), 7.49 (1 H, ddd, J 8.3, 6.7, 1.3), 7.41 (1 H, ddd, J 8.1, 6.7, 1.3), 6.98 (1 H, ddd, J 11.5, 2.5, 1.7).
δ_{C} (101 MHz, CDCl_3)	144.97, 137.95, 133.15, 128.83, 128.81, 128.16, 126.56, 126.47, 126.46, 123.91, 113.40.
δ_{B} (128 MHz, CDCl_3)	32.87 (d, J 95.7).
HRMS (EI)	$[\text{M}]^+$ Calcd for $\text{C}_{12}\text{H}_{10}\text{BN}$ 179.0906; Found 179.09095.

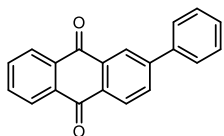
I.2.4 Synthesis of 2-Arylanthracenes 8a-c



General Procedure B: This procedure was adapted from Yamashita *et al.*¹²⁵

An oven dried 100 mL Schlenk flask equipped with a condenser and stir bar was cooled under vacuum. The nitrogen-filled flask was charged with 2-chloroanthraquinone, **6**, (1 equiv., 2.1 mmol, 0.50 g), the appropriate arylboronic acid (1.5 equiv., 3.1 mmol), and tetrakis(triphenylphosphine)palladium(0) (4.5 mol%, 0.09 mmol, 0.11 g). The flask was purged and backfilled three times with argon. The solids were dissolved in toluene (10.3 mL) and an argon-sparged aqueous solution of potassium carbonate (2 M, 4.1 mL) was added. The biphasic reaction mixture was heated to reflux (110 °C) with stirring under a positive pressure of argon for 14 hours. The reaction was cooled to room temperature and diluted with ethyl acetate (10 mL). The biphasic mixture was transferred to a separatory funnel and the organic layer was collected. The aqueous layer was washed with ethyl acetate (3 x 15 mL) and the combined organic layers were washed with a saturated aqueous sodium chloride solution then dried over sodium sulfate. The mixture was filtered and concentrated by rotary evaporation under reduced pressure. Products **7a-c** were purified by dissolving in a minimal quantity of dichloromethane, passing through a silica plug and eluting with 50% dichloromethane in hexanes.

2-Phenylanthracene-9,10-Dione (7a)



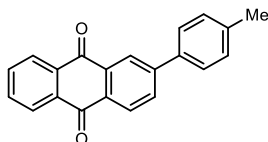
Synthesized according to General Procedure B using phenylboronic acid (1.5 equiv., 3.1 mmol, 0.38 g). Yield 0.53 g, 91%.

δ_{H} (400 MHz, CDCl_3) 8.46 (1 H, dd, J 1.9, 0.5), 8.33 – 8.24 (3 H, m), 7.96 (1 H, dd, J 8.1, 2.0), 7.80 – 7.73 (2 H, m), 7.71 – 7.66 (2 H, m), 7.52 – 7.39 (3 H, m).

δ_{C} (101 MHz, CDCl_3) 183.13, 182.80, 146.77, 138.90, 134.17, 134.05, 133.86, 133.62, 133.59, 132.32, 132.12, 129.17, 128.90, 128.04, 127.34, 127.28, 127.21, 125.52.

HRMS (EI) $[M]^+$ Calcd for $\text{C}_{20}\text{H}_{12}\text{O}_2$ 284.0837; Found 284.08341.

2-(p-Tolyl)Anthracene-9,10-Dione (7b)



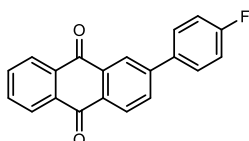
Synthesized according to General Procedure B using 4-tolylboronic acid (1.5 equiv., 3.1 mmol, 0.42 g). Yield 0.61 g, 99%.

δ_{H} (400 MHz, CDCl_3) 8.51 (1 H, dd, J 2.0, 0.5), 8.36 (0 H, d, J 0.5), 8.35 – 8.31 (3 H, m), 8.00 (1 H, dd, J 8.1, 2.0), 7.84 – 7.77 (2 H, m), 7.66 – 7.60 (2 H, m), 7.35 – 7.29 (2 H, m), 2.43 (3 H, s).

δ_{C} (101 MHz, CDCl_3) 183.41, 183.01, 146.91, 139.14, 136.13, 134.27, 134.13, 134.00, 133.80, 133.75, 132.21, 132.02, 129.99, 128.15, 127.39, 127.32, 127.28, 125.37, 21.37.

HRMS (EI) $[M]^+$ Calcd for $\text{C}_{21}\text{H}_{14}\text{O}_2$ 298.0994; Found 298.09976.

2-(4-Fluorophenyl)Anthracene-9,10-Dione (7c)



Synthesized according to General Procedure B using 4-fluorophenylboronic acid (1.5 equiv., 3.1 mmol, 0.43 g). Yield 0.61 g, 98%.

δ_{H} (400 MHz, CDCl_3) 8.46 (1 H, d, J 1.9), 8.35 (1 H, dd, J 8.1, 0.5), 8.34 – 8.29 (2 H, m), 7.95 (1 H, dd, J 8.1, 2.0), 7.84 – 7.78 (2 H, m), 7.73 – 7.66 (2 H, m), 7.23 – 7.16 (2 H, m).

δ_{C} (101 MHz, CDCl_3) 183.24, 182.88, 163.45 (d, J 249.1), 145.86, 135.19, 135.16, 134.34, 134.20, 134.01, 133.70, 133.65, 132.24, 129.23, 128.23, 127.40, 127.34, 125.44, 116.27 (d, J 21.6).

δ_F (376 MHz, CDCl₃) -112.81.

HRMS (EI) [M]⁺ Calcd for C₂₀H₁₁FO₂ 302.0743; Found 302.07418.

General Procedure C: This procedure was adapted from Tao *et al.*¹²⁶

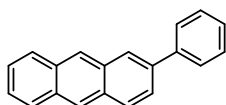
An oven dried 100 mL Schlenk flask equipped with a stir bar and sealed with a rubber septum was cooled under vacuum. The flask was charged with lithium aluminum hydride (4 equiv., 4.4 mmol, 0.17 g). The flask was purged and backfilled three times with argon and the LAH was suspended in THF (5.5 mL). The heterogeneous suspension was cooled to 0 °C in an ice water bath. The appropriate anthraquinone (1 equiv., 1.1 mmol) was dissolved in THF (8.8 mL) and added dropwise via syringe to the cooled lithium aluminum hydride suspension under a positive pressure of argon. The reaction mixture was allowed to stir for 1 hour at 0 °C, after which a second portion of lithium aluminum hydride (2 equiv., 2.2 mmol, 0.08 g) was added by quickly removing the septum, pouring in reagent, and resealing. The ice bath was removed and the reaction mixture was allowed to warm to room temperature and stirred for 2 hours.

The reaction was quenched by cooling to 0 °C with an ice water bath, followed by opening the reaction to air and the very slow dropwise addition of an aqueous solution of hydrochloric acid (6M, 5.5 mL) via syringe. The mixture was stirred 30 minutes at 0 °C then warmed to room temperature. The reaction mixture was diluted with dichloromethane (20 mL) and the biphasic mixture was transferred to a separatory funnel. The organic layer was collected and the aqueous layer was washed with dichloromethane (3 x10 mL). The combined organic layers were washed with a saturated aqueous sodium chloride solution and dried over sodium sulfate. After filtration, the organic solvents were removed by rotary evaporation under reduced pressure.

The product mixture was subjected to the reduction conditions for a second time using the same procedure.

The desired product was obtained after purification by silica gel chromatography (40 g column) eluting with a 20% dichloromethane in hexanes,

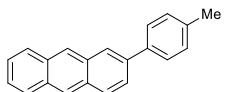
2-Phenylanthracene (4-H Ph Anthracene, 8a)



Synthesized according to General Procedure C using **7a** (1 equiv., 1.1 mmol, 0.31 g). Yield 0.093 g, 33%.

δ_{H} (400 MHz, CDCl_3)	8.48 (1 H, s), 8.45 (1 H, s), 8.21 (1 H, t, J 1.2), 8.12 – 8.07 (1 H, m), 8.05 – 7.99 (2 H, m), 7.78 (3 H, td, J 8.5, 1.7), 7.55 – 7.37 (5 H, m).
δ_{C} (101 MHz, CDCl_3)	141.18, 137.93, 132.19, 132.00, 131.94, 130.99, 129.04, 128.90, 128.36, 128.29, 127.57, 127.57, 126.70, 126.15, 125.80, 125.67, 125.63, 125.53.
HRMS (EI)	$[\text{M}]^+$ Calcd for $\text{C}_{21}\text{H}_{16}$ 254.1096; Found 254.10991.
Melting Point	213.6 °C

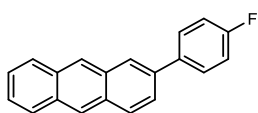
2-(p-Tolyl)Anthracene (4-Me Ph Anthracene, 8b)



Synthesized according to General Procedure C using **7b** (1 equiv., 1.1 mmol, 0.33 g). Yield 0.12 g, 40%.

δ_{H} (400 MHz, CDCl_3)	8.48 – 8.42 (2 H, m), 8.19 (1 H, dq, J 1.6, 0.8), 8.08 (1 H, dq, J 8.9, 0.8), 8.04 – 7.99 (2 H, m), 7.76 (1 H, dd, J 8.8, 1.8), 7.72 – 7.66 (2 H, m), 7.50 – 7.44 (2 H, m), 7.36 – 7.30 (2 H, m), 2.44 (3 H, s).
δ_{C} (101 MHz, CDCl_3)	138.25, 137.83, 137.40, 132.16, 132.06, 131.84, 130.93, 129.76, 128.80, 128.35, 128.26, 127.30, 126.56, 126.11, 125.67, 125.57, 125.42, 125.33, 21.31.
HRMS (EI)	$[\text{M}]^+$ Calcd for $\text{C}_{20}\text{H}_{14}$ 268.1252; Found 268.12554.

2-(4-Fluorophenyl)Anthracene (4-F Ph Anthracene, **8c**)



Synthesized according to General Procedure C using **7c** (1 equiv., 1.1 mmol, 0.33 g). Yield 0.040 g, 13%.

δ_{H} (400 MHz, CDCl_3) 8.47 (1 H, s), 8.45 (1 H, s), 8.15 (1 H, d, J 1.7), 8.11 – 8.06 (1 H, m), 8.05 – 7.98 (2 H, m), 7.77 – 7.67 (3 H, m), 7.51 – 7.44 (2 H, m), 7.24 – 7.14 (2 H, m).

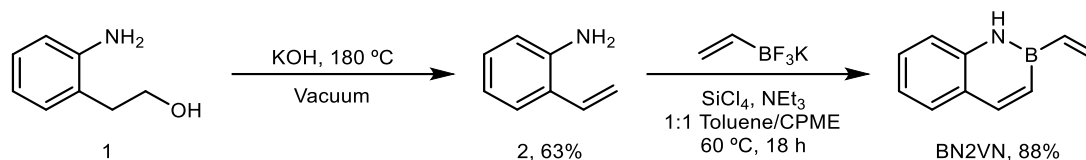
δ_{C} (101 MHz, CD_2Cl_2) 163.04 (d, J 246.2), 137.58 (d, J 3.3), 137.19, 132.58, 132.32, 132.25, 131.21, 129.38, 129.30, 129.26, 128.58, 128.49, 126.90, 126.41, 126.05, 125.93, 125.84, 125.83, 125.69, 116.12 (d, J 21.7).

δ_{F} (376 MHz, CDCl_3) -114.89.

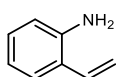
HRMS (EI) $[\text{M}]^+$ Calcd for $\text{C}_{20}\text{H}_{13}\text{F}$ 272.1001; Found 272.10074.

I.3 Experimental Details for Chapter 3: BN 2-Vinylnaphthalene (BN2VN) and Polymers

I.3.1 BN2VN Monomer Synthesis



2-Aminostyrene (**2**)



This reaction is adapted from Hoveyda *et al.*¹⁴⁰

An oven-dried 100 mL Schlenk flask equipped with a rare-earth² stir bar, short path distillation head, and tared receiving flask was cooled under vacuum and backfilled with argon. To the Schlenk flask was added 2-aminophenethyl alcohol (**1**) (1 equiv., 15.0 g, 109 mmol) and potassium hydroxide pellets (1 equiv., 6.1 g, 109 mmol). The entire distillation apparatus was purged and backfilled three times with argon, then returned to vacuum and heated to 180 °C. As the potassium hydroxide begins to melt the reaction mixture changes color from brown/purple to green. With continued heating and applied vacuum (1.3 Torr) the clear product distils over (83-90 °C) to the tared receiving flask which was ultimately sealed under argon with a septum and stored in the glove box for future use (yield 6.2 g, 63%).

Note: Depending on the source of 2-aminophenethyl alcohol, there may be contamination with dimethyl sulfoxide (DMSO) which codistils with **2**. DMSO may be removed with successive liquid-liquid extractions with deionized water, however DMSO contamination showed no noticeable effect on subsequent reactions.

δ_{H} (400 MHz, CDCl_3) 7.29 (1 H, ddt, J 7.7, 1.6, 0.5), 7.14 – 7.04 (1 H, m), 6.84 – 6.72 (2 H, m), 6.69 (1 H, ddd, J 8.0, 1.2, 0.4), 5.64 (1 H, dd, J 17.4, 1.5), 5.33 (1 H, dd, J 11.0, 1.5), 3.75 (2 H, s). δ_{C} (101 MHz, CDCl_3) 143.77, 132.87, 128.85, 127.46, 124.22, 119.05, 116.20, 115.82.

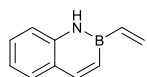
² A stronger magnet provided better stirring (Fischer Scientific Catalogue No. 14-513-511).

δ_c (101 MHz, CDCl₃) 143.77, 132.87, 128.85, 127.46, 124.22, 119.05, 116.20, 115.82.

HRMS (EI) m/z [M]⁺ Calcd for C₈H₉N 119.0735; Found 119.07365.

Data collected match published material on this compound,^{45,140} therefore no further spectra were obtained.

Small Scale: 2-Vinyl-1,2-Dihydrobenzo[e][1,2]Azaborinine (BN2VN)



This procedure was adapted from Molander *et al.*⁴⁵

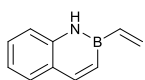
An oven-dried 500 mL Schlenk flask equipped with a stir bar and septum sealed reflux condenser was charged with potassium vinyltrifluoroborate (1.1 equiv., 18.6 mmol, 2.49 g) and purged and backfilled three times with argon. **2** (1 equiv., 16.9 mmol, 2.01 g), toluene (75 mL), cyclopentyl methyl ether (CPME) (75 mL), triethylamine (1.5 equiv., 25.3 mmol, 3.5 mL), then silicon tetrachloride (1.1 equiv., 18.6 mmol, 2.1 mL) were added and the reaction mixture was heated to 60 °C for 18 hours with stirring. The reaction mixture was cooled to room temperature, diluted with hexanes (100 mL), and passed through a plug of celite to remove solids, washing with hexanes (100 mL). The eluent was collected and concentrated by rotary evaporation. The product was purified by silica gel chromatography, eluting with hexanes, then ramping to 10% dichloromethane in hexanes. Fractions were concentrated by rotary evaporation and dried on vacuum (for a limited time due to sublimation, usually ~ 5 hours) to yield a white solid which was stored in a glove box freezer (-20 °C) for future use (yield 2.3 g, 88%).

Note: A 40% reduction in amount of toluene and CPME used led to only minor decreases in yield. This is advantageous for large scale reactions (**2**, >2 g), however vigorous stirring is needed to allow the reaction to become homogeneous after addition of silicon tetrachloride. Pure **2** can also be isolated by sublimation at room temperature and 1.3 Torr, following celite filtration.

δ_H (400 MHz, CD₂Cl₂) 8.09 (1 H, d, *J* 11.5), 7.92 (1 H, s), 7.66 (1 H, ddt, *J* 7.8, 1.3, 0.6), 7.45 (1 H, ddd, *J* 8.4, 7.1, 1.5), 7.29 (1 H, ddt, *J* 8.1, 1.3, 0.6), 7.22 (1 H, ddd, *J* 7.9, 7.1, 1.2), 7.12 (1 H, dd, *J* 11.5, 2.0), 6.56

	(1 H, dd, <i>J</i> 19.6, 13.3), 6.31 (1 H, dd, <i>J</i> 19.7, 3.7), 6.11 (1 H, dd, <i>J</i> 13.6, 3.5).
δ_c (101 MHz, CD ₂ Cl ₂)	145.46, 140.61, 132.63, 129.86, 128.82, 126.33, 121.52, 118.66. (β -carbon shift is 132 ppm, determined by DEPT 135 in CDCl ₃ .)
δ_B (128 MHz, CD ₂ Cl ₂)	32.45.
HRMS (EI)	<i>m/z</i> [M] ⁺ Calcd for C ₁₀ H ₁₀ BN 155.0906; Found 155.09057.
Anal.	Found: C, 77.4; H, 6.4; N, 9.1. Calc. for C ₁₀ H ₁₀ BN: C, 77.5; H, 6.5; N, 9.0.
Melting point:	66 °C.

Large Scale: 2-Vinyl-1,2-Dihydrobenzo[e][1,2]Azaborinine (BN2VN)



This procedure was adapted from Klausen *et al.*³⁵

An oven-dried 1 L Schlenk flask equipped with a stir bar and septum sealed reflux condenser was charged with potassium vinyltrifluoroborate (1.1 equiv., 86.4 mmol, 11.57 g) and purged and backfilled three times with argon. 2-Vinylalanine (1 equiv., 78.5 mmol, 9.36 g), toluene (208 mL), cyclopentyl methyl ether (CPME) (208 mL), triethylamine (1.5 equiv., 117.8 mmol, 16.5 mL), then silicon tetrachloride (1.1 equiv., 86.4 mmol, 9.9 mL) were added and the reaction mixture was heated to 60 °C for 18 hours with stirring under a positive pressure of argon. The reaction mixture was cooled to room temperature, diluted with hexanes (200 mL), and passed through a plug of silica to remove solids, washing with 25% dichloromethane in hexanes (300 mL). The eluent was collected and concentrated by rotary evaporation. The product was purified by silica gel chromatography, eluting with hexanes, then ramping to 10% dichloromethane in hexanes. Fractions were concentrated by rotary evaporation, transferred to a tared scintillation vial, and placed on the Schlenk line to dry under reduced pressure (for a limited time due to sublimation, usually ~ 5 hours) to yield a white solid which was stored in a glove box freezer (-20 °C) for future use (yield 10.5 g, 86%).

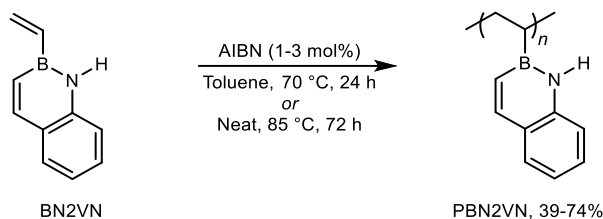
δ_H (400 MHz, CD ₂ Cl ₂)	8.05 (1H, d, <i>J</i> 11.6), 7.91 (1H, s), 7.62 (1H, ddq, <i>J</i> 7.8, 1.3, 0.6), 7.42 (1H, ddd, <i>J</i> 8.4, 7.1, 1.5), 7.28 (1H, ddt, <i>J</i> 8.2, 1.2, 0.6), 7.17
--	---

(1H, ddd, *J* 7.8, 7.1, 1.2), 7.05 (1H, dd, *J* 11.6, 2.0), 6.51 (1H, dd, *J* 19.6, 13.3), 6.24 (1H, dd, *J* 19.6, 3.7), 6.04 (1H, dd, *J* 13.1, 3.7).

δ_{B} (128 MHz, CD₂Cl₂) 32.45.

Data collected match published material on this compound³⁵ therefore no further spectra were obtained.

I.3.2 BN2VN Polymerization



PBN2VN₃₉ (Toluene Polymerization)

An oven-dried 15 mL heavy walled cylindrical pressure vessel equipped with a rare-earth³ stir bar was brought into the glove box and charged with **BN2VN** (17.9 mmol, 2.77 g), toluene (2.7 mL), and AIBN (0.2 M in toluene, 3 mol%, 0.54 mmol, 2.7 mL). The pressure vessel was tightly sealed with a Teflon cap, brought out of the glove box, wrapped in aluminum foil, and heated (in a pre-heated pie plate) to 70 °C for 24 hours with vigorous stirring. Polymerization was quenched by opening the reaction flask in air and immediately pipetting the solution into a beaker of methanol (200 mL). Over the course of 30 minutes the polymer precipitated from solution and was isolated by filtering off the methanol solution through a plug of celite. Collected polymer was washed with additional methanol (150 mL), then eluted with toluene (250 mL) into an empty round bottom flask. The toluene polymer solution was concentrated by rotary evaporation (to ~ 6 mL) and once again precipitated into methanol (200 mL). The second precipitation yielded a more powdery precipitate, which was filtered over a plug of celite, washed with methanol (150 mL), and then eluted with dichloromethane (200 mL) into an empty round bottom flask. The polymer solution was concentrated by rotary evaporation, divided among tared scintillation vials (3) for storage, concentrated by rotary evaporation, and then finally dried in a vacuum oven for about 36 hours at 85 °C (yield 2.04 g, 74%).

δ_{H} (400 MHz, CD₂Cl₂) 8.30 – 5.46(7 H, m), 2.39 – 0.43 (3 H, m).

δ_{C} (101 MHz, CD₂Cl₂) 143.82, 140.13, 129.16, 127.89, 125.23, 120.42, 117.73.

³ A stronger magnet provided better stirring (Fischer Scientific Catalogue No. 14-513-511).

δ_B (128 MHz, CD₂Cl₂) 32.8 (br).

Anal. Found: C, 77.1; H, 6.2; N, 9.1. Calc. for C₁₀H₁₀BN: C, 77.5; H, 6.5; N, 9.0.

PBN2VN₅₇ (Neat Polymerization)

An oven-dried 2-5 mL microwave vial equipped with a small stir bar was brought into the glove box and charged with **BN2VN** (2 mmol, 310.1 mg) and AIBN (1 mol%, 3.3 mg). The microwave vial was crimped with an aluminum/PTFE/silicone septum seal, brought out of the glove box, wrapped in aluminum foil, and heated (in a pre-heated pie plate) to 85 °C for 72 hours with vigorous stirring. Polymerization was quenched by opening the microwave vial in air, dissolving the solid polymer in dichloromethane (10 mL), and immediately pipetting the solution into a beaker of methanol (30 mL). Over the course of 30 minutes the polymer precipitated from solution and was isolated by filtering off the methanol solution through a plug of celite. Collected polymer was washed with additional methanol (20 mL) then eluted with dichloromethane (20 mL) into an empty round bottom flask. The dichloromethane polymer solution was concentrated by rotary evaporation, re-dissolved in dichloromethane (5 mL), and once again precipitated into methanol (30 mL). The second precipitation yielded a more powdery precipitate, which was filtered over a plug of celite, washed with methanol (20 mL), and then eluted with dichloromethane (20 mL) into an empty round bottom flask. The polymer solution was concentrated by rotary evaporation, transferred to a tared scintillation vial for storage, dried on the Schenk line for about 30 min, and then finally dried in a vacuum oven for about 36 hours at 85 °C (yield 119.5 mg, 39%).

Note: Due to the readiness of **BN2VN** to evaporate and condense at elevated temperatures in the absence of solvent, some monomer amassed at the top of the microwave vial (below, left). In order to limit characterization to the bulk polymer, the microwave vial was inverted and the top two thirds of the microwave vial was rinsed with dichloromethane (below, right). Potential for non-

representative polymerization above the bulk is possible due to splashing of the less viscous reaction mixture during early stages of polymerization.

δ_{H} (400 MHz, CD_2Cl_2) 8.19 – 5.43 (6 H, m), 2.56 – 0.32 (3 H, m).

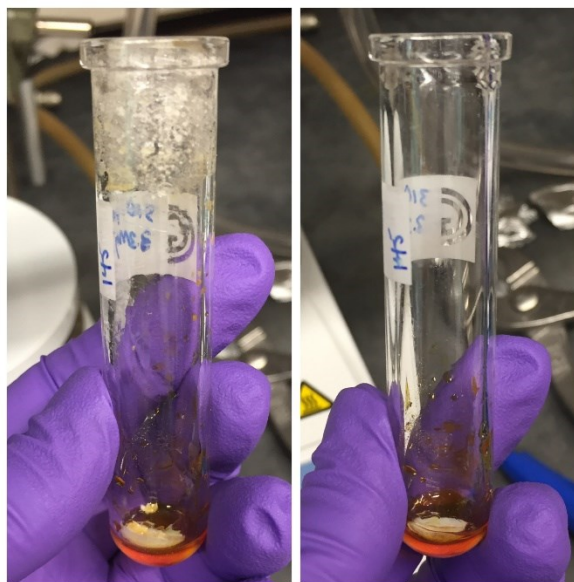
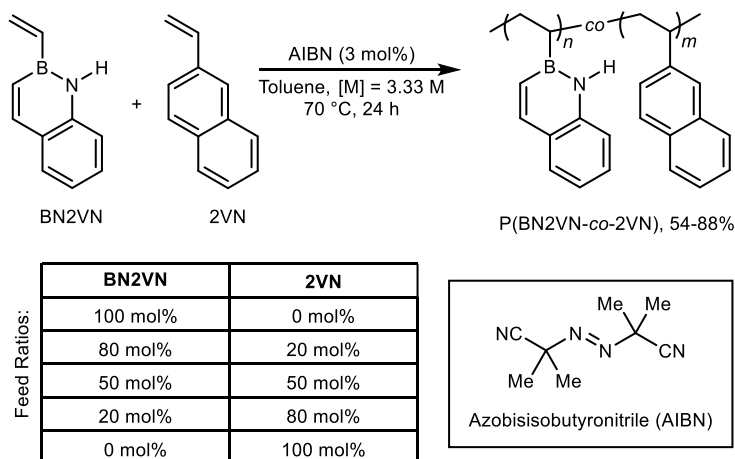


Figure I.1. Image of bulk polymerization reaction vessel. Left: condensed monomer appears at top of vial and bulk material at bottom. Right: Bulk reaction after removing condensed monomer.

I.4 Experimental Details for Chapter 4: BN2VN and 2-Vinylnaphthalene (2VN) Copolymers

I.4.1 Copolymerization of BN2VN and 2VN



General Procedure D: An oven-dried 15 mL heavy walled cylindrical pressure vessel equipped with a small stir bar was brought into the glove box and charged with the appropriate monomer(s) (2 mmol total), toluene (0.3 mL), and AIBN (0.2 M in toluene, 3 mol%, 0.06 mmol, 0.3 mL). The pressure vessel was tightly sealed with a Teflon cap, brought out of the glove box, wrapped in aluminum foil, and heated (in a pre-heated pie plate) to 70 °C for 24 hours with vigorous stirring. Polymerization was quenched by opening the reaction flask in air and immediately pipetting the solution into a beaker of methanol (30 mL). Over the course of 30 minutes the polymer precipitated from solution and was isolated by filtering off the methanol solution through a plug of celite. Collected polymer was washed with additional methanol (20 mL), then eluted with toluene (20 mL) into an empty round bottom flask. The toluene polymer solution was concentrated by rotary evaporation, re-dissolved in toluene (5 mL), and once again precipitated into methanol (30 mL). The second precipitation yielded a more powdery precipitate, which was filtered over a plug of celite, washed with methanol (20 mL), and then eluted with dichloromethane (20 mL) into an empty round bottom flask. The polymer solution was concentrated by rotary evaporation,

transferred to a tared scintillation vial for storage, dried on the Schenk line for about 30 min, and then finally dried in a vacuum oven for about 36 hours at 85 °C.

PBN2VN₃₉

Synthesized according to General Procedure D using **BN2VN** (2 mmol, 309.9 mg) (yield 178.1 mg, 58%).

δ_{H} (400 MHz, CD₂Cl₂) 8.17 – 5.43 (5 H, m), 2.26 – 0.46 (3 H, m).

δ_{C} (101 MHz, CD₂Cl₂) 144.26, 140.44, 129.67, 128.40, 125.73, 120.92, 118.21.

δ_{B} (128 MHz, CD₂Cl₂) 31.2 (br).

Anal. Found: C, 77.1; H, 6.2; N, 9.1. Calc. for C₁₀H₁₀BN: C, 77.5; H, 6.5; N, 9.0.

P(BN2VN₇₄-*co*-2VN₂₆)

Synthesized according to General Procedure D using **BN2VN** (1.6 mmol, 248.7 mg) and **2VN** (0.4 mmol, 61.6 mg) (yield 167.6 mg, 54%).

δ_{H} (400 MHz, CD₂Cl₂) 8.32 – 6.04 (6 H, m), 3.13 – 0.21 (3 H, m).

δ_{C} (101 MHz, CD₂Cl₂) 144.38, 140.41, 133.91, 132.64, 129.62, 127.97, 125.72, 120.93, 118.18.

δ_{B} (128 MHz, CD₂Cl₂) 33.1 (br).

Anal. Found: C, 81.0; H, 6.7; N, 6.8. Calc. for [C₁₀H₁₀BN]_{0.74}[C₁₂H₁₀]_{0.26}: C, 81.6; H, 6.5; N, 6.7.

P(BN2VN₄₉-*co*-2VN₅₁)

Synthesized according to General Procedure D using **BN2VN** (1 mmol, 156.1 mg) and **2VN** (1 mmol, 154.2 mg) (yield 190.5 mg, 61%).

δ_{H} (400 MHz, CD ₂ Cl ₂)	8.07 – 6.37 (6 H, m), 2.38 – 0.39 (3 H, m).
δ_{C} (101 MHz, CD ₂ Cl ₂)	144.20, 139.81, 133.39, 132.14, 129.13, 127.52, 127.37, 126.60, 125.67, 125.29, 125.00, 120.50, 117.72, 40.90.
δ_{B} (128 MHz, CD ₂ Cl ₂)	33.2 (br).
Anal.	Found: C, 85.6; H, 6.2; N, 3.6. Calc. for [C ₁₀ H ₁₀ BN] _{0.49} [C ₁₂ H ₁₀] _{0.51} : C, 85.6; H, 6.5; N, 4.4.

P(BN2VN₉-*c*o-2VN₉₁)

Synthesized according to General Procedure D using **BN2VN** (0.4 mmol, 61.9 mg) and **2VN** (1.6 mmol, 245.6 mg) (yield 171.1 mg, 56%).

δ_{H} (400 MHz, CD ₂ Cl ₂)	7.95 – 6.12 (7 H, m), 2.26 – 1.22 (3 H, m).
δ_{C} (101 MHz, CD ₂ Cl ₂)	142.88, 133.85, 132.59, 127.99, 127.79, 127.23, 126.14, 125.78, 125.44, 41.16.
δ_{B} (128 MHz, CD ₂ Cl ₂)	34.5 (br).
Anal.	Found: C, 91.0; H, 6.0; N, 0.71. Calc. for [C ₁₀ H ₁₀ BN] _{0.09} [C ₁₂ H ₁₀] _{0.91} : C, 92.0; H, 6.5; N, 0.81.

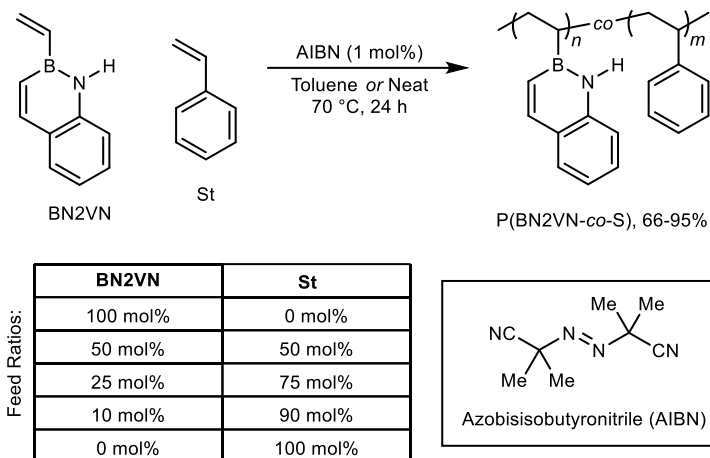
P2VN₅₄

Synthesized according to General Procedure D using **2VN** (2 mmol, 308.4 mg) (yield 271.0 mg, 88%).

δ_{H} (400 MHz, CD ₂ Cl ₂)	8.07 – 6.18 (7 H, m), 2.54 – 1.38 (3 H, m).
δ_{C} (101 MHz, CD ₂ Cl ₂)	143.49, 142.98, 133.90, 132.63, 128.03, 127.85, 127.20, 126.14, 125.48, 41.19.
Anal.	Found: C, 92.3; H, 6.2; N, 0.12. Calc. for C ₁₂ H ₁₀ : C, 93.5; H, 6.5. Found nitrogen incorporation likely reflects AIBN end groups.

I.5 Experimental Details for Chapter 5: BN2VN and Styrene Copolymers

I.5.1 Copolymerization of BN2VN and Styrene



General Procedure E: An oven-dried 2-5 mL microwave reaction vial equipped with a small stir bar was brought into a nitrogen filled glove box and charged with the appropriate monomer(s) (10 mmol total) and AIBN (1 mol%, 0.1 mmol, 16 mg). The microwave vial was capped with an aluminum and Teflon seal, brought out of the glove box, wrapped in aluminum foil, and heated (in a pre-heated pie plate) to 70 °C for 24 hours with vigorous stirring. Polymerization was quenched by opening the reaction flask in air, dissolving in dichloromethane (5 x 5 mL), and immediately pipetting the solution into a beaker of methanol (200 mL). Over the course of 20 minutes the polymer precipitated from solution and was isolated by filtering off the methanol solution through a medium fritted funnel. Collected polymer was washed with additional methanol (100 mL), then eluted with dichloromethane (35 mL) into an empty round bottom flask. The dichloromethane-polymer solution was once again precipitated into methanol (200 mL). The second precipitation yielded a more powdery precipitate, which was filtered through a medium fritted funnel, washed with methanol (100 mL), and then transferred to a tared scintillation vial for storage, dried on the Schenk line for about 30 min, and then finally dried in a vacuum oven for about 36 hours at 60 °C.

PBN2VN₁₃₂

Synthesized according to General Procedure E using **BN2VN** (10 mmol, 1.55 g) to yield a white powder (yield 1.17 g, 75%).

δ_{H} (400 MHz, CD ₂ Cl ₂)	8.23-5.57 (7 H, m), 2.54-0.14 (3 H, m).
δ_{C} (101 MHz, CD ₂ Cl ₂)	143.78, 139.93, 129.11, 127.77, 125.25, 120.40, 117.66, 38.28, 29.92.
δ_{B} (128 MHz, CD ₂ Cl ₂)	28.89 (br).
FTIR (KBr, thin film)	3381 (m), 3008 (w), 2885 (m), 2836 (m), 1613 (m), 1562 (m), 1437 (s), 807 (m), 761 (s) cm ⁻¹ .
Anal.	Found: C, 77.09; H, 6.44; N, 8.91. Calc. for C ₁₀ H ₁₂ BN: C, 76.49; H, 7.70; N, 8.92.

P(BN2VN₁₂₇-*co*-S₁₄₁)

Synthesized according to General Procedure E using **BN2VN** (5 mmol, 780 mg) and styrene (5 mmol, 520 mg) to yield a white powder (yield 1.12 g, 87%).

δ_{H} (400 MHz, CD ₂ Cl ₂)	8.11-6.08 (6 H, m), 2.71-0.48 (3 H, m).
δ_{C} (101 MHz, CD ₂ Cl ₂)	146.10, 144.00, 139.93, 129.15, 127.98, 125.65, 120.47, 117.82, 42.38, 40.63, 27.78, 25.71.
δ_{B} (128 MHz, CD ₂ Cl ₂)	31.78 (br).
FTIR (KBr, thin film)	3374 (w), 3025 (m), 2910 (m), 2844 (w), 1614 (m), 1562 (s), 1438 (s), 806 (m), 761 (s), 700 (s), 667 (w) cm ⁻¹ .
Anal.	Found: C, 83.46; H, 6.95; N, 5.07. Calc. for C ₁₀ H ₁₂ BN(0.47)+C ₈ H ₈ (0.53): C, 84.85; H, 7.72; N, 4.19.

P(BN2VN₈₇-*co*-S₂₃₆)

Synthesized according to General Procedure E using **BN2VN** (2.5 mmol, 390 mg) and styrene (7.5 mmol, 780 mg) to yield a white powder (yield 1.01 g, 86%).

δ_{H} (400 MHz, CD ₂ Cl ₂)	8.01-6.09 (6 H, m), 2.42-0.44 (3 H, m).
---	---

δ_{C} (101 MHz, CD ₂ Cl ₂)	145.47, 144.17, 139.86, 129.08, 127.93, 125.65, 120.41, 117.80, 42.13, 40.45.
δ_{B} (128 MHz, CD ₂ Cl ₂)	39.13 (br).
FTIR (KBr, thin film)	3373 (w), 3025 (m), 2920 (m), 2847 (w), 1614 (m), 1562 (m), 1493 (m), 1439 (m), 8078 (w), 761 (m), 699 (s), 667 (w) cm ⁻¹ .
Anal.	Found: C, 87.47; H, 7.34; N, 2.71. Calc. for C ₁₀ H ₁₂ BN(0.27)+C ₈ H ₈ (0.73): C, 88.00; H, 7.73; N, 2.41.

P(BN2VN₃₂-*co*-S₃₃₂)

Synthesized according to General Procedure E using **BN2VN** (1 mmol, 160 mg) and styrene (9 mmol, 940 mg) to yield a white powder (yield 970 mg, 89%).

δ_{H} (400 MHz, CD ₂ Cl ₂)	7.99-6.25 (5 H, m), 2.43-0.42 (3 H, m).
δ_{C} (101 MHz, CD ₂ Cl ₂)	145.48, 144.15, 139.87, 129.09, 128.01, 125.68, 120.42, 117.82, 44.45, 42.12, 40.48.
δ_{B} (128 MHz, CD ₂ Cl ₂)	37.87 (br).
FTIR (KBr, thin film)	3059 (w), 3026 (m), 2923 (m), 2849 (w), 1600 (m), 1561 (m), 1451 (m), 760 (m), 699 (s), 667 (w) cm ⁻¹ .
Anal.	Found: C, 90.55; H, 7.47; N, 1.14. Calc. for C ₁₀ H ₁₂ BN(0.09)+C ₈ H ₈ (0.91): C, 90.84; H, 7.74; N, 0.80.

PS₃₁₃

Synthesized according to General Procedure E using styrene (10 mmol, 1.05 g) to yield a white powder (yield 990 mg, 95%).

δ_{H} (400 MHz, CD ₂ Cl ₂)	7.48-6.08 (5 H, m), 2.46-0.82 (3 H, m).
δ_{C} (101 MHz, CD ₂ Cl ₂)	146.23, 145.85, 128.46, 128.06, 126.09, 44.54, 40.81.
FTIR (KBr, thin film)	3026 (m), 2924 (m), 2850 (w), 1601 (w), 1493 (m), 1452 (m), 756 (m), 699 (s) cm ⁻¹ .
Anal.	Found: C, 92.20; H, 7.68; N, < 0.02. Calc. for C ₈ H ₈ : C, 92.26; H, 7.74; N, 0.00.

General Procedure F: An oven-dried 2-5 mL microwave reaction vial equipped with a small stir bar was brought into a nitrogen filled glove box and charged with the appropriate monomer(s) (10 mmol total), AIBN (1 mol%, 0.1 mmol, 16 mg), and toluene (1 mL, [monomer]=10 M). The microwave vial was capped with an aluminum and Teflon seal, brought out of the glove box, wrapped in aluminum foil, and heated (in a pre-heated pie plate) to 70 °C for 24 hours with vigorous stirring. Polymerization was quenched by opening the reaction flask in air, dissolving in dichloromethane (2 x 5 mL), and immediately pipetting the solution into a beaker of methanol (200 mL). Over the course of 20 minutes the polymer precipitated from solution and was isolated by filtering off the methanol solution through a medium fritted funnel. Collected polymer was washed with additional methanol (100 mL), then eluted with dichloromethane (25 mL) into an empty round bottom flask. The dichloromethane-polymer solution was once again precipitated into methanol (200 mL). The second precipitation yielded a more powdery precipitate, which was filtered through a medium fritted funnel, washed with methanol (100 mL), and then transferred to a tared scintillation vial for storage, dried on the Schenk line for about 30 min, and then finally dried in a vacuum oven for about 36 hours at 60 °C.

P(BN2VN₄₈-co-S₅₁)

Synthesized according to General Procedure F using **BN2VN** (5 mmol, 780 mg) and styrene (5 mmol, 520 mg) to yield a white powder (yield 860 mg, 66%).

δ_{H} (400 MHz, CD ₂ Cl ₂)	8.04-6.03 (5 H, m), 2.56-0.39 (3 H, m).
δ_{C} (101 MHz, CD ₂ Cl ₂)	145.87, 143.96, 139.82, 129.04, 127.86, 125.43, 120.36, 117.72, 53.98, 42.46, 40.35.
δ_{B} (128 MHz, CD ₂ Cl ₂)	36.80 (br).
FTIR (KBr, thin film)	3373 (w), 3025 (m), 2915 (m), 2846 (w), 1614 (m), 1562 (m), 1439 (s), 807 (m), 761 (s), 700 (s), 667 (w) cm ⁻¹ .
Anal.	Found: C, 85.1; H, 7.09; N, 4.43. Calc. for C ₁₀ H ₁₂ BN(0.48)+C ₈ H ₈ (0.52): C, 84.69; H, 7.72; N, 4.28.

P(BN2VN₃₂-co-S₉₂)

Synthesized according to General Procedure F using **BN2VN** (2.5 mmol, 390 mg) and styrene (7.5 mmol, 790 mg) to yield a white powder (yield 860 mg, 73%).

δ_{H} (400 MHz, CD ₂ Cl ₂)	8.06-6.13 (5 H, m), 2.74-0.41 (3 H, m).
δ_{C} (101 MHz, CD ₂ Cl ₂)	145.44, 144.17, 139.80, 129.06, 127.92, 125.57, 120.38, 117.78, 117.74, 42.47, 40.41.
δ_{B} (128 MHz, CD ₂ Cl ₂)	37.84 (br).
FTIR (KBr, thin film)	3371 (w), 3026 (m), 2921 (m), 2848 (w), 1614 (m), 1562 (m), 1493 (m), 1450 (m), 807 (w), 761 (m), 669 (s), 667 (w) cm ⁻¹ .
Anal.	Found: C, 88.24; H, 7.37; N, 2.21. Calc. for C ₁₀ H ₁₂ BN(0.26)+C ₈ H ₈ (0.74): C, 88.16; H, 7.73; N, 2.32.

P(BN2VN₁₄-co-S₁₁₉)

Synthesized according to General Procedure F using **BN2VN** (1 mmol, 160 mg) and styrene (9 mmol, 940 mg) to yield a white powder (yield 840 mg, 77%).

δ_{H} (400 MHz, CD ₂ Cl ₂)	8.16-6.24 (5 H, m), 2.79-0.50 (3 H, m).
δ_{C} (101 MHz, CD ₂ Cl ₂)	145.46, 144.22, 139.87, 127.99, 125.70, 120.50, 117.75, 44.40, 40.41.
δ_{B} (128 MHz, CD ₂ Cl ₂)	35.77 (br).
FTIR (KBr, thin film)	3026 (m), 2923 (m), 2849 (w), 1600 (w), 1561 (m), 1493 (m), 1451 (m), 1028 (w), 760 (m), 699 (s), 667 (w) cm ⁻¹ .
Anal.	Found: C, 90.51; H, 7.62; N, 0.94. Calc. for C ₁₀ H ₁₂ BN(0.11)+C ₈ H ₈ (0.89): C, 90.53; H, 7.74; N, 0.98.

PS₁₂₉

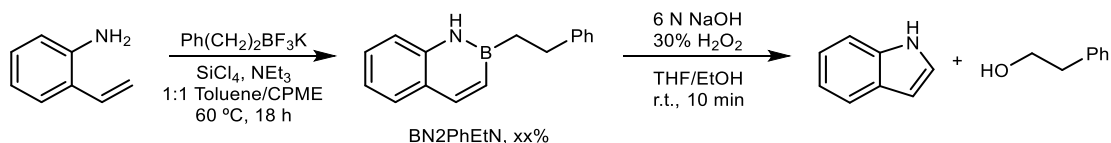
Synthesized according to General Procedure F using styrene (10 mmol, 1.04 g) to yield a white powder (yield 850 mg, 81%).

δ_{H} (400 MHz, CD ₂ Cl ₂)	7.54-6.21 (5 H, m), 2.78-0.79 (3 H, m).
---	---

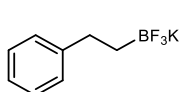
δ_c (101 MHz, CD ₂ Cl ₂)	145.85, 128.40, 126.10, 44.79, 40.81.
FTIR (KBr, thin film)	3026 (m), 2924 (m), 2850 (w), 1601(w), 1493 (m), 1452 (m), 756 (m), 699 (s) cm ⁻¹ .
Anal.	Found: C, 91.89; H, 7.89; N, < 0.02. Calc. for C ₈ H ₈ : C, 92.26; H, 7.74; N, 0.00.

I.6 Experimental Details for Chapter 6: Polymer Side Chain BN Oxidation

I.6.1 Small Molecule Oxidation Study



Potassium Phenethyltrifluoroborate



This reaction is adapted from Aggarwal *et al.*²¹⁵

To a 50 mL round bottom flask was added phenethylboronic acid (1 equiv., 456 mg, 3 mmol) and methanol (10 mL). Aqueous potassium hydrogen fluoride solution (4.5 M, 1.5 equiv., 2 mL, 9 mmol) was added dropwise to the methanol solution while swirling the reaction flask. The reaction flask was attached to the rotary evaporator and allowed to spin (without applied vacuum) in a 30 °C water bath for 30 minutes. After 30 minutes the water bath temperature was raised to 50 °C and vacuum was applied to remove the water/methanol azeotrope by rotary evaporation. Once dry, methanol (6 mL) and DI water (3-6 mL) was added to re-dissolve the reaction mixture followed by continued rotary evaporation to dryness; this was repeated a total of 4 times. After the final rotary evaporation, the reaction was placed on the Schlenk line to dry under reduced pressure, overnight. The following day the product was triturated away from insoluble salts with dry acetone (8 mL, then 3 x 2 mL), filtering the acetone solution through a cotton tipped pipette. The acetone solution was concentrated by rotary evaporation, transferred to a tared scintillation vial, and then placed on the Schlenk line to dry under reduced pressure to yield a white solid (yield 549 mg, 85%).

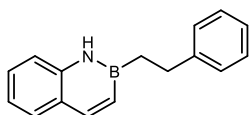
δ_{H} (400 MHz, CD₃CN) 7.24 – 7.18 (4H, m), 7.10 – 7.05 (1H, m), 2.53 – 2.48 (2H, m), 0.49 – 0.30 (2H, m).

δ_{C} (101 MHz, CD₃CN) 149.52, 128.95, 128.92, 125.48, 106.06, 33.17, 33.14.

δ_{B} (128 MHz, CD₃CN) 5.18, 4.68.

δ_F (282 MHz, CD ₃ CN)	-140.44, -140.72, -140.91.
HRMS (EI)	HRMS (EI) m/z: [M-KF] ⁺ Calcd for C ₈ H ₉ BF ₂ 154.0765; Found 154.07666.
Anal.	Found: C, 44.86; H, 3.97; N, < 0.02. Calc. for C ₈ H ₉ BF ₃ K: C, 45.31; H, 4.28; N, 0.00.

2-Phenethyl-1,2-Dihydrobenzo[e][1,2]Azaborinine (1)



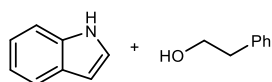
This procedure was adapted from Klausen *et al.*³⁵

An oven-dried 100 mL Schlenk flask equipped with a stir bar and septum sealed reflux condenser was charged with potassium phenethyltrifluoroborate (1.1 equiv., 2.9 mmol, 604 mg) and purged and backfilled three times with argon. 2-Vinylalanine (1 equiv., 2.6 mmol, 309 mg), toluene (11.4 mL), cyclopentyl methyl ether (CPME) (11.4 mL), triethylamine (1.5 equiv., 3.9 mmol, 0.54 mL), then silicon tetrachloride (1.1 equiv., 2.9 mmol, 0.33 mL) were added and the reaction mixture was heated to 60 °C for 16 hours with stirring under a positive pressure of argon. The reaction mixture was cooled to room temperature, diluted with hexanes (10 mL), and passed through a plug of silica to remove solids, washing with 20% dichloromethane in hexanes (150 mL). The eluent was collected and concentrated by rotary evaporation. The product was purified by silica gel chromatography, eluting with hexanes, then ramping to 10% dichloromethane in hexanes. Fractions were concentrated by rotary evaporation, transferred to a tared scintillation vial, and placed on the Schlenk line to dry under reduced pressure to yield a white solid that was stored in the glove box for future use (yield 503 mg, 83%).

δ_H (400 MHz, CD ₂ Cl ₂)	7.98 (1H, d, <i>J</i> 11.5), 7.77 (1H, s), 7.64 – 7.57 (1H, m), 7.39 (1H, ddd, <i>J</i> 8.5, 7.1, 1.5), 7.28 (4H, d, <i>J</i> 4.7), 7.24 – 7.12 (3H, m), 6.88 (1H, dd, <i>J</i> 11.5, 2.0), 3.00 – 2.91 (2H, m), 1.68 – 1.61 (2H, m).
δ_C (101 MHz, CD ₂ Cl ₂)	145.46, 144.64, 140.54, 129.62, 128.66, 128.43, 128.42, 125.85, 121.05, 118.20, 32.25.
δ_B (128 MHz, CD ₂ Cl ₂)	37.74.
HRMS (EI)	HRMS (EI) m/z: [M] ⁺ Calcd for C ₁₆ H ₁₆ BN 233.1376; Found 233.13713.

Anal. Found: C, 82.23; H, 6.66; N, 5.90. Calc. for C₁₆H₁₆BN: C, 82.44; H, 6.92; N, 6.01.
Melting point: 97 °C

Oxidation of 2-Phenethyl-1,2-Dihydrobenzo[e][1,2]Azaborinine (**1**)

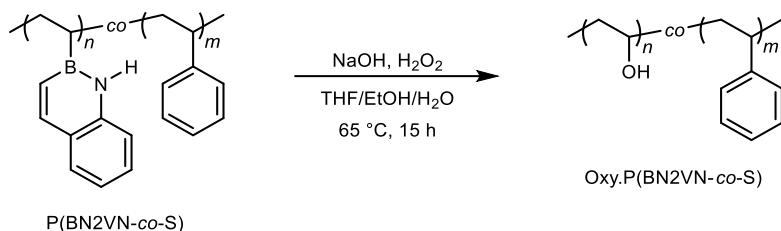


A two-dram vial equipped with a stir bar was added **1** (1 equiv., 0.2 mmol, 50 mg), tetrahydrofuran (THF) (2.0 mL), ethanol (EtOH) (0.5 mL), and aqueous sodium hydroxide (3 N, 1.0 mL). The stirred reaction mixture was cooled to 0 °C in an ice bath and aqueous hydrogen peroxide (30%, 1.0 mL) was added dropwise. The reaction mixture was allowed to stir at 0 °C for 10 minutes then decanted into a separatory funnel filled with aqueous saturated sodium chloride (5 mL), and the vial rinsed with diethyl ether (3 mL) into the separatory funnel. The organic layer was collected, dried with magnesium sulfate, concentrated by rotary evaporation, and then connected to the Schlenk line to dry under reduced pressure (for a limited time due to sublimation of indole and evaporation of phenethyl alcohol, 45 minutes) to yield a white solid suspended in a clear oil.

δ_{H} (400 MHz, CD₂Cl₂) 8.36 (1H, s), 7.65 (1H, dd, *J* 7.9, 1.2), 7.44 – 7.40 (1H, m), 7.38 – 7.28 (2H, m), 7.27 – 7.21 (5H, m), 7.20 – 7.17 (1H, m), 7.14 – 7.09 (1H, m), 3.84 (2H, t, *J* 6.6), 2.86 (2H, t, *J* 6.6), 1.68 (1H, s).
Indole: 8.36 (1H, s), 7.65 (1H, dd, *J* 7.9, 1.2), 7.44 – 7.40 (1H, m), 7.38 – 7.28 (2H, m), 7.20 – 7.17 (1H, m), 7.14 – 7.09 (1H, m).
Phenethyl Alcohol: 7.27 – 7.21 (5H, m), 3.84 (2H, t, *J* 6.6), 2.86 (2H, t, *J* 6.6), 1.68 (1H, s).

Data collected match authentic samples of these materials, therefore no further spectra were obtained.

I.6.2 Polymer Oxidation Study



General Procedure G: 200 mg of polymer was added to a 100 mL round bottom flask fit with a stir bar and dissolved in THF (25 mL). To this was added ethanol (5 mL) and aqueous sodium hydroxide (6 N, 5 mL), followed by the dropwise addition of aqueous hydrogen peroxide (30%, 10 mL) at room temperature. The reaction was allowed to stir in air for 30 minutes, then topped with an open topped reflux condenser and heated to 65 °C for 15 hours. The reaction mixture was allowed to cool to room temperature, then precipitated into deionized water (100 mL) in a 500 mL round bottom flask. Volatile organic solvents were removed by rotary evaporation and the precipitated polymer was filtered through a medium fritted funnel, then washed with excess deionized water. The polymer was eluted with dichloromethane (20 mL) into a small round bottom flask, then this solution was added to methanol (100-200 mL). The methanol solution was concentrated and brought to dryness by rotary evaporation, to facilitate the removal of borates. The dry polymer was dissolved in dichloromethane (~ 5 mL), transferred to a tared scintillation vial, concentrated by rotary evaporation, and then dried in a vacuum oven at 85 °C for 16 hours.

Oxy. P(BN2VN₁₂₇-co-S₁₄₁)

Synthesized according to General Procedure G using P(BN2VN₁₂₇-co-S₁₄₁) (200 mg) to yield an off white solid (yield 52.7 mg).

δ_{H} (400 MHz, CD₂Cl₂) 7.56-6.22 (5 H, m), 4.10-0.33 (5 H, m).

δ_c (101 MHz, CD₂Cl₂) 145.65, 128.49, 126.25, 44.96, 41.05.

FTIR (KBr, thin film) 3359 (w), 3383 (br), 3060 (m), 3026 (m), 2926 (m), 2851 (m), 1601 (m), 1493 (m), 1452 (m), 1029 (m), 760 (m), 700 (s) cm⁻¹.

Anal. Found: C, 84.79; H, 7.9; N, 0.31. Calc. for C₂H₄O(0.47)+C₈H₈(0.53): C, 74.5269; H, 8.4027; N, 0.00.

Oxy. P(BN2VN₈₇-*co*-S₂₃₆)

Synthesized according to General Procedure G using **P(BN2VN₈₇-*co*-S₂₃₆)** (200 mg) to yield a white solid (yield 156 mg).

δ_H (400 MHz, CD₂Cl₂) 7.37-6.33 (5 H, m), 3.66-0.42 (4 H, m).

δ_c (101 MHz, CD₂Cl₂) 145.28, 128.09, 125.71, 67.25, 44.43, 40.56.

FTIR (KBr, thin film) 3579 (w), 3428 (br), 3026 (m), 2925 (m), 2851 (w), 1601 (w), 1493 (m), 1452 (m), 1029 (w), 758 (m), 699 (s) cm⁻¹.

Anal. Found: C, 88.77; H, 7.29; N, 0.46. Calc. for C₂H₄O(0.27)+C₈H₈(0.75): C, 82.07; H, 8.12; N, 0.00.

Oxy. P(BN2VN₃₂-*co*-S₃₃₂)

Synthesized according to General Procedure G using **P(BN2VN₃₂-*co*-S₃₃₂)** (200 mg) to yield a white solid (yield 156 mg).

δ_H (400 MHz, CD₂Cl₂) 7.35-6.21 (5 H, m), 3.14-0.44 (3 H, m).

δ_c (101 MHz, CD₂Cl₂) 145.32, 128.04, 125.68, 44.37, 40.39.

FTIR (KBr, thin film) 3583 (w), 3439 (w), 3026 (m), 2924 (m), 2850 (w), 1601 (w), 1493 (m), 1452 (m), 1028 (w), 758 (m), 699 (s) cm⁻¹.

Anal. Found: C, 90.28; H, 7.85; N, 0.19. Calc. for C₂H₄O(0.09)+C₈H₈(0.91): C, 88.86; H, 7.87; N, 0.00.

Oxy. PS₃₁₃

Synthesized according to General Procedure G using **PS₃₁₃** (200 mg) to yield a white solid (yield 148.2 mg, 74%).

δ_{H} (400 MHz, CD ₂ Cl ₂)	7.32-63.23 (5 H, m), 2.51-0.76 (3 H, m).
δ_{C} (101 MHz, CD ₂ Cl ₂)	145.41, 128.02, 125.66, 44.14, 40.40.
FTIR (KBr, thin film)	3026 (m), 2923 (m), 2850 (w), 1601 (w), 1493 (m), 1452 (m), 1028 (w), 756 (m), 699 (s) cm ⁻¹ .
Anal.	Found: C, 88.16; H, 7.37; N, < 0.02. Calc. for C ₈ H ₈ : C, 92.26; H, 7.74; N, 0.00.

Oxy. P(BN2VN₄₈-co-S₅₁)

Synthesized according to General Procedure G using **P(BN2VN₄₈-co-S₅₁)** (200 mg) to yield an off white solid (yield 55 mg).

δ_{H} (400 MHz, CD ₂ Cl ₂)	7.59-6.16 (5 H, m), 4.14-0.12 (6 H, m).
δ_{C} (101 MHz, CD ₂ Cl ₂)	145.59, 128.51, 126.31, 67.69, 44.73, 41.11.
FTIR (KBr, thin film)	3557 (w), 3384 (br), 3026 (m), 2927 (m), 1601 (w), 1493 (m), 1452 (m), 1068 (m), 760 (m), 700 (s) cm ⁻¹ .
Anal.	Found: C, 83.67; H, 8.05; N, 0.35. Calc. for C ₂ H ₄ O(0.5)+C ₈ H ₈ (0.5): C, 74.1496; H, 8.4168; N, 0.00.

Oxy. P(BN2VN₃₂-co-S₉₂)

Synthesized according to General Procedure G using **P(BN2VN₃₂-co-S₉₂)** (200 mg) to yield a white solid (yield 121 mg).

δ_{H} (400 MHz, CD ₂ Cl ₂)	7.46-6.25 (5 H, m), 3.55-0.42 (4 H, m).
δ_{C} (101 MHz, CD ₂ Cl ₂)	145.38, 128.06, 125.68, 67.20, 44.06, 40.42.
FTIR (KBr, thin film)	3580 (w), 3426 (w), 3026 (m), 2925 (m), 2851 (w), 1601 (w), 1493 (m), 1452 (m), 1029 (w), 759 (m), 699 (s) cm ⁻¹ .
Anal.	Found: C, 87.85; H, 7.73; N, 0.35. Calc. for C ₂ H ₄ O(0.25)+C ₈ H ₈ (0.75): C, 82.45; H, 8.10; N, 0.00.

Oxy. P(BN2VN₁₄-co-S₁₁₉)

Synthesized according to General Procedure G using **P(BN2VN₁₄-co-S₁₁₉)** (200 mg) to yield a white solid (yield 185 mg).

δ_{H} (400 MHz, CD₂Cl₂) 7.54-6.22 (5 H, m), 3.10-0.39 (3 H, m).

δ_{C} (101 MHz, CD₂Cl₂) 145.33, 128.05, 125.69, 67.24, 44.39, 40.39.

FTIR (KBr, thin film) 3587 (w), 3448 (w), 3026 (m), 2925 (m), 2851 (m), 1601 (m), 1493 (m), 1452 (m), 1029 (m), 758 (m), 699 (s) cm⁻¹.

Anal. Found: C, 90.9; H, 6.07; N, 0.33. Calc. for C₂H₄O(0.1)+C₈H₈(0.9): C, 88.11; H, 7.90; N, 0.00.

Oxy. PS₁₂₉

Synthesized according to General Procedure G using **PS₁₂₉** (200 mg) to yield a white solid (yield 172 mg, 86%).

δ_{H} (400 MHz, CD₂Cl₂) 7.54-6.26 (5 H, m), 2.49-0.79 (3 H, m).

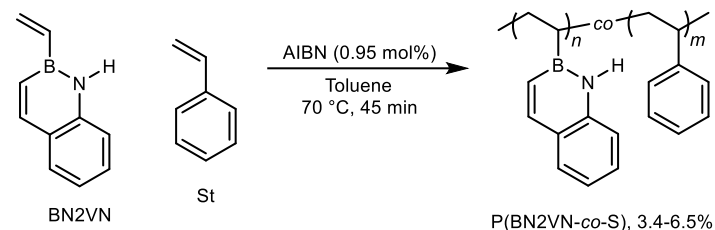
δ_{C} (101 MHz, CD₂Cl₂) 145.34, 127.98, 125.68, 44.43, 40.38.

FTIR (KBr, thin film) 3026 (m), 2924 (m), 2850 (m), 1601 (m), 1493 (m), 1452 (m), 1028 (m), 756 (m), 699 (s) cm⁻¹.

Anal. Found: C, 91.58; H, 7.53; N, < 0.02. Calc. for C₈H₈: C, 92.26; H, 7.74; N, 0.00.

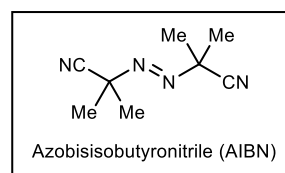
I.7 Experimental Details for Chapter 7: Reactivity Ratios of BN2VN and Styrene

I.7.1 Low Conversion BN2VN and Styrene Copolymerization



Feed Ratios:

BN2VN	St
90 mol%	10 mol%
80 mol%	20 mol%
70 mol%	30 mol%
60 mol%	40 mol%
50 mol%	50 mol%
40 mol%	60 mol%
30 mol%	70 mol%
20 mol%	80 mol%
10 mol%	90 mol%



General Procedure H: Stock solutions of St and BN2VN (3.00 M in toluene) and AIBN (31.2 mg/mL in toluene) were prepared. In a nitrogen atmosphere glove box, monomers (10.00 mmol total) and AIBN (0.095 mmol) were added to microwave reaction vials and vials were sealed. The sealed vials were heated in a pre-heated pie plate at 70 °C for 45 minutes with vigorous stirring. Upon opening to air, solutions were immediately transferred to a beaker of methanol (80 mL). The microwave vial was rinsed with dichloromethane (2 x 1 mL) and rinsates added to the methanol. Precipitated polymer was isolated by filtration through a thin pad of Celite (~3-5 mm), washed with methanol (10 mL), then eluted with dichloromethane (2 x 5 mL). Methanol precipitation was repeated a second time. The purified polymer was dried in a vacuum oven for about 18 hours at 85 °C.

P(BN2VN₄-*c*O**-S₁₀₃)**

Synthesized according to the General Procedure H using BN2VN (0.33 mL, 1.00 mmol) and St (3.00 mL, 9.00 mmol) to yield a white powder (yield 67.3 mg, 6.2%).

δ_{H} (400 MHz, CD₂Cl₂) 8.01-6.18 (br, 4.83 H), 2.77-0.44 (br, 3.00 H).

FTIR (KBr, thin film) 3060 (m), 3026 (m), 2924 (m), 2850 (w), 1601 (w), 1560 (w), 1493 (m), 1452 (m), 1028 (w), 759 (m), 698 (s), 541 (w) cm⁻¹.

P(BN2VN₁₀-*c*O**-S₈₆)**

Synthesized according to the General Procedure H using BN2VN (0.667 mL, 2.00 mmol) and St (2.67 mL, 8.00 mmol) to yield a white powder (yield 74.6 mg, 6.5%).

δ_{H} (400 MHz, CD₂Cl₂) 8.02-6.15 (br, 4.87 H), 2.80-0.34 (br, 3.00 H).

FTIR (KBr, thin film) 3059 (w), 3025 (m), 2923 (m), 2849 (w), 1615 (m), 1562 (m), 1493 (m), 1452 (m), 806 (w), 760 (m), 689 (s), 541 (w) cm⁻¹.

P(BN2VN₁₅-*c*O**-S₈₁)**

Synthesized according to the General Procedure H using BN2VN (1.00 mL, 3.00 mmol) and St (2.33 mL, 7.00 mmol) to yield a white powder (yield 62.2 mg, 5.2%).

δ_{H} (400 MHz, CD₂Cl₂) 8.01-6.06 (br, 4.99 H), 2.75-0.45 (br, 3.00 H).

FTIR (KBr, thin film) 3059 (w), 3025 (m), 2923 (br), 2848 (w), 1615 (m), 1598 (m), 1563 (m), 1493 (m), 1452 (m), 761 (m), 698 (s) cm⁻¹.

P(BN2VN₂₀-*c*O**-S₇₀)**

Synthesized according to the General Procedure H using BN2VN (1.33 mL, 4.00 mmol) and St (2.00 mL, 6.00 mmol) to yield a white powder (yield 66.5 mg, 5.3%).

δ_{H} (400 MHz, CD₂Cl₂) 8.01-6.05 (br, 5.03 H), 2.79-0.39 (br, 3.00 H).

FTIR (KBr, thin film) 3059 (w), 3025 (m), 2920 (br), 2847 (w), 1614 (m), 1597 (w), 1563 (m), 1493 (m), 1452 (m), 1439 (m), 806 (w), 761 (m), 698 (s) cm^{-1} .

P(BN2VN₂₅-*co*-S₆₁)

Synthesized according to the General Procedure H using BN2VN (1.67 mL, 5.00 mmol) and St (1.67 mL, 5.00 mmol) to yield a white powder (yield 63.8 mg, 4.9%).

δ_{H} (400 MHz, CD_2Cl_2) 8.04-6.08 (br, 5.13 H), 2.84-0.39 (br, 3.00 H).

FTIR (KBr, thin film) 3372 (br), 3059 (w), 3025 (m), 2918 (br), 2847 (w), 1614 (m), 1596 (w), 1562 (m), 1540 (w), 1493 (m), 1452 (m), 1438 (m), 1387 (w), 1345 (w), 1137 (m), 806 (m), 761 (s), 699 (s), 458 (m) cm^{-1} .

P(BN2VN₃₂-*co*-S₄₆)

Synthesized according to the General Procedure H using BN2VN (2.00 mL, 6.00 mmol) and St (1.33 mL, 4.00 mmol) to yield a white powder (yield 63.7 mg, 4.7%).

δ_{H} (400 MHz, CD_2Cl_2) 8.11-5.90 (br, 5.28 H), 2.79-0.36 (br, 3.00 H).

FTIR (KBr, thin film) 3373 (br), 3058 (w), 3025 (m), 2915 (br), 2845 (w), 1614 (m), 1596 (m), 1562 (s), 1493 (m), 1451 (m), 1439 (m), 806 (m), 760 (s), 699 (s), 458 (m) cm^{-1} .

P(BN2VN₃₈-*co*-S₃₅)

Synthesized according to the General Procedure H using BN2VN (2.33 mL, 7.00 mmol) and St (1.00 mL, 3.00 mmol) to yield a white powder (yield 47.6 mg, 3.4%).

δ_{H} (400 MHz, CD_2Cl_2) 8.03-6.10 (br, 5.40 H), 2.60-0.38 (br, 3.00 H).

FTIR (KBr, thin film) 3373 (br), 3025 (m), 2911 (br), 2844 (w), 1614 (s), 1596 (m), 1562 (s), 1493 (m), 1438 (s), 1137 (w), 806 (m), 760 (s), 700 (s), 458 (m) cm^{-1} .

P(BN2VN₄₁-*co*-S₂₀)

Synthesized according to the General Procedure H using BN2VN (2.67 mL, 8.00 mmol) and St (0.667 mL, 2.00 mmol) to yield a white powder (yield 55.7 mg, 3.8%).

δ_{H} (400 MHz, CD₂Cl₂) 8.10-5.95 (br, 5.55 H), 2.66-0.33 (br, 3.00 H).

FTIR (KBr, thin film) 3375 (br), 3024 (m), 2903 (br), 2842 (m), 1614 (s), 1597 (m), 1562 (s), 1492 (m), 1472 (m), 1439 (s), 1136 (m), 806 (m), 761 (s), 700 (m), 459 (m) cm⁻¹.

P(BN2VN₃₉-*co*-S₁₁)

Synthesized according to the General Procedure H using BN2VN (3.00 mL, 9.00 mmol) and St (0.333 mL, 1.00 mmol) to yield a white powder (yield 57.9 mg, 3.9%).

δ_{H} (400 MHz, CD₂Cl₂) 8.07-5.87 (br, 6.58 H), 2.50-0.30 (br, 3.00 H).

FTIR (KBr, thin film) 3375 (br), 3024 (w), 2897 (br), 2841 (m), 1614 (s), 1596 (m), 1562 (s), 1474 (m), 1438 (s), 1136 (m), 806 (m), 760 (s), 700 (m), 458 (m) cm⁻¹.

Appendix II: Bibliography

- (1) Al-Ali AlMa'adeed, M.; Krupa, I. Introduction; 2015; pp 1–11.
- (2) Hutley, T. J.; Ouederni, M. Polyolefins—The History and Economic Impact; 2015; pp 13–50.
- (3) Severn, J. R.; Chadwick, J. C. *Tailor-Made Polymers: Via Immobilization of Alpha-Olefin Polymerization Catalysts*; Severn, J. R., Chadwick, J. C., Eds.; Wiley-VCH Verlag GmbH & Co. KGaA: Weinheim, Germany, 2008.
- (4) Scheirs, J.; Priddy, D. *Modern Styrenic Polymers: Polystyrenes and Styrenic Copolymers*; Scheirs, J., Priddy, D. B., Eds.; Wiley Series in Polymer Science; John Wiley & Sons, Ltd: Chichester, UK, 2003.
- (5) Maul, J.; Frushour, B. G.; Kontoff, J. R.; Eichenauer, H.; Ott, K.; Schade, C. Polystyrene and Styrene Copolymers. In *Ullmann's Encyclopedia of Industrial Chemistry*; Wiley-VCH Verlag GmbH & Co. KGaA: Weinheim, Germany, 2007.
- (6) Crabtree, R. H. *The Organometallic Chemistry of the Transition Metals*, 6th ed.; John Wiley & Sons, Incorporated: New York, 2014.
- (7) Sinturel, C.; Bates, F. S.; Hillmyer, M. A. High X–Low *N* Block Polymers: How Far Can We Go? *ACS Macro Lett.* **2015**, *4* (9), 1044–1050.
- (8) de Dardel, F.; Arden, T. V. Ion Exchangers. In *Ullmann's Encyclopedia of Industrial Chemistry*; Wiley-VCH Verlag GmbH & Co. KGaA: Weinheim, Germany, 2008.
- (9) Jaymand, M. Recent Progress in the Chemical Modification of Syndiotactic Polystyrene. *Polym. Chem.* **2014**, *5* (8), 2663–2690.
- (10) Jäkle, F.; Vidal, F. Functional Polymeric Materials Based on Main Group Elements. *Angew. Chemie Int. Ed.* **2018**, DOI: 10.1002/anie.201810611.
- (11) Jäkle, F. Advances in the Synthesis of Organoborane Polymers for Optical, Electronic, and Sensory Applications. *Chem. Rev.* **2010**, *110* (7), 3985–4022.
- (12) Wade, C. R.; Broomsgrove, A. E. J.; Aldridge, S.; Gabbai, F. P. Fluoride Ion Complexation and Sensing Using Organoboron Compounds. *Chem. Rev.* **2010**, *110* (7), 3958–3984.
- (13) Ji, L.; Griesbeck, S.; Marder, T. B. Recent Developments in and Perspectives on Three-Coordinate Boron Materials: A Bright Future. *Chem. Sci.* **2017**, *8* (2), 846–863.
- (14) Meng, B.; Ren, Y.; Liu, J.; Jäkle, F.; Wang, L. P-*n* Conjugated Polymers Based on Stable

- Triarylborane with n-Type Behavior in Optoelectronic Devices. *Angew. Chemie Int. Ed.* **2018**, *57* (8), 2183–2187.
- (15) Bélanger-Chabot, G.; Braunschweig, H.; Roy, D. K. Recent Developments in Azaborinine Chemistry. *Eur. J. Inorg. Chem.* **2017**, *2017*(38–39), 4353–4368.
- (16) Giustra, Z. X.; Liu, S. Y. The State of the Art in Azaborine Chemistry: New Synthetic Methods and Applications. *J. Am. Chem. Soc.* **2018**, *140*(4), 1184–1194.
- (17) Staubitz, A.; Presa Soto, A.; Manners, I. Iridium-Catalyzed Dehydrocoupling of Primary Amine-Borane Adducts: A Route to High Molecular Weight Polyaminoboranes, Boron-Nitrogen Analogues of Polyolefins. *Angew. Chemie Int. Ed.* **2008**, *47*(33), 6212–6215.
- (18) Ayhan, O.; Eckert, T.; Plamper, F. A.; Helten, H. Poly(Iminoborane)s: An Elusive Class of Main-Group Polymers? *Angew. Chemie Int. Ed.* **2016**, *55*(42), 13321–13325.
- (19) Lorenz, T.; Lik, A.; Plamper, F. A.; Helten, H. Dehydrocoupling and Silazane Cleavage Routes to Organic-Inorganic Hybrid Polymers with NBN Units in the Main Chain. *Angew. Chemie Int. Ed.* **2016**, *55*(25), 7236–7241.
- (20) Lorenz, T.; Crumbach, M.; Eckert, T.; Lik, A.; Helten, H. Poly(p-Phenylene Iminoborane): A Boron-Nitrogen Analogue of Poly(p-Phenylene Vinylene). *Angew. Chemie - Int. Ed.* **2017**, *56*(10), 2780–2784.
- (21) Staubitz, A. Generation of High-Molecular-Weight Polymers with Diverse Substituents: An Unusual Metal-Free Synthesis of Poly(Aminoborane)s. *Angew. Chemie Int. Ed.* **2018**, *57*(21), 5990–5992.
- (22) De Albuquerque Pinheiro, C. A.; Roiland, C.; Jehan, P.; Alcaraz, G. Solventless and Metal-Free Synthesis of High-Molecular-Mass Polyaminoboranes from Diisopropylaminoborane and Primary Amines. *Angew. Chemie Int. Ed.* **2018**, *57*(6), 1519–1522.
- (23) Helten, H. B=N Units as Part of Extended n-Conjugated Oligomers and Polymers. *Chem. - A Eur. J.* **2016**, *22*(37), 12972–12982.
- (24) Zhang, W.; Li, G.; Xu, L.; Zhuo, Y.; Wan, W.; Yan, N.; He, G. 9,10-Azaboraphenanthrene-Containing Small Molecules and Conjugated Polymers: Synthesis and Their Application in Chemodosimeters for the Ratiometric Detection of Fluoride Ions. *Chem. Sci.* **2018**, *9*(19), 4444–4450.
- (25) Baggett, A. W.; Guo, F.; Li, B.; Liu, S.-Y.; Jäkle, F. Regioregular Synthesis of Azaborine Oligomers and a Polymer with a Syn Conformation Stabilized by NH...n Interactions. *Angew. Chemie Int. Ed.* **2015**, *54*(38), 11191–11195.
- (26) Hall, D. G. *Boronic Acids: Preparation and Applications in Organic Synthesis, Medicine and Materials*; Hall, D. G., Ed.; Wiley-VCH Verlag GmbH & Co. KGaA: Weinheim, Germany, 2011.
- (27) Rygus, J. P. G.; Crudden, C. M. Enantiospecific and Iterative Suzuki–Miyaura Cross-Couplings. *J. Am.*

- Chem. Soc.* **2017**, *139*(50), 18124–18137.
- (28) Baranac-Stojanovic, M. Aromaticity and Stability of Azaborines. *Chem. - A Eur. J.* **2014**, *20*(50), 16558–16565.
- (29) Stojanović, M.; Baranac-Stojanović, M. Mono BN-Substituted Analogues of Naphthalene: A Theoretical Analysis of the Effect of BN Position on Stability, Aromaticity and Frontier Orbital Energies. *New J. Chem.* **2018**, *42*(15), 12968–12976.
- (30) Su, K.; Remsen, E. E.; Thompson, H. M.; Sneddon, L. G. Syntheses and Properties of Poly(B-Vinylborazine) and Poly(Styrene-Co-B-Vinylborazine) Copolymers. *Macromolecules* **1991**, *24*(13), 3760–3766.
- (31) Wan, W.-M.; Baggett, A. W.; Cheng, F.; Lin, H.; Liu, S.-Y.; Jäkle, F. Synthesis by Free Radical Polymerization and Properties of BN-Polystyrene and BN-Poly(Vinylbiphenyl). *Chem. Commun.* **2016**, *52*, 13616–13619.
- (32) Thiedemann, B.; Gliese, P. J.; Hoffmann, J.; Lawrence, P. G.; Sönnichsen, F. D.; Staubitz, A. High Molecular Weight Poly(N-Methyl-B-Vinylazaborine) – a Semi-Inorganic B–N Polystyrene Analogue. *Chem. Commun.* **2017**, *53*, 7258–7261.
- (33) van de Wouw, H. L.; Awuyah, E. C.; Baris, J. I.; Klausen, R. S. An Organoborane Vinyl Monomer with Styrene-like Radical Reactivity: Reactivity Ratios and Role of Aromaticity. *Macromolecules* **2018**, *51*(16), 6359–6368.
- (34) Mendis, S. N.; Zhou, T.; Klausen, R. S. Syndioselective Polymerization of a BN Aromatic Vinyl Monomer. *Macromolecules* **2018**, acs.macromol.8b01707.
- (35) van de Wouw, H. L.; Lee, J. Y.; Klausen, R. S. Gram-Scale Free Radical Polymerization of an Azaborine Vinyl Monomer. *Chem. Commun.* **2017**, *53*(53), 7262–7265.
- (36) van de Wouw, H. L.; Lee, J. Y.; Awuyah, E. C.; Klausen, R. S. A BN Aromatic Ring Strategy for Tunable Hydroxy Content in Polystyrene. *Angew. Chemie Int. Ed.* **2018**, *57*(6), 1673–1677.
- (37) Dewar, M. J. S.; Dietz, R.; Kubba, V. P.; Lepley, A. R. New Heteroaromatic Compounds. Part X. Grignard Reactions and Hydride Reductions of B-Oxides Derived from 10,9-Borazarophenanthrene and 2,1-Borazaronaphthalene. *J. Am. Chem. Soc.* **1961**, *83*(7), 1754–1756.
- (38) Dewar, M. J. S.; Dietz, R. 546. New Heteroaromatic Compounds. Part III. 2,1-Borazaro-Naphthalene (1,2-Dihydro-1-Aza-2-Boranaphthalene). **1959**, *0*(0).
- (39) Ashe, A. J.; Fang, X. A Synthesis of Aromatic Five- and Six-Membered B-N Heterocycles via Ring Closing Metathesis. *Org. Lett.* **2000**, *2*(14), 2089–2091.
- (40) Morgan, M. M.; Piers, W. Efficient Synthetic Methods for the Installation of Boron-Nitrogen Bonds in Conjugated Organic Molecules. *Dalt. Trans.* **2015**, 5920–5924.

- (41) Lynch, A. T.; Sneddon, L. G. Transition-Metal-Promoted Reactions of Boron Hydrides. 10. Rhodium-Catalyzed Syntheses of B-Alkenylborazines. *J. Am. Chem. Soc.* **1987**, *109* (19), 5867–5868.
- (42) Pellon, J.; Deichert, W. G.; Thomas, W. M. Polymerization of Vinyl Monomers Containing Boron. I. B-Trivinyl-N-Triphenylborazine and B-Triallyl-N-Triphenylborazine. *J. Polym. Sci.* **1961**, *55* (161), 153–160.
- (43) Pan, J.; Kampf, J. W.; Ashe, A. J. The Ligand Properties of 2-Vinyl-1,2-Azaboratabenzene. *J. Organomet. Chem.* **2009**, *694* (7–8), 1036–1040.
- (44) Abbey, E. R.; Lamm, A. N.; Baggett, A. W.; Zakharov, L. N.; Liu, S.-Y. Protecting Group-Free Synthesis of 1,2-Azaborines: A Simple Approach to the Construction of BN-Benzenoids. *J. Am. Chem. Soc.* **2013**, *135* (34), 12908–12913.
- (45) Wisniewski, S. R.; Guenther, C. L.; Argintaru, O. A.; Molander, G. A. A Convergent, Modular Approach to Functionalized 2,1-Borazaronaphthalenes from 2-Aminostyrenes and Potassium Organotrifluoroborates. *J. Org. Chem.* **2014**, *79* (1), 365–378.
- (46) Fazen, P. J.; Beck, J. S.; Lynch, A. T.; Remsen, E. E.; Sneddon, L. G. Thermally Induced Borazine Dehydropolymerization Reactions. Synthesis and Ceramic Conversion Reactions of a New High-Yield Polymeric Precursor to Boron Nitride. *Chem. Mater.* **1990**, *2* (2), 96–97.
- (47) Jackson, L. A.; Allen, C. W. Alkenylborazines. *Phosphorus. Sulfur. Silicon Relat. Elem.* **1989**, *41* (3–4), 341–346.
- (48) Woods, W. G.; Bengelsdorf, I. S.; Hunter, D. L. 2-Vinyl-4,4,6-Trimethyl-1,3,2-Dioxaborinane. I. Synthesis and Properties. *J. Org. Chem.* **1966**, *31* (9), 2766–2768.
- (49) Mulvaney, J. E.; Ottaviani, R. A.; Laverty, J. J. Preparation of Vinyl Boronate Copolymers and Reactions. *J. Polym. Sci. Polym. Chem. Ed.* **1982**, *20* (7), 1949–1952.
- (50) van de Wouw, H. L.; Awuyah, E. C.; Baris, J. I.; Klausen, R. S. An Organoborane Vinyl Monomer with Styrene-like Radical Reactivity: Reactivity Ratios and Role of Aromaticity. *Macromolecules* **2018**, *51* (16).
- (51) van de Wouw, H. L.; Lee, J. Y.; Siegler, M. A.; Klausen, R. S. Innocent BN Bond Substitution in Anthracene Derivatives. **2016**, *14* (12), 3256–3263.
- (52) Vala, M. T.; Haebig, J.; Rice, S. A. Experimental Study of Luminescence and Excitation Trapping in Vinyl Polymers, Paracyclophanes, and Related Compounds. *J. Chem. Phys.* **1965**, *43* (3), 886–897.
- (53) Frank, C. W. Excimer Formation in Vinyl Polymers. III. Fluid and Rigid Solutions of Poly(4-vinylbiphenyl). *J. Chem. Phys.* **1974**, *61* (5), 2015–2022.
- (54) *Handbook of Radical Polymerization*; Matyjaszewski, K., Davis, T. P., Eds.; John Wiley & Sons, Inc.: Hoboken, NJ, USA, 2002.

- (55) *Handbook of RAFT Polymerization*; Barner-Kowollik, C., Ed.; Wiley-VCH Verlag GmbH & Co. KGaA: Weinheim, Germany, 2008.
- (56) Tang, C. N.; Paz-Pazos, M.; Dao, A. H.; Pugh, C.; Samtani, O. Correlation of Free Radical Copolymerization Behavior and Copolymer Properties with the Strength of π - π Stacking Interactions between Aromatic Fluorocarbons and Aromatic Hydrocarbons: Copolymerization of Styrene and Fluorinated Styrenes at the Two Extreme. *Macromolecules* **2007**, *40* (23), 8178–8188.
- (57) Patrick, C. R.; Prosser, G. S. A Molecular Complex of Benzene and Hexafluorobenzene. *Nature* **1960**, *187*(4742), 1021.
- (58) Vrbancich, J.; Ritchie, G. L. D. Quadrupole Moments of Benzene, Hexafluorobenzene and Other Non-Dipolar Aromatic Molecules. *J. Chem. Soc. Faraday Trans. 2* **1980**, *76* (0), 648.
- (59) Madruga, E. L. From Classical to Living/Controlled Statistical Free-Radical Copolymerization. *Prog. Polym. Sci.* **2002**, *27*(9), 1879–1924.
- (60) Klumperman, B.; O'Driscoll, K. F. Interpreting the Copolymerization of Styrene with Maleic Anhydride and with Methyl Methacrylate in Terms of the Bootstrap Model. *Polymer (Guildf)*. **1993**, *34* (5), 1032–1037.
- (61) Odian, G. *Principles of Polymerization*, 4th ed.; WILEY-VCH Verlag, 2004.
- (62) Herman, J. J.; Teyssié, P. Determination of Vinyl Monomers Reactivity by Carbon-13 Nuclear Magnetic Resonance Spectroscopy. *Macromolecules* **1978**, *11* (4), 839–840.
- (63) Pugh, C.; Paz-Pazos, M.; Tang, C. N. Correlation of Free Radical Copolymerization Behavior and Copolymer Properties with the Strength of π - π Stacking Interactions between Aromatic Fluorocarbons and Aromatic Hydrocarbons: Comparison of the Copolymerization Behavior of 2,3,4,5,6-Pentafluorosty. *J. Polym. Sci. Part A Polym. Chem.* **2009**, *47* (2), 331–345.
- (64) Minsk, L. M.; Priest, W. J.; Kenyon, W. O. The Alcoholysis of Polyvinyl Acetate. *J. Am. Chem. Soc.* **1941**, *63* (10), 2715–2721.
- (65) Tubbs, R. K. Sequence Distribution of Partially Hydrolyzed Poly(Vinyl Acetate). *J. Polym. Sci. Part A-1 Polym. Chem.* **1966**, *4* (3), 623–629.
- (66) Budhlall, B. M.; Landfester, K.; Sudol, E. D.; Dimonie, V. L.; Klein, A.; El-Aasser, M. S. Characterization of Partially Hydrolyzed Poly(Vinyl Alcohol). Effect of Poly(Vinyl Alcohol) Molecular Architecture on Aqueous Phase Conformation. *Macromolecules* **2003**, *36* (25), 9477–9484.
- (67) Miscellaneous Vinyl Thermoplastics. *Brydson's Plast. Mater.* **2017**, 427–440.
- (68) Hirai, T.; Okazaki, A.; Hayashi, S. Effect of Sequence Distribution of Poly(Vinyl Alcohol-Vinyl Acetate) on the Coloring Reaction with Iodine. *J. Appl. Polym. Sci.* **1986**, *32* (3), 3919–3928.
- (69) 栄一長井; 典男相根. ポリビニルアルコールに関する研究. *Kobunshi Kagaku* **1955**, *12* (121), 195–

- 199.
- (70) Scholtens, B. J. R.; Bijsterbosch, B. H. Molecular Architecture and Physicochemical Properties of Some Vinyl Alcohol-Vinyl Acetate Copolymers. *J. Polym. Sci. Polym. Phys. Ed.* **1979**, *17*(10), 1771–1787.
- (71) Morishima, Y.; Fujisawa, K.; Nozakura, S. Sequence Length Required for Poly(Vinyl Acetate)—Iodine and Poly(Vinyl Alcohol)—Iodine Color Reactions. *Polym. J.* **1978**, *10*(3), 281–285.
- (72) Finley, J. H. Spectrophotometric Determination of Polyvinyl Alcohol in Paper Coatings. *Anal. Chem.* **1961**, *33*(13), 1925–1927.
- (73) Monte-Bovi, A. J.; Sciarra, J. J. Study of the Polyvinyl Alcohol-Borate-Iodine Complex II. Test Papers. *J. Pharm. Sci.* **1961**, *50*(3), 198–200.
- (74) Monte-Bovi, A. J. Qualitative Determination of Borates by Poly(Vinyl Alcohol). *Drug Stand.* **1959**, *27*, 15–17.
- (75) Chung, T. C.; Raate, M.; Berluce, E.; Schulz, D. N. Synthesis of Functional Hydrocarbon Polymers with Well-Defined Molecular Structures. *Macromolecules* **1988**, *21*(7), 1903–1907.
- (76) Kondo, Y.; García-Cuadrado, D.; Hartwig, J. F.; Boen, N. K.; Wagner, N. L.; Hillmyer, M. A. Rhodium-Catalyzed, Regiospecific Functionalization of Polyolefins in the Melt. *J. Am. Chem. Soc.* **2002**, *124*(7), 1164–1165.
- (77) Bae, C.; Hartwig, J. F.; Chung, H.; Harris, N. K.; Switek, K. A.; Hillmyer, M. A. Regiospecific Side-Chain Functionalization of Linear Low-Density Polyethylene with Polar Groups. *Angew. Chemie Int. Ed.* **2005**, *44*(39), 6410–6413.
- (78) Bae, C.; Hartwig, J. F.; Boen Harris, N. K.; Long, R. O.; Anderson, K. S.; Hillmyer, M. A. Catalytic Hydroxylation of Polypropylenes. *J. Am. Chem. Soc.* **2005**, *127*(2), 767–776.
- (79) Chung, T. C. Synthesis of Polyalcohols via Ziegler-Natta Polymerization. *Macromolecules* **1988**, *21*(4), 865–869.
- (80) St. Laurent, J. B.; de Buzzaccarini, F.; De Clerck, K.; Demeyere, H.; Labeque, R.; Lodewick, R.; van Langenhove, L. Laundry Cleaning of Textiles. *Handb. Cleaning/Decontamination Surfaces* **2007**, 57–102.
- (81) Pham, A. N.; Xing, G.; Miller, C. J.; Waite, T. D. Fenton-like Copper Redox Chemistry Revisited: Hydrogen Peroxide and Superoxide Mediation of Copper-Catalyzed Oxidant Production. *J. Catal.* **2013**, *301*, 54–64.
- (82) Franssen, N. M. G.; Reek, J. N. H.; de Bruin, B. Synthesis of Functional 'Polyolefins': State of the Art and Remaining Challenges. *Chem. Soc. Rev.* **2013**, *42*(13), 5809–5832.
- (83) Boffa, L. S.; Novak, B. M. Copolymerization of Polar Monomers with Olefins Using Transition-Metal

- Complexes. *Chem. Rev.* **2000**, *100* (4), 1479–1493.
- (84) Jeremic, D. Polyethylene. *Ullmann's Encyclopedia of Industrial Chemistry*, 2014.
- (85) Nakamura, A.; Ito, S.; Nozaki, K. Coordination–Insertion Copolymerization of Fundamental Polar Monomers. *Chem. Rev.* **2009**, *109* (11), 5215–5244.
- (86) Liu, D.; Wang, M.; Wang, Z.; Wu, C.; Pan, Y.; Cui, D. Stereoselective Copolymerization of Unprotected Polar and Nonpolar Styrenes by an Yttrium Precursor: Control of Polar-Group Distribution and Mechanism. *Angew. Chemie Int. Ed.* **2017**, *56* (10), 2714–2719.
- (87) Ittel, S. D.; Johnson, L. K.; Brookhart, M. Late-Metal Catalysts for Ethylene Homo- and Copolymerization. *Chem. Rev.* **2000**, *100* (4), 1169–1203.
- (88) Mayo, F. R.; Lewis, F. M.; Walling, C. Copolymerization. VIII. The Relation Between Structure and Reactivity of Monomers in Copolymerization ¹. *J. Am. Chem. Soc.* **1948**, *70* (4), 1529–1533.
- (89) Mayo, F. R.; Walling, C.; Lewis, F. M.; Hulse, W. F. Copolymerization. V. Some Copolymerizations of Vinyl Acetate. *J. Am. Chem. Soc.* **1948**, *70* (4), 1523–1525.
- (90) Hallensleben, M. L.; Fuss, R.; Mummy, F. Polyvinyl Compounds, Others. In *Ullmann's Encyclopedia of Industrial Chemistry*; Wiley-VCH Verlag GmbH & Co. KGaA: Weinheim, Germany, 2015; pp 1–23.
- (91) Nord, F. F. Über Die Dehydrierungsleistungen von Fusarium Lini B. *Naturwissenschaften* **1936**, *24* (48), 763–763.
- (92) Finch, C. A. *Polyvinyl Alcohol: Developments*; Wiley, 1992.
- (93) Solaro, R.; Corti, A.; Chiellini, E. Biodegradation of Poly(Vinyl Alcohol) with Different Molecular Weights and Degree of Hydrolysis. *Polym. Adv. Technol.* **2000**, *11* (8–12), 873–878.
- (94) Albertsson, A.-C.; Karlsson, S. Aspects of Biodeterioration of Inert and Degradable Polymers. *Int. Biodeterior. Biodegradation* **1993**, *31* (3), 161–170.
- (95) Ho, B. T.; Roberts, T. K.; Lucas, S. An Overview on Biodegradation of Polystyrene and Modified Polystyrene: The Microbial Approach. *Crit. Rev. Biotechnol.* **2018**, *38* (2), 308–320.
- (96) Coates, G. W. Precise Control of Polyolefin Stereochemistry Using Single-Site Metal Catalysts. *Chem. Rev.* **2000**, *100* (4), 1223–1252.
- (97) Hassan, C. M.; Peppas, N. A. Structure and Morphology of Freeze/Thawed PVA Hydrogels. *Macromolecules* **2000**, *33* (7), 2472–2479.
- (98) Peppas, N. A.; Hilt, J. Z.; Khademhosseini, A.; Langer, R. Hydrogels in Biology and Medicine: From Molecular Principles to Bionanotechnology. *Adv. Mater.* **2006**, *18* (11), 1345–1360.
- (99) Lyoo, W. S.; Chvalun, S.; Ghim, H. Do; Kim, J. P.; Blackwell, J. Small-Angle and Wide-Angle X-Ray Analyses of Syndiotactic Poly(Vinyl Alcohol) Microfibrils. *Macromolecules* **2001**, *34* (8), 2615–2623.

- (100) Choi, J. H.; Ko, S. W.; Kim, B. C.; Blackwell, J.; Lyoo, W. S. Phase Behavior and Physical Gelation of High Molecular Weight Syndiotactic Poly(Vinyl Alcohol) Solution. *Macromolecules* **2001**, *34* (9), 2964–2972.
- (101) Horii, F.; Masuda, K.; Kaji, H. CP/MAS ¹³C NMR Spectra of Frozen Solutions of Poly(Vinyl Alcohol) with Different Tacticities. *Macromolecules* **1997**, *30* (8), 2519–2520.
- (102) Murahashi, S.; Nozakura, S.; Sumi, M. A New Route to Stereoregular Poly(Vinyl Alcohols). *J. Polym. Sci. Part B Polym. Lett.* **1965**, *3* (4), 245–249.
- (103) Okamura, S.; Kodama, T.; Higashimura, T. The Cationic Polymerization of T-butyl Vinyl Ether at Low Temperature and the Conversion into Polyvinyl Alcohol of Poly-t-butyl Vinyl Ether. *Die Makromol. Chemie* **1962**, *53* (1), 180–191.
- (104) Higashimura, T.; Suzuoki, K.; Okamura, S. Cationic Stereospecific Polymerization of T-butyl Vinyl Ether. *Die Makromol. Chemie* **1965**, *86* (1), 259–270.
- (105) Yamamoto, T.; Fukae, R.; Saso, T.; Sangen, O.; Kamachi, M.; Sato, T.; Fukunishi, Y. Synthesis of High-Molecular Weight Poly(Vinyl Alcohol) of Various Tactic Contents through Photo-Emulsion Copolymerization of Vinyl Acetate and Vinyl Pivalate. *Polym. J.* **1992**, *24* (1), 115–119.
- (106) Lyoo, W. S.; Blackwell, J.; Ghim, H. Do. Structure of Poly(Vinyl Alcohol) Microfibrils Produced by Saponification of Copoly(Vinyl Pivalate/Vinyl Acetate). *Macromolecules* **1998**, *31* (13), 4253–4259.
- (107) Ishihara, N.; Seimiya, T.; Kuramoto, M.; Uoi, M. Crystalline Syndiotactic Polystyrene. *Macromolecules* **1986**, *19* (9), 2464–2465.
- (108) Schellenberg, J. Recent Transition Metal Catalysts for Syndiotactic Polystyrene. *Prog. Polym. Sci.* **2009**, *34* (8), 688–718.
- (109) Grassi, A.; Saccheo, S.; Zambelli, A.; Laschi, F. Reactivity of the $[(\eta^5\text{-C}_5\text{Me}_5)\text{TiCl}_3][\text{RB}(\text{C}_6\text{F}_5)_3]$ Complexes Identified as Active Species in Syndiospecific Styrene Polymerization. *Macromolecules* **1998**, *31* (17), 5588–5591.
- (110) Schleyer, P. von R. Introduction: Aromaticity. **2001**.
- (111) Dewar, M. J. S.; Kubba, V. P.; Pettit, R. 624. New Heteroaromatic Compounds. Part I. 9-Aza-10-Boraphenanthrene. *J. Chem. Soc.* **1958**, *0* (0), 3073.
- (112) Campbell, P. G.; Marwitz, A. J. V.; Liu, S.-Y. Recent Advances in Azaborine Chemistry. *Angew. Chemie Int. Ed.* **2012**, *51* (25), 6074–6092.
- (113) Marwitz, A. J. V.; Matus, M. H.; Zakharov, L. N.; Dixon, D. A.; Liu, S.-Y. A Hybrid Organic/Inorganic Benzene. *Angew. Chemie Int. Ed.* **2009**, *48* (5), 973–977.
- (114) Arthur J. Ashe, I. and; Fang, X. A Synthesis of Aromatic Five- and Six-Membered B–N Heterocycles via Ring Closing Metathesis. **2000**.

- (115) Wisniewski, S. R.; Guenther, C. L.; Argintaru, O. A.; Molander, G. A. A Convergent, Modular Approach to Functionalized 2,1-Borazaronaphthalenes from 2-Aminostyrenes and Potassium Organotrifluoroborates. *J. Org. Chem.* **2014**, *79* (1), 365–378.
- (116) Molander, G. A.; Wisniewski, S. R. Accessing Molecularly Complex Azaborines: Palladium-Catalyzed Suzuki–Miyaura Cross-Couplings of Brominated 2,1-Borazaronaphthalenes and Potassium Organotrifluoroborates. *J. Org. Chem.* **2014**, *79* (14), 6663–6678.
- (117) Ishibashi, J. S. A.; Dargelos, A.; Darrigan, C.; Chrostowska, A.; Liu, S.-Y. BN Tetracene: Extending the Reach of BN/CC Isosterism in Acenes. *Organometallics* **2017**, *36* (14), 2494–2497.
- (118) Sanyal, S.; Manna, A. K.; Pati, S. K. BN-Decorated Graphene Nanoflakes with Tunable Opto-Electronic and Charge Transport Properties. *J. Mater. Chem. C* **2014**, *2* (16), 2918–2928.
- (119) Ishibashi, J. S. A.; Marshall, J. L.; Mazière, A.; Lovinger, G. J.; Li, B.; Zakharov, L. N.; Dargelos, A.; Graciaa, A.; Chrostowska, A.; Liu, S.-Y. Two BN Isosteres of Anthracene: Synthesis and Characterization. *J. Am. Chem. Soc.* **2014**, *136* (43), 15414–15421.
- (120) Knapp, D. M.; Gillis, E. P.; Burke, M. D. A General Solution for Unstable Boronic Acids: Slow-Release Cross-Coupling from Air-Stable MIDA Boronates. *J. Am. Chem. Soc.* **2009**, *131* (20), 6961–6963.
- (121) Islas, R.; Chamorro, E.; Robles, J.; Heine, T.; Santos, J. C.; Merino, G. Borazine: To Be or Not to Be Aromatic. *Struct. Chem.* **2007**, *18* (6), 833–839.
- (122) *CRC Handbook of Chemistry and Physics*, 96TH ed.
- (123) McL Mathieson, A.; Robertson, J. M.; Sinclair, V. C.; IUCr. The Crystal and Molecular Structure of Anthracene. I. X-Ray Measurements. *Acta Crystallogr.* **1950**, *3* (4), 245–250.
- (124) Anthony, J. E. The Larger Acenes: Versatile Organic Semiconductors. *Angew. Chemie Int. Ed.* **2008**, *47* (3), 452–483.
- (125) Chiba, H.; Nishida, J.; Yamashita, Y. Tetracyanoanthraquinodimethanes Having Biaryl Substituents: Synthesis, Crystal Structures, and Physical Properties. *Chem. Lett.* **2012**, *41* (5), 482–484.
- (126) Famil Valiyev, †; Wei-Shan Hu, ‡; Hsing-Yin Chen, †,§; Ming-Yu Kuo, †; Ito Chao, *, † and; Yu-Tai Tao*, †, ‡. Synthesis and Characterization of Anthra[2,3-b]Thiophene and Tetraceno[2,3-b]Thiophenes for Organic Field-Effect Transistor Applications. **2007**.
- (127) Byrd, L.; Miller, L. L.; Pletcher, D. The Oxidation of Aromatic Hydrocarbons in Methylene Chloride at -70°C. *Tetrahedron Lett.* **1972**, *13* (24), 2419–2422.
- (128) Dietrich, M.; Mortensen, J.; Heinze, J. Electrochemical Oxidation of Anthracene and 9,9'-Bianthryl to the Respective Dication and Tetracation. *Angew. Chemie Int. Ed. English* **1985**, *24* (6), 508–509.
- (129) Josefík, F.; Mikysek, T.; Svobodová, M.; Šimůnek, P.; Kvapilová, H.; Ludvík, J. New Triazaborine Chromophores: Their Synthesis via Oxazaborines and Electrochemical and DFT Study of Their

Fundamental Properties. *Organometallics* **2014**, *33* (18), 4931–4939.

- (130) Bosdet, M. J. D.; Piers, W. E. B-N as a C-C Substitute in Aromatic Systems. *Can. J. Chem.* **2009**, *87* (1), 8–29.
- (131) Lepeltier, M.; Lukoyanova, O.; Jacobson, A.; Jeeva, S.; Perepichka, D. F.; Matzger, A. J.; Brédas, J.-L.; Cingolani, R.; Gigli, G. New Azaborine-Thiophene Heteroacenes. *Chem. Commun.* **2010**, *46* (37), 7007.
- (132) Hatakeyama, T.; Hashimoto, S.; Seki, S.; Nakamura, M. Synthesis of BN-Fused Polycyclic Aromatics via Tandem Intramolecular Electrophilic Arene Borylation. *J. Am. Chem. Soc.* **2011**, *133* (46), 18614–18617.
- (133) Baggett, A. W.; Guo, F.; Li, B.; Liu, S.-Y.; Jäkle, F. Regioregular Synthesis of Azaborine Oligomers and a Polymer with a *Syn* Conformation Stabilized by N·H···n Interactions. *Angew. Chemie Int. Ed.* **2015**, *54* (38), 11191–11195.
- (134) Wang, X.-Y.; Zhuang, F.-D.; Wang, J.-Y.; Pei, J. Incorporation of Polycyclic Azaborine Compounds into Polythiophene-Type Conjugated Polymers for Organic Field-Effect Transistors. *Chem. Commun.* **2015**, *51* (99), 17532–17535.
- (135) Wan, W.-M.; Baggett, A. W.; Cheng, F.; Lin, H.; Liu, S.-Y.; Jäkle, F. Synthesis by Free Radical Polymerization and Properties of BN-Polystyrene and BN-Poly(Vinylbiphenyl). *Chem. Commun.* **2016**, *52* (Scheme 1).
- (136) Thiedemann, B.; Gliese, P. J.; Hoffmann, J.; Lawrence, P. G.; Sönnichsen, F. D.; Staubitz, A.; Fahmi, A.; Scheer, M. High Molecular Weight Poly(N-Methyl-B-Vinylazaborine) – a Semi-Inorganic B–N Polystyrene Analogue. **2017**, No. 53.
- (137) Molander, G. A.; Wisniewski, S. R.; Amani, J. Accessing an Azaborine Building Block: Synthesis and Substitution Reactions of 2-Chloromethyl-2,1-Borazaronaphthalene. *Org. Lett.* **2014**, *16* (21), 5636–5639.
- (138) Watanabe, K.; Yamagiwa, N.; Torisawa, Y. Cyclopentyl Methyl Ether as a New and Alternative Process Solvent. *Organic Process Research and Development*. American Chemical Society 2007, pp 251–258.
- (139) *ACS GCI Pharmaceutical Roundtable Solvent Selection Guide*; 2011.
- (140) Dolman, S. J.; Schrock, R. R.; Hoveyda, A. H. Enantioselective Synthesis of Cyclic Secondary Amines through Mo-Catalyzed Asymmetric Ring-Closing Metathesis (ARCM). *Org. Lett.* **2003**, *5* (25), 4899–4902.
- (141) Ryou, J. H.; Ha, C. S.; Cho, W. J. Miscibility of Poly(Vinyl Methyl Ether) and Poly(Styrene-Co-2-Vinylnaphthalene) Blends by FT-IR Spectroscopy and Tg Measurements. *J. Polym. Sci. Part A Polym. Chem.* **1993**, *31* (2), 325–333.

- (142) Parab, K.; Venkatasubbaiah, K.; Jäkle, F. Luminescent Triarylborane-Functionalized Polystyrene: Synthesis, Photophysical Characterization, and Anion-Binding Studies. *J. Am. Chem. Soc.* **2006**, *128* (39), 12879–12885.
- (143) van de Wouw, H. L.; Lee, J. Y.; Klausen, R. S. Gram-Scale Free Radical Polymerization of an Azaborine Vinyl Monomer. *Chem. Commun.* **2017**, *53* (53), 7262–7265.
- (144) Resendiz-Lara, D. A.; Stubbs, N. E.; Arz, M. I.; Pridmore, N. E.; Sparkes, H. A.; Manners, I. Boron–nitrogen Main Chain Analogues of Polystyrene: Poly(B-Aryl)Aminoboranes via Catalytic Dehydrocoupling. *Chem. Commun.* **2017**, *53* (85), 11701–11704.
- (145) Lorenz, T.; Crumbach, M.; Eckert, T.; Lik, A.; Helten, H. Poly(*p*-Phenylene Iminoborane): A Boron–Nitrogen Analogue of Poly(*p*-Phenylene Vinylene). *Angew. Chemie Int. Ed.* **2017**, *56* (10), 2780–2784.
- (146) Wisniewski, S. R.; Guenther, C. L.; Argintaru, O. A.; Molander, G. A. A Convergent, Modular Approach to Functionalized 2,1-Borazaronaphthalenes from 2-Aminostyrenes and Potassium Organotrifluoroborates. *J. Org. Chem.* **2014**, *79* (1), 365–378.
- (147) Liu, Z.; Ishibashi, J. S. A.; Darrigan, C.; Dargelos, A.; Chrostowska, A.; Li, B.; Vasiliu, M.; Dixon, D. A.; Liu, S.-Y. The Least Stable Isomer of BN Naphthalene: Toward Predictive Trends for the Optoelectronic Properties of BN Acenes. *J. Am. Chem. Soc.* **2017**, *139* (17), 6082–6085.
- (148) Dewar, M. J. S.; Gleicher, G. J.; Robinson, B. P. Synthesis and Nuclear Magnetic Resonance Spectrum of 10,9-Borazaronaphthalene. *J. Am. Chem. Soc.* **1964**, *86* (24), 5698–5699.
- (149) Yanai, T.; Tew, D. P.; Handy, N. C. A New Hybrid Exchange–correlation Functional Using the Coulomb-Attenuating Method (CAM-B3LYP). *Chem. Phys. Lett.* **2004**, *393* (1–3), 51–57.
- (150) Latelli, N.; Ouddai, N.; Arotçaréna, M.; Chaumont, P.; Mignon, P.; Chermette, H. Mechanism of Addition-Fragmentation Reaction of Thiocarbonyls Compounds in Free Radical Polymerization. A DFT Study. *Comput. Theor. Chem.* **2014**, *1027*, 39–45.
- (151) Mazière, A.; Chrostowska, A.; Darrigan, C.; Dargelos, A.; Graciaa, A.; Chermette, H. Electronic Structure of BN-Aromatics: Choice of Reliable Computational Tools. *J. Chem. Phys.* **2017**, *147* (16), 164306.
- (152) Kranz, M.; Clark, T. Azaborines: An Ab Initio Study. *J. Org. Chem.* **1992**, *57* (20), 5492–5500.
- (153) Ghosh, D.; Periyasamy, G.; Pati, S. K.; Poater, J.; Sola, M.; Subramanian, V.; Giri, S.; Geerlings, P. Density Functional Theoretical Investigation of the Aromatic Nature of BN Substituted Benzene and Four Ring Polyaromatic Hydrocarbons. *Phys. Chem. Chem. Phys.* **2011**, *13* (46), 20627.
- (154) Klooster, W. T.; Koetzle, T. F.; Siegbahn, P. E. M.; Richardson, T. B.; Crabtree, R. H. Study of the N–H···H–B Dihydrogen Bond Including the Crystal Structure of BH₃NH₃ by Neutron Diffraction. *J. Am. Chem. Soc.* **1999**, *121* (27), 6337–6343.

- (155) Alcaraz, G.; Vendier, L.; Clot, E.; Sabo-Etienne, S. Ruthenium Bis(σ -B-H) Aminoborane Complexes from Dehydrogenation of Amine-Boranes: Trapping of H₂B-NH₂. *Angew. Chemie - Int. Ed.* **2010**, *49* (5), 918–920.
- (156) Paetzold, P. New Perspectives in Boron-Nitrogen Chemistry - I. *Pure Appl. Chem.* **1991**, *63* (3), 345–350.
- (157) McKinley, N. F.; O'Shea, D. F. Efficient Synthesis of Aryl Vinyl Ethers Exploiting 2,4,6-Trivinylcyclotriboroxane as a Vinylboronic Acid Equivalent. *J. Org. Chem.* **2004**, *69* (15), 5087–5092.
- (158) Adler Yañez, R. A.; Kehr, G.; Daniliuc, C. G.; Schirmer, B.; Erker, G. Formation of a Dihydroborole by Catalytic Isomerization of a Divinylborane. *Dalt. Trans.* **2014**, *43* (28), 10794.
- (159) Schleyer, P. von R.; Maerker, C.; Dransfeld, A.; Jiao, H.; van Eikema Hommes, N. J. R. Nucleus-Independent Chemical Shifts: A Simple and Efficient Aromaticity Probe. *J. Am. Chem. Soc.* **1996**, *118* (26), 6317–6318.
- (160) Chen, Z.; Wannere, C. S.; Corminboeuf, C.; Puchta, R.; von Ragué Schleyer, P. Nucleus-Independent Chemical Shifts (NICS) as an Aromaticity Criterion. *Chemical Reviews*. American Chemical Society 2005, pp 3842–3888.
- (161) London, F. Théorie Quantique Des Courants Interatomiques Dans Les Combinaisons Aromatiques. *J. Phys. le Radium* **1937**, *8* (10), 397–409.
- (162) McWeeny, R. Perturbation Theory for the Fock-Dirac Density Matrix. *Phys. Rev.* **1962**, *126* (3), 1028–1034.
- (163) Ditchfield, R. Self-Consistent Perturbation Theory of Diamagnetism. *Mol. Phys.* **1974**, *27* (4), 789–807.
- (164) Wolinski, K.; Hinton, J. F.; Pulay, P. Efficient Implementation of the Gauge-Independent Atomic Orbital Method for NMR Chemical Shift Calculations. *J. Am. Chem. Soc.* **1990**, *112* (23), 8251–8260.
- (165) Cheeseman, J. R.; Trucks, G. W.; Keith, T. A.; Frisch, M. J. A Comparison of Models for Calculating Nuclear Magnetic Resonance Shielding Tensors. *J. Chem. Phys.* **1998**, *104* (14), 5497.
- (166) Chrostowska, A.; Xu, S.; Mazière, A.; Boknevtz, K.; Li, B.; Abbey, E. R.; Dargelos, A.; Graciaa, A.; Liu, S.-Y. UV-Photoelectron Spectroscopy of BN Indoles: Experimental and Computational Electronic Structure Analysis. *J. Am. Chem. Soc.* **2014**, *136* (33), 11813–11820.
- (167) Del Bene, J. E.; Yañez, M.; Alkorta, I.; Elguero, J. An Ab Initio Study of the Structures and Selected Properties of 1,2-Dihydro-1,2-Azaborine and Related Molecules. *J. Chem. Theory Comput.* **2009**, *5* (9), 2239–2247.
- (168) Catão, A. J. L.; López-Castillo, A. Stability and Molecular Properties of the Boron-Nitrogen

- Alternating Analogs of Azulene and Naphthalene: A Computational Study. *J. Mol. Model.* **2017**, *23* (4), 119.
- (169) Davies, G. H. M.; Molander, G. A. Synthesis of Functionalized 1,3,2-Benzodiazaborole Cores Using Bench-Stable Components. *J. Org. Chem.* **2016**, *81* (9), 3771–3779.
- (170) Schleyer, P. von R.; Jiao, H.; Hommes, N. J. R. van E.; Malkin, V. G.; Malkina, O. L. An Evaluation of the Aromaticity of Inorganic Rings: Refined Evidence from Magnetic Properties. *J. Am. Chem. Soc.* **1997**, *119* (51), 12669–12670.
- (171) Wu, Y.-D.; Wong, C.-L.; Chan, K. W. K.; Ji, G.-Z.; Jiang, X.-K. Substituent Effects on the C–H Bond Dissociation Energy of Toluene. A Density Functional Study. *J. Org. Chem.* **1996**, *61* (2), 746–750.
- (172) Szwarc, M. The C–H Bond Energy in Toluene and Xylenes. *J. Chem. Phys.* **1948**, *16* (2), 128–136.
- (173) Stephen J. Blanksby*, † and; G. Barney Ellison*, ‡. Bond Dissociation Energies of Organic Molecules. **2003**.
- (174) Ochterski, J. W. Thermochemistry in Gaussian | Gaussian.com <http://gaussian.com/thermo/> (accessed May 25, 2018).
- (175) Moad, G.; Solomon, D. H.; Johns, S. R.; Willing, R. I. Fate of the Initiator in the Azobis(Isobutyronitrile)-Initiated Polymerization of Styrene. *Macromolecules* **1984**, *17* (5), 1094–1099.
- (176) Patil, A. O.; Schulz, D. N.; Novak, B. M. *Functional Polymers: Modern Synthetic Methods and Novel Structures*; Patil, A. O., Schulz, D. N., Novak, B. M., Eds.; ACS Symposium Series; American Chemical Society: Washington, DC, 1998; Vol. 704.
- (177) Padwa, A. R. Functionally Substituted Poly (α -Olefins). *Progress in Polymer Science*. Pergamon January 1989, pp 811–833.
- (178) Chan, P. K.; Rey, A. D. Polymerization-Induced Phase Separation. 2. Morphological Analysis. *Macromolecules* **1997**, *30* (7), 2135–2143.
- (179) Mayo, F. R.; Lewis, F. M. Copolymerization I. A Basis for Comparing the Behavior of Monomers in Copolymerization; the Copolymerization of Styrene and Methyl Methacrylate. *J. Am. Chem. Soc.* **1944**, *66* (1939), 1594–1601.
- (180) Coca, A. Boron Reagents in Synthesis. *ACS Symp. Ser.* **2016**, *1236*, 1–523.
- (181) Thomas, S. E. *Organic Synthesis: The Roles of Boron and Silicon*; Oxford University Press, 1992.
- (182) Brown, H. C.; Subba Rao, B. C. A New Technique for the Conversion of Olefins into Organoboranes and Related Alcohols. *Journal of the American Chemical Society*. American Chemical Society November 1956, pp 5694–5695.

- (183) Cox, P. A.; Leach, A. G.; Campbell, A. D.; Lloyd-Jones, G. C. Protodeboronation of Heteroaromatic, Vinyl, and Cyclopropyl Boronic Acids: PH-Rate Profiles, Autocatalysis, and Disproportionation. *J. Am. Chem. Soc.* **2016**, *138* (29), 9145–9157.
- (184) Baggett, A. W.; Liu, S.-Y. A Boron Protecting Group Strategy for 1,2-Azaborines. *J. Am. Chem. Soc.* **2017**, *139* (42), 15259–15264.
- (185) Hsiao, T.-J.; Tsai, J.-C. End-Functionalization of Syndiotactic Polystyrene by Vinylsilane Inducing Selective Chain Transfer Reactions. *J. Polym. Sci. Part A Polym. Chem.* **2010**, *48* (8), 1690–1698.
- (186) Chung, T. C. Synthesis of Diblock Copolymers Containing Both Polydiene and Polyalcohol Blocks. *J. Polym. Sci. Part A Polym. Chem.* **1989**, *27* (10), 3251–3261.
- (187) Chung, T. C.; Lu, H. L.; Li, C. L. Synthesis and Functionalization of Unsaturated Polyethylene: Poly(Ethylene-Co-1,4-Hexadiene). *Macromolecules* **1994**, *27* (26), 7533–7537.
- (188) Chung, T. C.; Rhubright, D. Functionalization of Polypropylene by Hydroboration. *J. Polym. Sci. Part A Polym. Chem.* **1993**, *31* (11), 2759–2763.
- (189) Krimm, S.; Liang, C. Y.; Sutherland, G. B. B. M. Infrared Spectra of High Polymers. V. Polyvinyl Alcohol. *J. Polym. Sci.* **1956**, *22* (101), 227–247.
- (190) Silverstein, R. M.; Bassler, G. C.; Morrill, T. C. *Spectrometric Identification of Organic Compounds*; Wiley, 1981.
- (191) Liang, C. Y.; Krimm, S. Infrared Spectra of High Polymers. VI. Polystyrene. *J. Polym. Sci.* **1958**, *27* (115), 241–254.
- (192) van de Wouw, H. L.; Lee, J. Y.; Klausen, R. S. Gram-Scale Free Radical Polymerization of an Azaborine Vinyl Monomer. *Chem. Commun.* **2017**, *53*, 7262–7265.
- (193) Giustra, Z. X.; Liu, S.-Y. The State of the Art in Azaborine Chemistry: New Synthetic Methods and Applications. *J. Am. Chem. Soc.* **2018**, *140* (4), 1184–1194.
- (194) Campbell, P. G.; Abbey, E. R.; Neiner, D.; Grant, D. J.; Dixon, D. A.; Liu, S.-Y. Resonance Stabilization Energy of 1,2-Azaborines: A Quantitative Experimental Study by Reaction Calorimetry. *J. Am. Chem. Soc.* **2010**, *132* (51), 18048–18050.
- (195) Gershoni-Poranne, R.; Stanger, A. Magnetic Criteria of Aromaticity. *Chem. Soc. Rev.* **2015**, *44* (18), 6597–6615.
- (196) Su, K.; Remsen, E. E.; Thompson, H. M.; Sneddon, L. G. Syntheses and Properties of Poly(B-Vinylborazine) and Poly(Styrene-Co-B-Vinylborazine) Copolymers. *Macromolecules* **1991**, *24* (13), 3760–3766.
- (197) Lynch, A. T.; Sneddon, L. G. Transition-Metal-Promoted Reactions of Boron Hydrides. 12. Syntheses, Polymerizations, and Ceramic Conversion Reactions of B-Alkenylborazines. *J. Am. Chem.*

- Soc.* **1989**, *111* (16), 6201–6209.
- (198) Mirabelli, M. G. L.; Lynch, A. T.; Sneddon, L. G. Molecular and Polymeric Precursors to Boron-Based Ceramics. *Solid State Ionics* **1989**, *32–33*, 655–660.
- (199) Baggett, A. W.; Guo, F.; Li, B.; Liu, S.-Y.; Jäkle, F. Regioregular Synthesis of Azaborine Oligomers and a Polymer with a Syn Conformation Stabilized by N·H···n Interactions. *Angew. Chemie Int. Ed.* **2015**, *54* (38), 11191–11195.
- (200) Chrostowska, A.; Xu, S.; Lamm, A. N.; Mazière, A.; Weber, C. D.; Dargelos, A.; Baylère, P.; Graciaa, A.; Liu, S.-Y. UV-Photoelectron Spectroscopy of 1,2- and 1,3-Azaborines: A Combined Experimental and Computational Electronic Structure Analysis. *J. Am. Chem. Soc.* **2012**, *134* (24), 10279–10285.
- (201) Ihara, E.; Kurokawa, A.; Itoh, T.; Inoue, K. Homopolymerization and Copolymerization with Styrene of Various Alkoxyvinylsilanes and Oxidative Transformation of C-Si Bond in the Resulting Copolymers to Afford Poly[(Vinyl Alcohol)-Co-Styrene]S. *Polym. J.* **2008**, *40* (12), 1140–1148.
- (202) Ihara, E.; Kurokawa, A.; Itoh, T.; Inoue, K. A Novel Synthetic Strategy for Copolymers of Vinyl Alcohol: Radical Copolymerization of Alkoxyvinylsilanes with Styrene and Oxidative Transformation of C-Si(OR)₂Me into C-OH in the Copolymers to Afford Poly(Vinyl Alcohol-Ran-Styrene)S. *J. Polym. Sci. Part A Polym. Chem.* **2007**, *45* (16), 3648–3658.
- (203) Joshi, R. M. A Brief Survey of Methods of Calculating Monomer Reactivity Ratios. *J. Macromol. Sci. Part A - Chem.* **1973**, *7* (6), 1231–1245.
- (204) Scott, A.; Penlidis, A. Computational Package for Copolymerization Reactivity Ratio Estimation: Improved Access to the Error-in-Variables-Model. *Processes* **2018**, *6* (1), 8.
- (205) Van Herk, A. M.; Dröge, T. Nonlinear Least Squares Fitting Applied to Copolymerization Modeling. *Macromol. Theory Simulations* **1997**, *6* (6), 1263–1276.
- (206) Fineman, M.; Ross, S. D. Linear Method for Determining Monomer Reactivity Ratios in Copolymerization. *J. Polym. Sci.* **1950**, *V* (2), 259–265.
- (207) Kelen, T.; Tüdös, F. Analysis of the Linear Methods for Determining Copolymerization Reactivity Ratios. I. A New Improved Linear Graphic Method. *J. Macromol. Sci. Part A - Chem.* **1975**, *9* (1), 1–27.
- (208) Wrackmeyer, B. Carbon-13 NMR Spectroscopy of Boron Compounds. *Prog. Nucl. Magn. Reson. Spectrosc.* **1979**, *12* (4), 227–259.
- (209) Claudy, P.; Létoffé, J. M.; Camberlain, Y.; Pascault, J. P. Glass Transition of Polystyrene versus Molecular Weight. *Polym. Bull.* **1983**, *9–9* (4–5), 208–215.
- (210) Fox, T. G.; Flory, P. J. Second-Order Transition Temperatures and Related Properties of Polystyrene. I. Influence of Molecular Weight. *J. Appl. Phys.* **1950**, *21* (6), 581–591.

- (211) Höhne, G. W. H.; Hemminger, W. F.; Flammersheim, H.-J. Applications of Differential Scanning Calorimetry. In *Differential Scanning Calorimetry*; Springer Berlin Heidelberg: Berlin, Heidelberg, 2003; pp 147–244.
- (212) Valk, J.-M.; van Belzen, R.; Boersma, J.; Spek, A. L.; van Koten, G. Carbon–hydrogen and C–X (X = Cl or SiMe₃) Bond Activation. 1-Cyclopalladation and Oxidation of Some Derivatives of 2-[(Dimethylamino)Methyl]Naphthalene. *J. Chem. Soc., Dalt. Trans.* **1994**, 0(15), 2293–2302.
- (213) Gunstone, F. D.; Tucker, S. H. 1-CHLORO-2,6-DINITROBENZENE. *Org. Synth.* **1952**, 32, 23.
- (214) Bräse, S.; Gil, C.; Knepper, K.; Zimmermann, V. Organic Azides: An Exploding Diversity of a Unique Class of Compounds. *Angew. Chemie Int. Ed.* **2005**, 44(33), 5188–5240.
- (215) Larouche-Gauthier, R.; Elford, T. G.; Aggarwal, V. K. Ate Complexes of Secondary Boronic Esters as Chiral Organometallic-Type Nucleophiles for Asymmetric Synthesis. *J. Am. Chem. Soc.* **2011**, 133(42), 16794–16797.

Appendix III: Curriculum Vitae

Heidi Lee van de Wouw was born May 10th, 1990 to Monica Ann and John Allan van de Wouw. Heidi grew up alongside her younger sister, Jody Ann van de Wouw, in Redondo Beach, California. Heidi was a part of the Lanakila Outrigger Canoe Club as a steersman for most of her youth and competed on the Redondo Union High School Sailing Team. In addition to enjoying her time on the ocean, Heidi organized a community service project, earning the Girl Scout Gold Award.

After graduation from Redondo Union High School in 2008, Heidi began college at Sonoma State University. Here she double majored in Chemistry and Environmental Studies and Planning with an Emphasis in Water Quality. In college she began her research career under the supervision of both Dr. Carmen F. Works and the late Dr. Stephen A. Norwick. Heidi was an avid participant in the Sonoma State University Chemistry Club and in her senior year Heidi was voted to be club President. Heidi also held a student internship at the North Coast Water Quality Control Board under the direction of Cherie Blatt on the newly promulgated North Coast Dairy Permitting Program. Heidi graduated *cum laude* from Sonoma State University with two B.S. degrees in 2012.

In July 2013 Heidi joined the newly hired Dr. Rebekka S. Klausen in the Department of Chemistry at Johns Hopkins University to help set up their laboratory. Heidi officially joined the Klausen Group in the winter of 2013. Upon completion of her Ph.D., Heidi is to join the lab of Dr. Ellen M. Sletten in the Department of Chemistry and Biochemistry at the University of California, Los Angeles.

Heidi L. van de Wouw

Johns Hopkins University
Department of Chemistry
3400 N. Charles St, Remsen 219

Baltimore, MD 21218
Phone: (310) 804-1670
hvandew1@jhu.edu

Education

- 2013-present Johns Hopkins University, Baltimore, MD
Ph.D. Candidate in Chemistry, *expected graduation January 2019*
Anticipated Dissertation: Stable Aromatic Organoborane Materials
Advisor: Prof. Rebekka S. Klausen
- 2008-2012 Sonoma State University, Rohnert Park, CA
B.S. in Chemistry with Distinction, *cum laude*
B.S. in Environmental Studies and Planning, *cum laude*
Thesis: Quantum Yield Determination of Bimetallic Carbonyl Dithiolates
Thesis: Reducing the Toxicity of Cr(VI) in Soil using *Pseudomonas veronii*
Advisors: Prof. Carmen F. Works and Prof. Stephen A. Norwick

Publications ([†] = undergraduate co-author)

6. [van de Wouw, H. L.](#); Klausen, R. S. "BN Polystyrenes: Emerging Optical Materials & Versatile Intermediates." *J. Org. Chem.* **2019**, *84*, 1117-1125.
5. [van de Wouw, H. L.](#); Awuyah, E. C.[†]; Baris, J. I.[†]; Klausen, R. S. "An Organoborane Vinyl Monomer with Styrene-like Radical Reactivity: Reactivity Ratios and Role of Aromaticity." *Macromol.* **2018**, *51*, 6359–6368.
4. [van de Wouw, H. L.](#); Lee, J. Y.[†]; Awuyah, E. C.[†]; Klausen, R. S. "A BN Aromatic Ring Strategy for Tunable Hydroxy Content in Polystyrene." *Angew. Chem., Int. Ed.* **2018**, *57*, 1673–1677.
3. [van de Wouw, H. L.](#); Lee, J. Y.[†]; Klausen, R. S. "Gram-Scale Free Radical Polymerization of an Azaborine Vinyl Monomer." *Chem. Commun.* **2017**, *53*, 7262–7265.
2. [van de Wouw, H. L.](#); Lee, J. Y.[†]; Siegler, M. A.; Klausen, R. S. "Innocent BN Bond Substitution in Anthracene Derivatives." *Org. Biomol. Chem.* **2016**, *14*, 3256–3263.
1. [van de Wouw, H. L.](#); Chamorro, J.[†]; Quintero, M.[†]; Klausen, R. S. "Opposites Attract: Organic Charge Transfer Salts." *J. Chem. Educ.* **2015**, *92*, 2134–2139.

Patent Applications

1. [van de Wouw, H. L.](#); Lee, J. Y.; Klausen, R. S. "ORGANOBORANE POLYMERS FOR TUNABLE HYDROPHILICITY AND WETTABILITY." Provisional, filed October 16, 2017.

Awards and Achievements

- 2018 JHU Department of Chemistry Ernest M. Marks Award. *In recognition of teaching excellence.*
2018 Future Faculty Workshop Mentee. *Mentorship to senior graduate students aspiring to become independent academic researchers in the broad areas of Chemistry, Chemical Engineering, Materials Science, and Polymer Science, with a focus on soft materials and biomaterials.*
- 2017 ACS Women Chemists Committee and Eli Lilly & Company Travel Award. *Registration, travel, and lodging support awarded to female students presenting at an ACS National Meeting.*

- Discussion Leader, Physical Organic Chemistry Gordon Research Seminar. *Registration support for facilitating discussion between the audience and the keynote speaker.*
- 2016 JHU Department of Chemistry Harry and Cleio Greer Fellowship. *One full year support plus 10% stipend supplement awarded to an outstanding advanced-year graduate student.*
- JHU Excellence in Teaching Award Finalist. *Student nominated and school-wide award commending care and concern taken by a T.A. towards their subject and their students.*
- NOBCChE Advancing Science Conference Grant. *Registration, travel, and lodging support awarded to students presenting at the NOBCChE Annual Conference.*
- 2012 Sonoma State University Chemistry Departmental Distinction Award. *Honor judged by the department recognizing academic excellence within the discipline or extraordinary contributions to the department, university, or community.*
- 2011 Nancy Foster Glasmeier Research and Writing Award. *Project and educational expense support awarded to an outstanding undergraduate student engaged in a project addressing pressing environmental issues.*

Presentations

- 2018 "Molecular Diversity Through Stable Organoboranes" (Invited Oral Presentation). Sonoma State University Chemistry Department Group Meeting, Rohnert Park, CA, September 2018.
- "A BN Aromatic Ring Strategy for Tunable Hydroxy Content in Polystyrene" (Poster). 256th National American Chemical Society Meeting, POLY: Polymer Chemistry for Functional Materials Poster Session, Boston, MA, August 2018.
- "A BN Aromatic Ring Strategy for Tunable Hydroxy Content in Polystyrene" (Poster). 4th Functional Polymeric Materials Conference, Nassau, Bahamas, June 2018.
- 2017 "Exploring BN for CC Bond Substitution in Materials" (Poster). 254th National American Chemical Society Meeting, Women Chemists Committee and Eli Lilly & Company Travel Award Poster Session, Washington, DC, August 2017.
- "Gram-Scale Free Radical Polymerization of an Azaborine Vinyl Monomer" (Oral Presentation). 254th National American Chemical Society Meeting, Organic Division, Washington, DC, August 2017.
- "Exploring BN for CC Bond Substitution in Materials" (Poster). Physical Organic Chemistry Gordon Research Symposium and Conference, Holderness, NH, June 2017.
- 2016 "Klausen Group: Rational Synthesis to Well-Designed Electronic Materials" (Poster). 2016 NOBCChE National Conference, Raleigh, NC, November 2016.
- "Research and Pedagogy in Organic Electronics" (Poster). 2016 ACS Summer School of Green Chemistry and Sustainable Energy at Colorado School of Mines, Golden, CO, June 2016.
- 2012 "Quantum Yield Determinations of Iron-Iron Hydrogenase Model Compounds" (Oral Presentation). 24th Annual American Chemical Society Northern California Undergraduate Research Symposium, Oakland, CA, April 2012.
- "Photochemical Studies of Iron-Iron Hydrogenase Model Compounds in Various Solvents" (Poster). 243rd National American Chemical Society Meeting, San Diego, CA, March 2012.

"The Synthesis and Quantum Yield Determination of Bimetallic Carbonyl Dithiolates" (Oral Presentation). Sonoma State University, Chemistry Department Seminar Series, Rohnert Park, CA, March 2012.

- 2011 "Reducing the Toxicity of Chromium (VI) in Soil Using *Pseudomonas veronii*" (Poster). 23rd Annual American Chemical Society Northern California Undergraduate Research Symposium, San Jose, CA, May 2011.

Outreach and Service

- 2017-2018 JHU STEM Achievement in Baltimore Elementary Schools (SABES). *After school mentor and science coach, 3rd grade.*
- 2016-2018 ChemDNA (Diversity, Networking, and Advancement), JHU Chemistry. *Recruitment Weekend Subcommittee chair, founding board member.*
- 2015-2018 National Organization for the Professional Advancement of Black Chemists and Chemical Engineers (NOBCChE), JHU Student Chapter. *Vice president, secretary.*
- 2015-2018 Mt. Royal Middle School Science Fair. *Judge.*
- 2015 Food not Bombs at Baltimore Free Farm. *Cook, in solidarity with the Freddie Grey Unrest*
- 2014-2016 JHU Department of Chemistry Student Safety Committee. *Stockroom Safety Supplies Subcommittee chair, graduate student representative.*
- 2008-2012 Sonoma State University Chemistry Club. *President, treasurer.*